CHEMICAL RESEARCH, DEVELOPMENT & ENGINEERING CENTER

CRDEC-CR-87001

CLOTHING PENETRATION MECHANISM

by   Gunilla Gillberg

CELANESE CORPORATION
Summit, NJ   07901

October 1986

U.S. ARMY
ARMAMENT
MUNITIONS
CHEMICAL COMMAND

Aberdeen Proving Ground, Maryland   21010-5423

86 12 09 109

Disclaimer

The findings in this report are not to be construed as an official Department of the Army position unless so designated by other authorizing documents.

Distribution Statement

Approved for public release; distribution is unlimited.

REPORT DOCUMENTATION PAGE

1a. REPORT SECURITY CLASSIFICATION UNCLASSIFIED	1b. RESTRICTIVE MARKINGS
2a. SECURITY CLASSIFICATION AUTHORITY	3. DISTRIBUTION/AVAILABILITY OF REPORT Approved for public release; distribution is unlimited.
2b. DECLASSIFICATION/DOWNGRADING SCHEDULE	

4. PERFORMING ORGANIZATION REPORT NUMBER(S) CRDEC-CR-87001	5. MONITORING ORGANIZATION REPORT NUMBER(S)

6a. NAME OF PERFORMING ORGANIZATION Celanese Corporation	6b. OFFICE SYMBOL (If applicable)	7a. NAME OF MONITORING ORGANIZATION
6c. ADDRESS (City, State, and ZIP Code) 86 Morris Avenue Summit, NJ 07901		7b. ADDRESS (City, State, and ZIP Code)

8a. NAME OF FUNDING/SPONSORING ORGANIZATION CRDEC	8b. OFFICE SYMBOL (If applicable) SMCCR-RSC-P	9. PROCUREMENT INSTRUMENT IDENTIFICATION NUMBER DAAK11-84-C-0050

8c. ADDRESS (City, State, and ZIP Code) Aberdeen Proving Ground, MD 21010-5423	10. SOURCE OF FUNDING NUMBERS			
	PROGRAM ELEMENT NO.	PROJECT NO.	TASK NO.	WORK UNIT ACCESSION NO.

11. TITLE (Include Security Classification)

Clothing Penetration Mechanism

12. PERSONAL AUTHOR(S)
Gillberg, Gunilla

13a. TYPE OF REPORT Contractor	13b. TIME COVERED FROM 84 Jun TO 85 Oct	14. DATE OF REPORT (Year, Month, Day) 1986 October	15. PAGE COUNT 105

16. SUPPLEMENTARY NOTATION
COR: E. Penski, SMCCR-RSC-P, (301) 671-3953

17.	COSATI CODES		18. SUBJECT TERMS (Continue on reverse if necessary and identify by block number)
FIELD	GROUP	SUB-GROUP	Fabric penetration Contact angle
15	05		Liquids Polypropylene
			Capillary flow Viscosity (continued on reverse)

19 ABSTRACT (Continue on reverse if necessary and identify by block number)

The penetration of a liquid drop through a barrier fabric into a receiver material consisting of a 50/50 polyethylene terephthalate/cotton knit was studied for 25 pure liquids representing a large range of physico-chemical properties and 4 plain weave barrier fabrics (rayon, polybenzimidazole, polyethylene terephthalate, and polypropylene). The experiments were performed with constant drop volume, minimal deposition energy, constant barrier-receiver contact pressure, and constant penetration time. The contact angles of the liquids with the barrier polymers were determined by single fiber wettability studies. The penetration studies showed that extremely careful control and observation of all experimental parameters are necessary. The amount of liquid transferred by contact from a 50 µL drop thus was shown to depend on the viscosity of the liquid, the wettability of the barrier fabric, the evaporation rate of the liquid, and the barrier-receiver contact pressure. The rate of penetration was too fast to be determined by the experimental procedure specified. The degree of penetration was

(continued on reverse)

20. DISTRIBUTION/AVAILABILITY OF ABSTRACT ☒ UNCLASSIFIED/UNLIMITED ☐ SAME AS RPT. ☐ DTIC USERS	21. ABSTRACT SECURITY CLASSIFICATION UNCLASSIFIED
22a. NAME OF RESPONSIBLE INDIVIDUAL TIMOTHY E. HAMPTON	22b. TELEPHONE (Include Area Code) (301) 671-2914 22c. OFFICE SYMBOL SMCCR-SPS-T

DD FORM 1473, 84 MAR 83 APR edition may be used until exhausted. SECURITY CLASSIFICATION OF THIS PAGE
All other editions are obsolete.

UNCLASSIFIED

18. Subject Terms (continued)

    Rayon
    Polybenzimidazole
    Polyethylene terephthalate

19. Abstract (continued)

shown to be dependent on the construction of the barrier fabric and its wettability but
did not follow the general equations for capillary flow. The PBI barrier fabric showed
an unexpected low degree of penetration. Only liquids with a contact angle less than
60° will wet a fabric. No good correlations between the physico-chemical properties of
the liquid and the degree of penetration were established. Generally, the larger the
difference in surface energy between the barrier material and the liquid, the higher
the degree of penetration. Acetonitrile showed the highest penetration on the average
for all barrier fabrics.

PREFACE

The work described in this report was authorized under Contract DAAK11-84-C-0050. This work was started in June 1984 and completed in October 1985.

The use of trade names or manufacturers' names in this report does not constitute an official endorsement of any commercial products. This report may not be cited for purposes of advertisement.

Reproduction of this document in whole or in part is prohibited except with permission of the Commander, U.S. Army Chemical Research, Development and Engineering Center, ATTN: SMCCR-SPS-T, Aberdeen Proving Ground, Maryland 21010-5423. However, the Defense Technical Information Center and the National Technical Information Service are authorized to reproduce the document for U.S. Government purposes.

This report has been approved for release to the public.

Acknowledgments

DTIC
ELECTED
DEC 1 0 1986
B

DTIC
COPY
INSPECTED

Accession For		
NTIS GRA&I	✓	
DTIC TAB	☐	
Unannounced	☐	
Justification		
By		
Distribution/		
Availability Codes		
Dist	Avail and/or Special	
A-1		

3

Blank

CONTENTS

LIST OF FIGURES

LIST OF FIGURES

LIST OF TABLES

CLOTHING PENETRATION MECHANISM

SECTION 1. INTRODUCTION

The interaction between a liquid drop and a fabric is a complex process. The drop can fail to wet the fabric and remains pearled on the surface. If the drop enters the fabric, several different behaviors can be observed. In some cases, the liquid will wick out rapidly in intra- and interyarn spaces of the fabric. The wicking rate in the warp yarns can again differ to those of the filler yarn. In other cases, the main process will be a penetration of the liquid perpendicularly through the fabric in the interyarn spaces. The fabric construction will thus have a great influence in the wetting behavior of the liquid.

L. C. Buckles, F. W. Minor, A. M. Schwartz and E. A. Wulkow extensively studied the interaction of liquid drops with fibers, yarns and fabrics in the late 50's and early 60's[1-5]. They showed that the wicking of a liquid in a yarn (intrayarn migration) followed Washburn equation for flow in a cylindrical capillary before the drop had sunk completely into the yarn. The amount of migration thereafter consisted of movement of liquid from large capillary spaces to small ones. The penetration of liquid through a fabric into a substrate was shown to be extremely dependent on the chosen experimental conditions. The dominating liquid transport mechanism for a given fabric-liquid pair depended on the drop size, the impact force of the drop onto the fabric, applied pressure on the wetted fabric and the point of time this pressure was applied as well as the absorptive properties of the substrate on which the fabric was resting.

B. Miller and H. K. Perkins studied fabric penetration by liquids under breakthrough conditions both in the case of limited and unlimited liquid supply[6]. They developed an apparatus, Model LV-III, which allowed a controlled contact pressure to be applied across the barrier fabric and the receiver fabrics. They found that the degree of penetration could be explained in terms of differences in pore sizes within the barrier and receiver fabrics, the wettability of the fiber and the liquid viscostiy. The dominant factor determining the degree of penetration appeared thus to be capillary effects. A decrease in the amount of penetrated liquid with time (reversal effect) was observed for some systems. F. W. Minor, et al[4] showed, in addition, that the weight of liquid per unit area of fabric at the instant the drop entered the fabric strongly influenced the penetration.

While considerable research has been performed on fabric penetration, there have been no studies devoted to develop the scientific principles for relating the physico-chemical properties of the liquid and barrier material to droplet penetration. This study reports the results of penetration studies performed with a large number of pure liquids selected to have a range of combination of surface tension, acid and base properties as described by Kamlet and Taft solvatochromic parameters[7], and

9

polarities as described by the partial solubility parameters[8]. The barrier fabrics were also chosen to have large differences in hydrophilicity and thus in liquid wettability. The other parameters known to affect the penetration such as type of receiver materials, contact pressure across the barrier fabric and receiver material, applied droplet size and penetration time were kept constant to isolate the fluid barrier interaction. The penetration studies were performed using a Model LV-III apparatus as developed by B. Miller and H. K. Perkins under Contract No. DAAK11-82-C-0143[6]. The results of the penetration data were analyzed by using Washburn's equation for capillary transport and the laws of fluid mechanics. Linear regression analysis were used to determine any correlations between the wettability data and the partial solubility parameters and Kamlet and Taft's solvatochromic parameters respectively.

The principal investigator was Celanese Research Company, Summit, New Jersey. The penetration studies were originally performed by the Specialty Fibers/Products Development of Celanese Fibers Operations, Charlotte. North Carolina. A restudy of the penetration was later performed at Celanese Research Company.

The materials, equipment, and procedures used in the studies are described in Sections 2 and 3. Experimental results of the wettability and penetration studies are given in Section 5 and these results are analyzed and discussed in Section 6. Finally, our conclusions for the penetration mechanism are given in Section 7.

SECTION 2. MATERIALS

The water used in the studies was doubly distilled. The methanol was glass distilled (EM Science) and the ethanol was a 200 proof quality from Publicker Industries. All other liquids were purchased from Aldrich Chemical Company and were their Gold Label or best available quality. The purity of the liquids was confirmed by surface tension measurements with a Prolabo surface tensiometer which uses the Wilhelmy plate method with a platinum blade. The measured surface tension values agreed with literature values[9]. These data as well as the viscosity[9], density[9], Kamlet and Taft's solvatochromic parameters[7] and the partial solubility parameters[8] are given in Table A-1 Appendix A.

The four barrier fabrics viz. polybenzimidazole (PBI), rayon, polyethylene terephthalate (PET) and polypropylene (PP) were chosen to encompass a wide range of physico-chemical properties. Their structures and some estimated physico-chemical properties are given in Figure 1. The rayon, PET, and PP all contained titanium oxide as a delusterant. The PBI was the heat stable sulfuric acid treated PBI fibers. All barrier fabrics were made from staple yarn and constructed in plain weave. The PBI, rayon and PET fabrics were made at Celanese. The polypropylene fabric was a gift from Hercules, Inc. The receiver fabric was a 50/50 cotton/PET blend knit. The total denier and area weight of the barrier fabrics are given in Table 1.

10
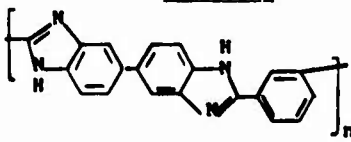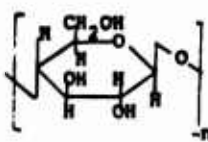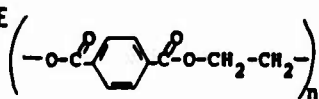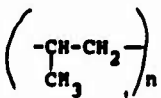
POLYMER	STRUCTURE	SOLUBILITY PARAMETER	SURFACE ENERGY	CROSS-SECTION
POLYBENZIMIDAZOLE (PBI)		11-12	42-45	DUMB-BELL
RAYON		15.7	42-44	CRENULATED
POLYETHYLENE TEREPHTHALATE (PET)		9.8 AND 12.1	38-43	ROUND
POLYPROPYLENE (PP)		9.2	29-34	ROUND

FIGURE 1. FIBER MATERIAL PROPERTIES

TABLE 1. BARRIER FABRICS

Fiber	Yarn Total Denier	Area Weight g/m^2
Polybenzimidazole (PBI)	347	247
Rayon	384	267
Polyethylene terephthalate (PET)	217	174
Polypropylene (PP)	805	262

The same fiber materials as used in the barrier fabrics were also obtained as filament yarns for the wettability studies. Table 2 gives a description of the filament yarns.

All fabrics and filaments were extracted twice ultrasonically with methanol to remove finishes and dirt and then dried in a 40°C oven. The cleaned fabrics and filaments were stored at constant temperature and humidity and allowed to reach their constant water regain before use (13% for PBI, 15% for rayon).

11

TABLE 2. FILAMENT YARNS

Polymer	Denier	No. of Fils	Dpf
Polybenzimidazole (PBI)	280	200	1.40
Rayon	300	80	3.75
Polyethylene terephthalate (PET)	300	66	4.55
Polypropylene (PP)	480	480	1.00

SECTION 3. EQUIPMENT AND PROCEDURES

3.1 Penetration Experiments

The penetration experiments were performed with a limited volume of liquid using a copy of the Model LV-III apparatus developed by B. Miller and H. K. Perkins[6], (Figure 2). Their general experimental procedures were also followed. A single layer of barrier fabric (15 cm X 15 cm) on top of multiple receiver layers (5 cm circles) were used in all experiments. The barrier fabric was held in a embroidery hoop (10 cm diameter) to prevent slippage when pressure was applied. Enough layers of receiver material was placed within the retainer ring (Figure 2) so that their total uncompressed thickness was equal to that of the retainer ring. Both the barrier fabric and receiver fabrics were changed after each experiment. The procedure of each experiment was to record the weight of the receiver layers, to position these and the barrier fabric on the LV-Model III apparatus, to load down the pressure ring with a 1 lb weight to keep barrier layer in place and then to apply a constant barrier-receiver contact pressure by the application of a 50 cm hydrostatic head to the bottom of the flexible rubber membrane (Figure 2), (for an analysis of the pressure across the fabrics and pressure drops across membranes, see reference 6). A constant size liquid drop was to be transferred to the barrier fabric without any impact by letting the drop come into light contact with the fabric.

The hydrostatic pressure was removed and the barrier and receiver fabrics separated 20 seconds after the drop had contacted the barrier fabric. The receiver layers were immediately weighed. The procedure was repeated five times or until satisfactory reproducibility was achieved for each solvent.

The penetration studies were performed by Celanese Fibers Operations following this procedure. The penetration apparatus was placed in a fume hood of a constant temperature-humidity room to reduce the risk of possible exposure to solvent vapors. The same equipment and procedure was to be used in a subsequent contract DAAK15-85-C-0008, Clothing Penetration Mechanism, Partially Volatile Mixtures by Celanese Research Company. It was discovered during the initial penetration studies under this contract that the penetration test method was extremely sensitive

12
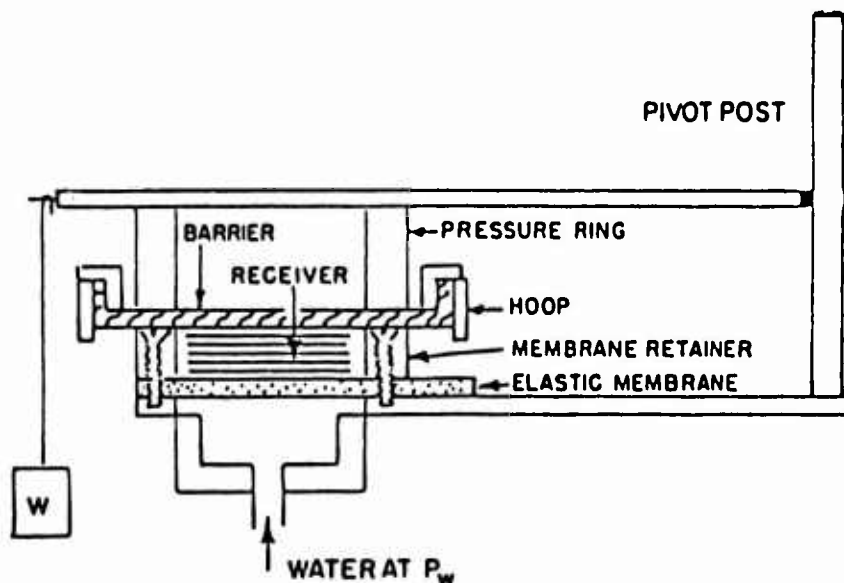
FIGURE 2. APPARATUS USED FOR MEASURING FLUID PENETRATION
(DEVELOPED AT TRI UNDER CONTRACT NO. DAAK11-32-C-0143)

---

to several previously not reported experimental parameters.
Significant changes in the water regain of the fabrics, even the
hydrophobic ones, result from small changes in the relative
humidity. The water regain of the barrier fabric can change
under the tension exhibited by the embroidery hoop. (This was
the case with the rayon barrier fabric.) Significant evaporative
losses can occur during both the penetration experiments and the
weighing operations even for liquids with boiling points above
100°C. The amount of the liquid drop actually transferred to a
barrier fabric depends on the type of barrier fabric, on the size
of the applied barrier-receiver contact pressure and on the
surface tension and viscosity of the liquid. The following
revised penetration procedure was therefore used in a restudy.

The experiments were performed in a constant temperature-
humidity room and at an area with as slow air movement as
possible. The local humidity was continuously monitored.

The average amount of liquid delivered to the barrier fabric
and receiver material was determined by weighing the mounted
barrier fabric and receiver materials before and immediately
after the liquid was transferred to the fabrics by a light
contact of the liquid drop to the barrier fabric mounted on the
penetration apparatus in the presence of the contact pressure.
The time from the liquid contact to the first weight reading was
monitored and the weight as function of time was studied in order
to estimate rate of evaporation. This procedure was repeated
five times.

The average amount of liquid penetrated into the receiver
material during 20 seconds of contact pressure was determined as
previously described.

A slightly modified procedure was used in the case of the rayon barrier fabric since this fabric showed a significant decrease in its water regain when under tension. The rayon barrier fabrics were therefore mounted on the embroidery hoops and allowed to equilibrate to constant weight before use. The added tension on the fabric caused by the application of a 50 cm hydrostatic head was also determined and found to be negligible.

3.2 Liquid Dispenser

A constant and large drop size (a drop diameter of 4 mm) or volume of 34 μL was desirable. The drop was also to be transferred to the barrier fabric in absence of any impact velocity. This demanded that the drop was preformed at the tip of the dispenser and transferred to the fabric by a light contact. The volume of a liquid which detaches itself from the tip of a vertical tube under the gravitational pull is very dependent on the surface tension of the liquid. Theoretically, the volume is determined by[10].

$$V = \frac{2 \pi r \cdot \gamma_{LV}}{g \cdot \rho} \tag{1}$$

where

$$
\begin{aligned}
V &= \text{volume of the drop} \\
r &= \text{outer radius of the vertical tube} \\
\gamma_{LV} &= \text{surface tension of liquid} \\
g &= \text{gravitational acceleration} \\
\rho &= \text{density of liquid}
\end{aligned}
$$

In reality, the volume obtained is less than the ideal volume due to some of the liquid remaining on the tip. Calculations show that an outer tube diameter of at least 5 mm would be needed to give a 4 mm drop of a liquid with a surface tension of 20 dyn/cm. Experiments showed that thin walled tubes of the needed size would not yield a controlled formation of liquid drops due to the capillary forces being too low. A method was developed which allowed the controlled formation of large drops. The method used a 50 μL Hamilton glass syringe as liquid reservoir and a Hamilton syringe needle, gauge 29 with 90° blunt cut tip fitted with a concentric Kontes glass capillary as a vertical tube (Figure 3). The glass capillary was glued onto the needle by a small amount of epoxy glue at the top end of the capillary. The formed vertical tubes thus had a bore with a diameter of 0.18 mm and an outer diameter of 5-6 mm. Approximately 50 μL drops could be formed at the end of this thick walled tube of all liquids used in the study. However, drops formed from liquids with a low viscosity and low surface tension showed strong tendency to necking. These drops could easily be dislodged prematurely by small vibrations. Only part of the drops were actually transferred when brought in light contact with the barrier fabric. The amount transferred depended on the liquid properties as well as on the properties of the barrier fabric and the size of the contact pressure.

HAMILTON GLASS SYRINGE, 50 μL

HAMILTON SYRINGE NEEDLE GAUGE 29
WITH 90° BLUNT CUT TIP;
O.D. 0.33 mm; I.D. 0.18 mm

KONTES GLASS CAPILLARY
O.D. 5-6 mm; I.D. 0.40 mm
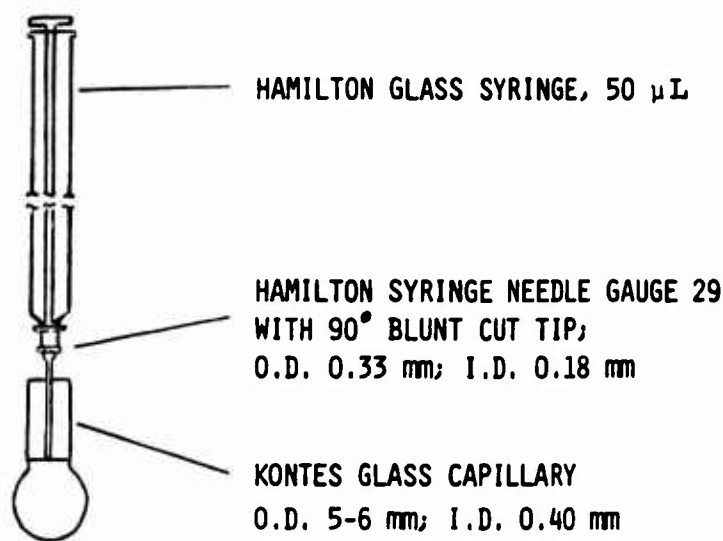
FIGURE 3. EQUIPMENT FOR THE DELIVERY OF A CONSTANT DROP SIZE

3.3 Fiber Wettability

The advancing and receding contact angles were determined by measuring the Wilhelmy pulling force on a single fiber inserted in a liquid by a modified autobalance (Figure 4)[11]. The advancing contact angle was calculated from the average wetting force measured when the liquid advanced slowly along the dry fiber; the receding contact angle from the average wetting force when the liquid was retracted from the prewetted fiber. Contributions from the buoyance forces could be neglected for all fibers. The wetting behavior of five to six fibers were determined for each liquid-fiber pair.

15
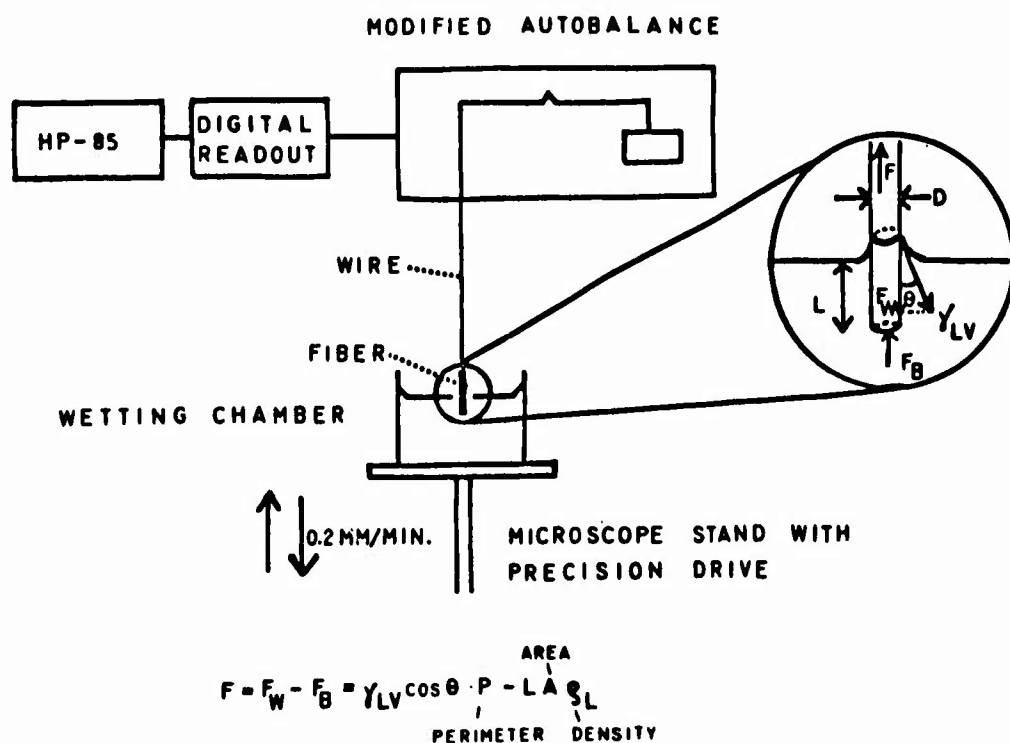
FIGURE 4. SCHEMATIC PICTURE OF APPARATUS FOR MEASURING THE WETTABILITY OF FIBERS OR RIBBONS ACCORDING TO THE WILHELMY METHOD

SECTION 4. RESULTS

4.1 Fiber Wetting Studies

The average wetting force calculated from the averages for each fiber are given in the second column of Tables A-2 - A-9, Appendix A. The wetting force F, depends on the perimeter of the fiber, P, the liquid surface tension, γ_{LV}, and the contact angle, θ , according to the Wilhelmy equation:

$$F = P \cdot \gamma_{LV} \cdot \cos \theta \qquad (2)$$

The perimeter can either be determined microscopically or from wetting studies with liquids which are known to give a zero contact angle with the fiber material. Our first approach was to use the standard microscopic techniques for determining the diameter of the two fiber materials with circular cross-sections (polypropylene and PET) and to use image analysis of cross-sections for the two fibers with irregular cross-sections (rayon and PBI). Both microscopic methods are afflicted by a slight inaccuracy in exact definition of the borderline of the fibers. However, the advantage of using an independently determined perimeter is that no preassumptions of the contact angles are needed.

Zisman and his coworkers have extensively studied the contact angles of pure liquids in a variety of solids. They found that approximately straight lines were obtained when the cosine of the contact angle was plotted against the surface tension[12]. The critical surface tension for wetting was defined by the intercept between the straight line plot of cos θ vs. γ_{LV} and the horizontal line of cos θ = 1. Liquids with a surface tensic less than the critical surface tension of wetting should all giv a contact angle of zero i.e., a cos θ of 1. However, the Zisman plot for the rayon fibers showed all liquids but water and formamide to be scattered around a cos θ of 0.8 when an average perimeter of 115 µm as determined by image analysis was used to calculate the contact angles from the wettability data (Figure 5). No contact angle hysteresis was observed which suggested that the contact angles should be close to zero. Both facts implied that the perimeter determined by image analysis was too large. A contribution to this could be the fact that the fibers had to be dyed with a water soluble dye to yield needed contrast for the image analysis and this could have caused a slight swelling of the fibers. Both water and formamide showed a continuously increasing wetting force for 20 minutes after contact. This increase could originate from a capillary rise of liquid in the interstices on the fiber surface or more probably from a swelling of the fibers. The measured force thus contained contributions from both the weight of liquid and the wetting force. Figure 6 gives the Zisman plot for the data using a perimeter of 90 µm estimated to give an average contact angle of zero. The scatter around cos θ equal to 1 reflects the variability in fiber diameters. The impossible cos θ values of formamide and water are due to fiber swelling.

17
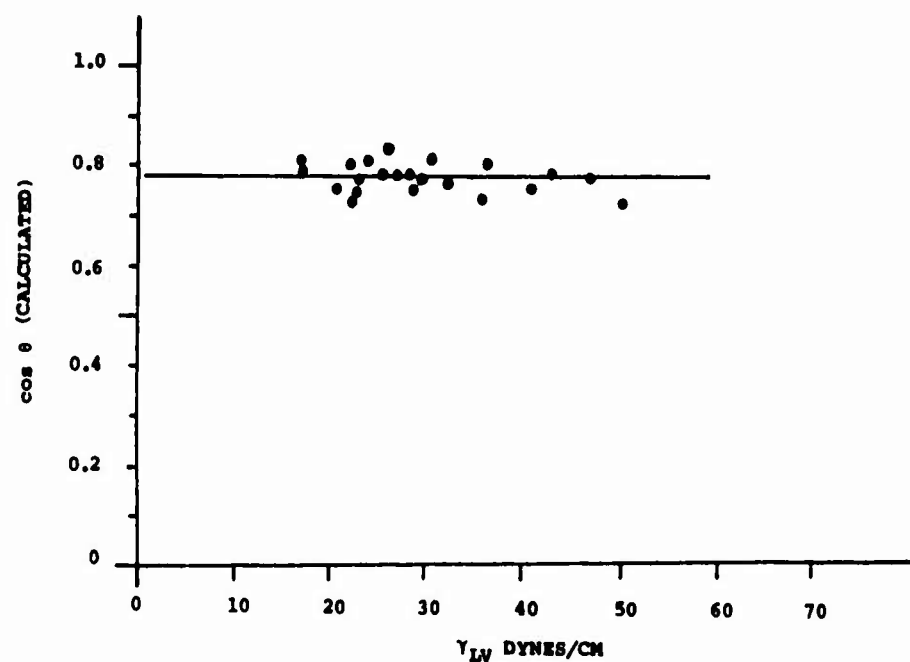
FIGURE 5.   RAYON – DETERMINATION OF ZISMAN'S CRITICAL SURFACE
TENSION, γ_C, FOR RAYON FIBERS.   THE AVERAGE PERIMETER
WAS DETERMINED TO BE 115 µm FROM FIBER CROSS-SECTIONS
BY IMAGE ANALYSIS
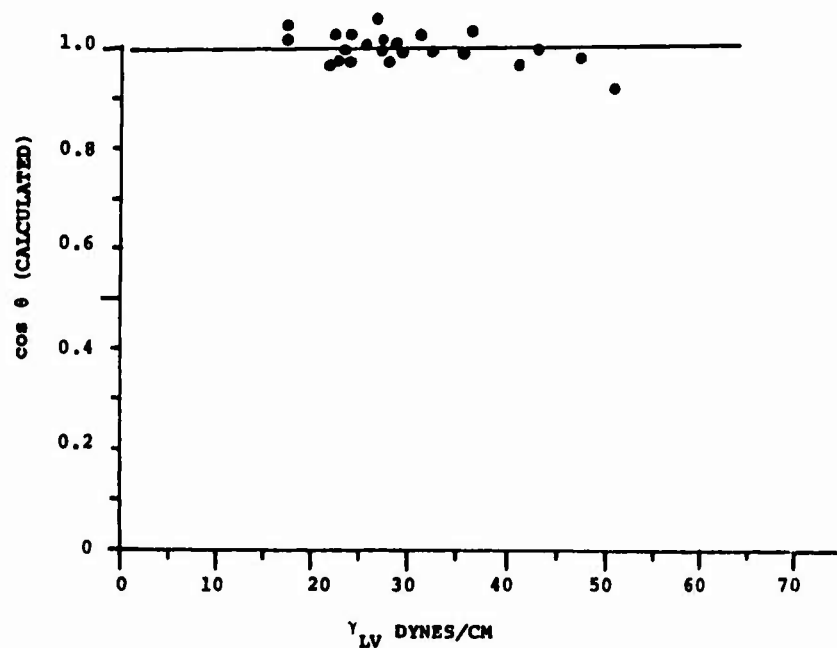
FIGURE 6.   RAYON – DETERMINATION OF ZISMAN'S CRITICAL SURFACE
TENSION, γ_C, FOR RAYON FIBERS.   THE AVERAGE PERIMETER
WAS ESTIMATED TO BE 90 µm FROM THE WETTABILITY DATA

18

The contrast between the cross-section of the PBI fibers and the used embedding medium was not optimal for image analysis. Two different instruments gave average perimeters of 50 and 42 μm respectively. A perimeter value of 46 μm was determined from the wettability data (Figure 7) and was used in the calculations (Tables A-4, A-5, Appendix A). The critical surface tension of the PBI fibers is 40 dynes/cm.

The diameter of the PET fibers was determined to be 22.5 μm using an optical microscope equipped with a filar unit and video monitor and with the fibers immersed in a matching refractive index oil. This value is in good agreement with the diameter value of 23 μm as determined from the wettability data (Figure 8). The Zisman plot gave a critical surface tension of 40 dynes/cm for the PET fibers. The wettability data and the calculated parameters are given in Tables A-6 and A-7, Appendix A.

The diameter of the polypropylene fibers was determined to be 13 μm both by microscopy and from the wettability data. The critical surface tension was determined to be 26 dynes/cm from the Zisman plot (Figure 9). The calculated data are given in Tables A-7 and A-8, Appendix A.
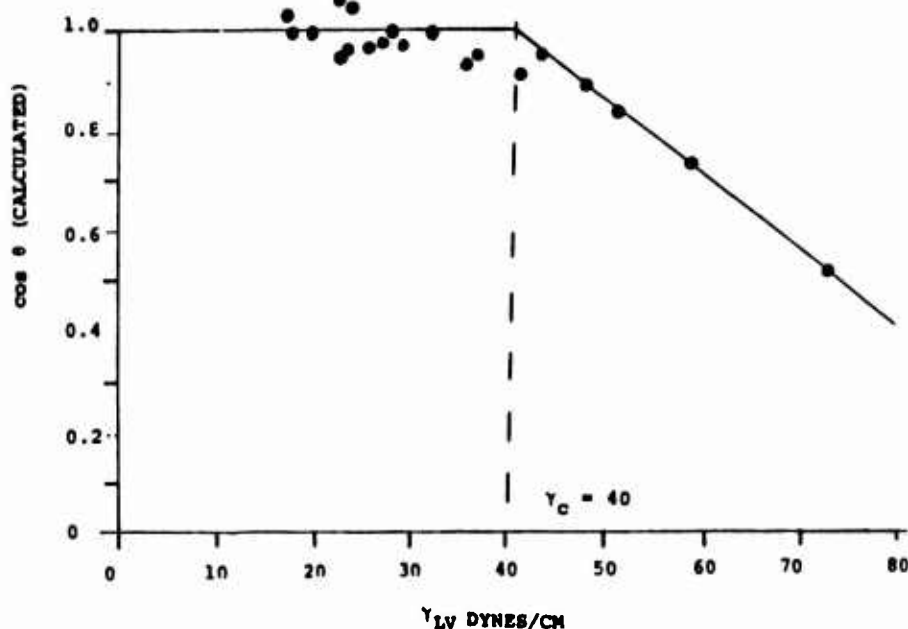
FIGURE 7. PBI – DETERMINATION OF ZISMAN'S CRITICAL SURFACE TENSION, γ_C, FOR PBI FIBERS. THE AVERAGE PERIMETER WAS ESTIMATED TO BE 46 μm FROM THE WETTABILITY DATA
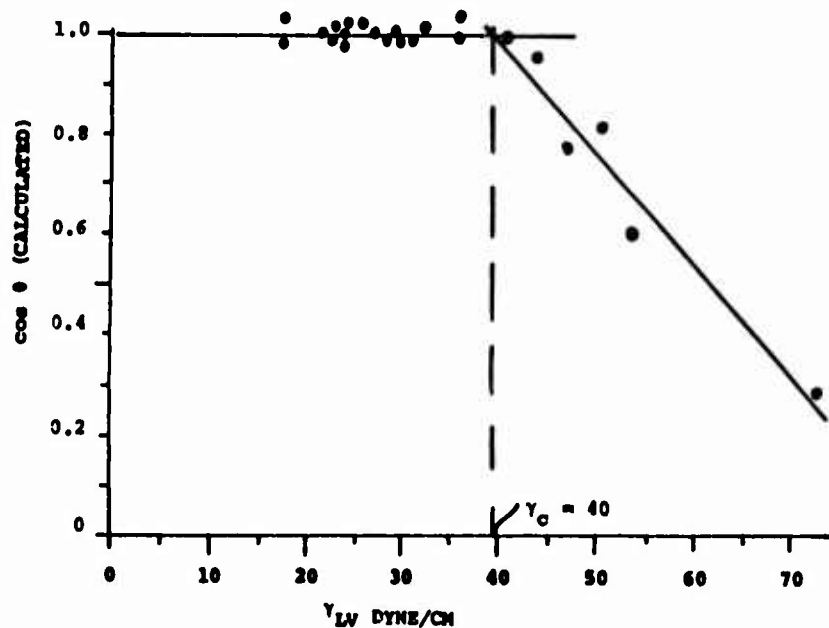
FIGURE 8.   PET DETERMINATION OF ZISMAN'S CRITICAL SURFACE
TENSION, γ_C, FOR PET FIBERS.   THE AVERAGE DIAMETER
WAS ESTIMATED   TO BE 23 μm FROM THE WETTABILITY DATE
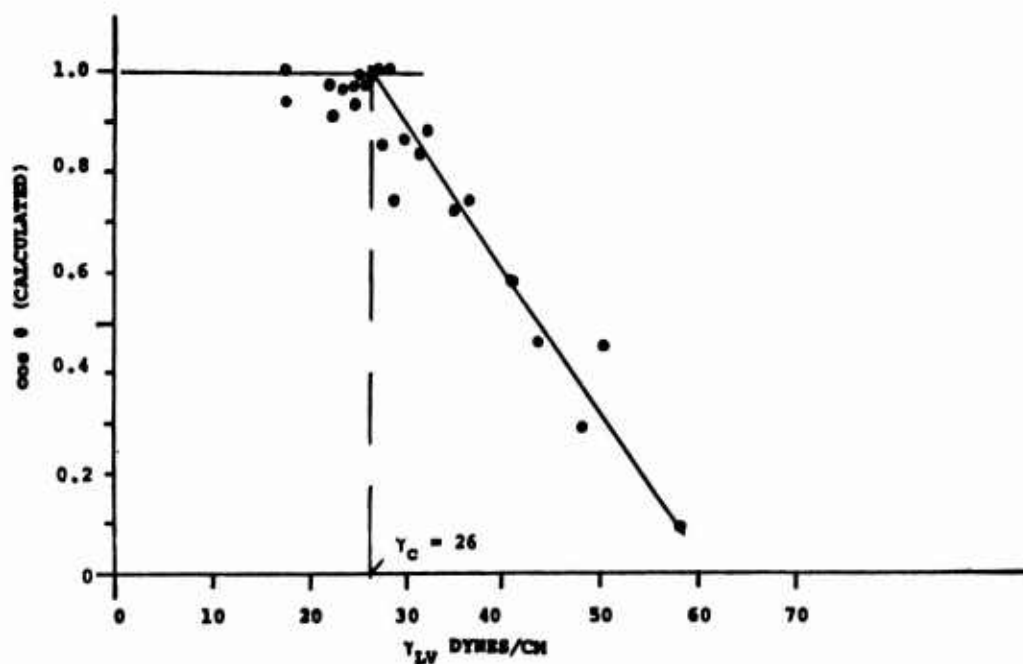
FIGURE 9.   POLYPROPYLENE - DETERMINATION OF ZISMAN'S CRITICAL
SURFACE TENSION, γ_C, FOR POLYPROPYLENE FIBERS.   THE
AVERAGE DIAMETER WAS ESTIMATED TO BE 13.0 μm FROM THE
WETTABILITY STUDIES

20

Another method commonly used for estimating the surface energy of polymers is generally referred to as the Kaelble's method[13] although originally introduced by Owens and Wendt[14]. It is based on Fowkes' suggestion that the attractive forces at an interface as measured by the work of adhesion can be written as the sum of the contributions from the different types of intermolecular interactions such as London dispersion forces, hydrogen bonds, dipole-dipole interaction, etc. The surface tension is also assumed to be the sum of its components. Owens and Wendt grouped all types of polar interaction into one component and assumed that the polar interactions as well as the dispersion interactions could be described by a geometric mean expression. The surface energy of the polymer is estimated by using the wettability data determined for liquids with known partial surface tensions (for details see Appendix B). The estimated surface energy, γ_S, calculated from the partial surface energies as well as Zisman's critical surface energy for wetting are given in Table 3.

TABLE 3. ESTIMATED SURFACE ENERGIES OF THE POLYMERIC MATERIALS OF THE BARRIER FABRICS

Polymer	γ_C	γ_S^D	γ_S^P	γ_S
Rayon	>72			
PBI	40	23	22	45
PET	40	27	11	38
Polypropylene	26	27	0.4	27

Fowkes[15] has pointed out the incorrectness of predicting hydrogen bonding with a geometric mean expression. Further polar interactions derived from Lewis donor-acceptor interactions will be very dependent on the system under consideration. Very small polar interactions will result if the liquid and the solid are both acidic or both basic while a large polar interaction will exist when one is a donor and the other an acceptor. Fowkes, therefore, suggested that Drago's correlation of treating the interactions based on only dispersion forces and acid-base interactions is correct. He proposed for the work of adhesion:

$$W_{ADH} = 2\sqrt{\gamma_A^D \cdot \gamma_B^D} + f(C_A C_B + E_A E_B) \cdot$$

$$x \frac{\text{moles of acid-base pairs}}{\text{unit area}} + W_A^P \tag{3}$$

where:

f = a constant

C_A, E_A = Drago's parameters for the acid

C_B, E_B = Drago's parameters for the base strength

W_A^P = Dipole-dipole interaction forces

Experiments showed that W_A^P is negligibly small. The determination of acid-base interactions is regarded as very important in modern adhesion studies.

Drago's E and C parameters have been determined only for a limited number of liquids. Kamlet and Taft have shown that many solvent-solute interactions can be accurately described by linear energy relationships of the generalized form[16].

$$SP = SP_0 + \text{cavity term} + \text{dipolar term} + \text{hydrogen bonding term(s)} \qquad (4)$$

$$SP = SP_0 + A \, (\delta^2)_1 \overline{V}_2 + B \cdot \pi_1^* \cdot \pi_2^* + C \cdot \alpha_1 \cdot \beta_2 + D \cdot \alpha_2 \cdot \beta_1 \qquad (5)$$

where the SP_0 A, B, C and D are constants and the solvatochromic parameters π^*, α and β are an index of solvent dipolarity/polarizability, measure of hydrogen bond donor (acidity) and hydrogen bond acceptor (basicity) respectively. δ is the Hildebrand solubility parameter and $\overline{V}_2$ is the solute molar volume. Published data of these parameters exist for more than 250 liquids.

Combining the approaches of Fowkes and Kamlet and Taft we have analyzed the wettability data according to the relationship.

$$W_{ADH} = \gamma_{LV}(1 + \cos \theta) + \pi_e = \text{const.} + p \cdot \pi_L^* + a \cdot \beta_L + b \cdot \alpha_L \qquad (6)$$

where p, a and b are constants characteristic for the dipolarity/polarizability, hydrogen bond donor and hydrogen bond acceptor properties of the polymer. In the first approach we assumed π_e to be negligibly small for all liquids.

The multiple linear regression analysis was performed using an all possible subsets regression program from BMDP Statistical Software, Inc. Very poor correlations were obtained when all 25 liquids used in the wettability studies were included. The best subset for the different fiber materials are given in Table 4. Further analysis has allowed an understanding of this poor correlation. The work of adhesion as determined from wettability data (Equation 6) will only depend on interactions between the liquid and the solid in the case of liquids which exhibit a contact angle larger than zero. In the case of zero contact angle, the work of adhesion becomes equal to the work of cohesion of the

22

liquid $(2 \cdot \gamma_{LV})$ which cannot be expected to correlate to interaction forces involving the solid. Limiting the liquids used in the linear regression analysis to those having a surface tension close to or larger than the estimated surface energy of the polymer proved to give very good correlations for PBI and PET, slightly less for polypropylene. All three polymers show interactions caused by dipolarity/polarizibility to be dominating. The PBI showed a higher basicity than the PET which would be expected from a structural point of view.

Linear regression analysis of the work of adhesion as function of the partial solubility parameters gave poorer correlations than those reported in Table 4 for cases of limited number of liquids.

4.2 Acid/Base Properties Of The Fibers

Inverse gas chromatography (IGC) is of great value in studies of various polymer-solvent interactions[17] and has been used for characterizing the acid/base properties of polymers[18]. The polymer is used as the stationary phase and small amounts of volatile solutes are injected as molecular "probes" in the IGC experiments. The polymer can be either coated onto a standard stationary phase, ground up into a powder, chopped up into small pieces or loaded as intact fibers. The IGC experiment has several advantages over wettability studies for investigations of polymer-solvent interactions. Very small volumes of the liquids are used and no exposure to the surrounding is needed. The polymer can be in any shape. The variable shapes of natural fibers make them difficult to study by wettability methods. Finally, a direct measure of the interaction energies is obtainable. We decided to see if IGC studies could be used as an alternative to wettability studies for an estimate of specific polymer-solvent interactions. We decided to start with the determination of the acid/base properties of the polymers using t-butyl alcohol as the acidic probe, n-butylamine as the basic probe and n-heptane as a neutral probe[18]. The interaction of other neutral probes were also studied in order to get a feel for boiling point effects. The columns were loaded with intact fibers[19] in order to minimize end effects. It was our original intention to study all solvents for one of the polymers by IGC and to determine the correlation between the IGC data and the wettability data. However, the IGC experiments were not as straight forward as expected from literature and the influence of several experimental variables had to be established (see Appendix C).

The retention volume of the probes were determined at 30, 60 and 90°C and the results analyzed to give an estimate of the interaction enthalpy between the probe molecules and column packings. (Higher temperatures 75, 90 and 105°C were needed in case of the PP column.) The results of the IGC investigation (Table 5) showed the PBI column to be distinctively acidic and the PET column to be basic. The rayon and PP columns were slightly acidic. The acidity of the PBI as determined by IGC is

23

TABLE 4. BEST SUBSET FROM LINEAR REGRESSION ANALYSIS OF THE WETTABILITY DATA CORRELATED TO KAMLET AND TAFT SOLVATOCHROMIC PARAMETERS ACCORDING TO THE RELATIONSHIP

$$W_{ADH} = \gamma_{LV}(1 + \cos\theta) = CONST. + p\cdot\pi_L^* + a\cdot\beta_L + b\cdot\alpha_L$$

Polymer	Selected Liquids	const.	p	a	b	R²	R
Rayon	All 25	29.3	62.7	-23.6	23.3	0.58	0.76
PBI	All 25	29.2	49.8	0	0	0.56	0.75
PET	All 25	17.7	-15.0	0	6.3	0.50	0.70
Polypropylene	All 25	1.2	-0.6	0	-0.4	0.55	0.74
PBI	$\gamma_{LV} \geq \gamma_c, \gamma_s$ (10)	6.1	77.0	0	18.7	0.95	0.97
PET	$\gamma_{LV} \geq \gamma_c, \gamma_s$ (10)	14.7	69.4	0	6.5	0.90	0.95
Polypropylene	$\gamma_{LV} \geq \gamma_c, \gamma_s$ (12)	29.2	38.9	0	-4.0	0.74	0.86

TABLE 5.	RELATIVE INTERACTION ENTHALPIES AS DETERMINED BY IGC			
Probe	Relative Interaction Enthalpy $(-\Delta H/R)$			
	Rayon	PBI	PET	PP
n-Butylamine	38.3	103.9	4.6	165.8
t-Butanol	28.1	31.7	9.1	117.4
n-Heptane	21.6	38.7	10.0	224.9

in contrast to the result of the linear regression analysis using Kamlet and Taft's solvatochromic parameters. One possible explanation to the difference is the different water content of the fibers in the two types of experiments. The wettability studies as well as the penetration studies were performed with fibers containing the equilibrium amount of water regain. This water is most probably lost during the IGC experiment. The "acidity" of the PP column reflects most probably a difference in the interaction between a branched and straight hydrocarbon chain with the polypropylene.

4.3 Fabric Characterization

All four barrier fabrics were made in plain weave from staple yarn but it was not possible to obtain fabrics with the same total denier of the yarn and denier per fiber. Photomicrographs of the four barrier fabrics and the receiver fabric are shown in Figures 10-14. It is evident from the photomicrographs that the PET barrier fabric had the largest transplanar openings and the polypropylene the smallest of the barrier fabrics. The rayon and PET barrier fabrics are the most similar in construction. The light transmittance through the fabric gives an estimate of the level of continuous transplanar pores. The transmittance, i.e., the percent of area open to passage of light shone at 90° angle to the fabric surface was determined by image analysis for the four barrier fabrics and the results are given in Table 6 as well as the measured thickness of the fabrics.

The fabrics were also submitted to the Textile Research Institute (TRI) for the determination of air permeability, spontaneous water up-take and pore size distribution. The air permeability was obtained using a Frazier instrument and driving pressure of 0.5 inches of water. The spontaneous water up-take was measured by the TRI method using a 1% aqueous nonionic surfactant (Triton X-100) solution[20] and the pore size distribution data by the TRI extrusion method with the same surfactant solution[21]. The results are given in Table 7.

The transplanar pores observed in the photomicrographs with light shone through the fabrics agree in size with the larger pores determined by the TRI extrusion method for the PBI and rayon fabrics. However, the very large pore observed in the PET
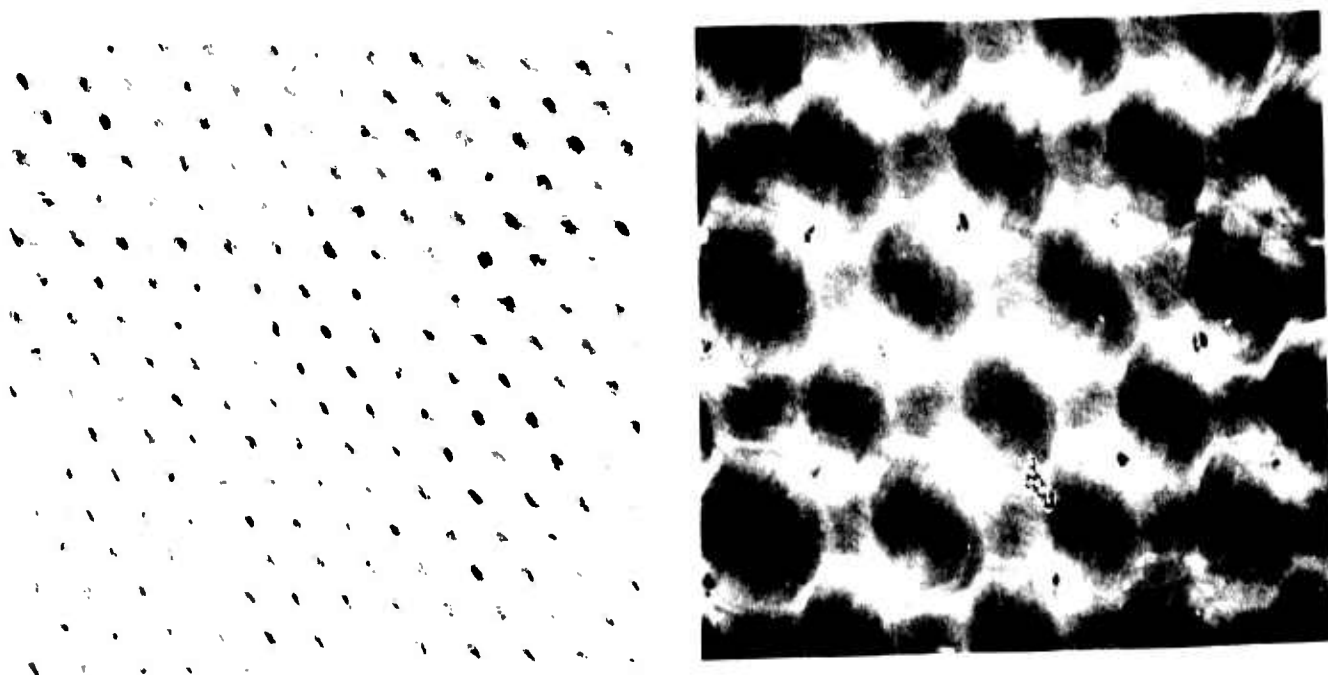
FIGURE 10. PHOTOMICROGRAPHS OF RAYON BARRIER FABRIC. REFLECTED LIGHT, 12X (LEFT); TRANSMITTED LIGHT, 40X (RIGHT)
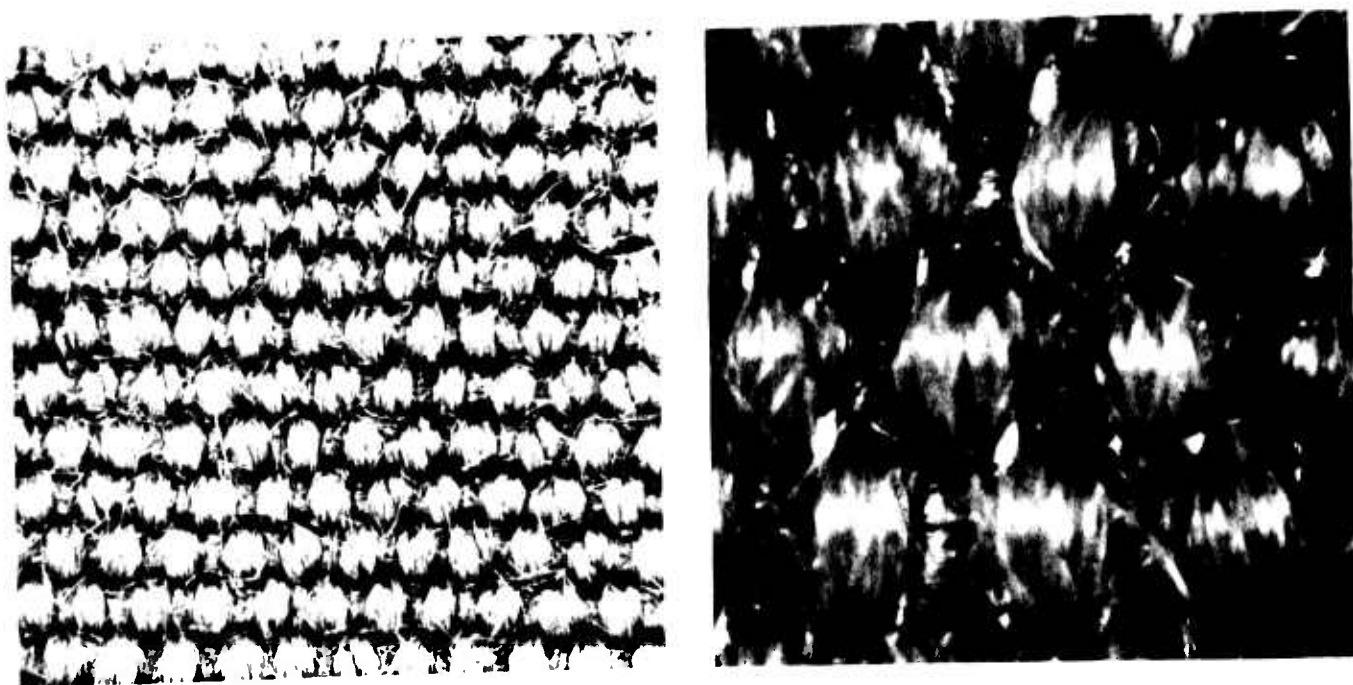
FIGURE 11. PHOTOMICROGRAPHS OF PBI BARRIER FABRIC. REFLECTED LIGHT , 12X (LEFT); TRANSMITTED LIGHT, 40X (RIGHT)
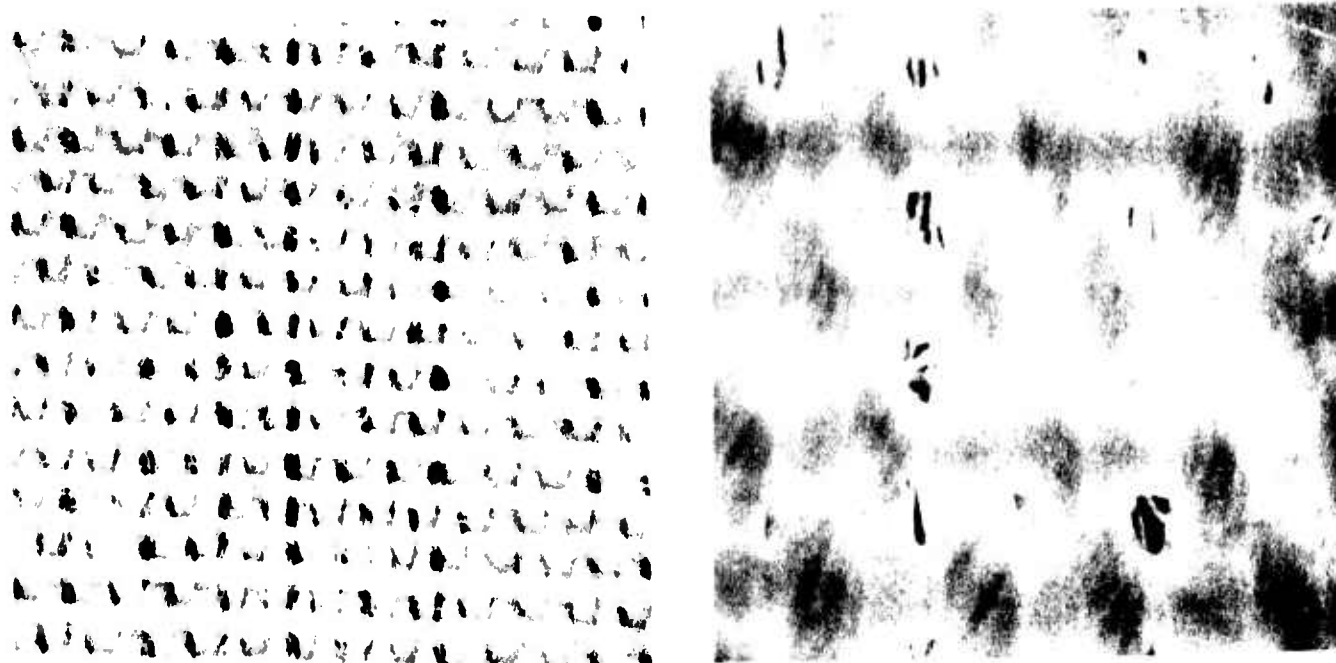
FIGURE 12.   PHOTOMICROGRAPHS OF PET BARRIER FABRIC.   REFLECTED
LIGHT, 12X (LEFT); TRANSMITTED LIGHT, 40X (RIGHT)
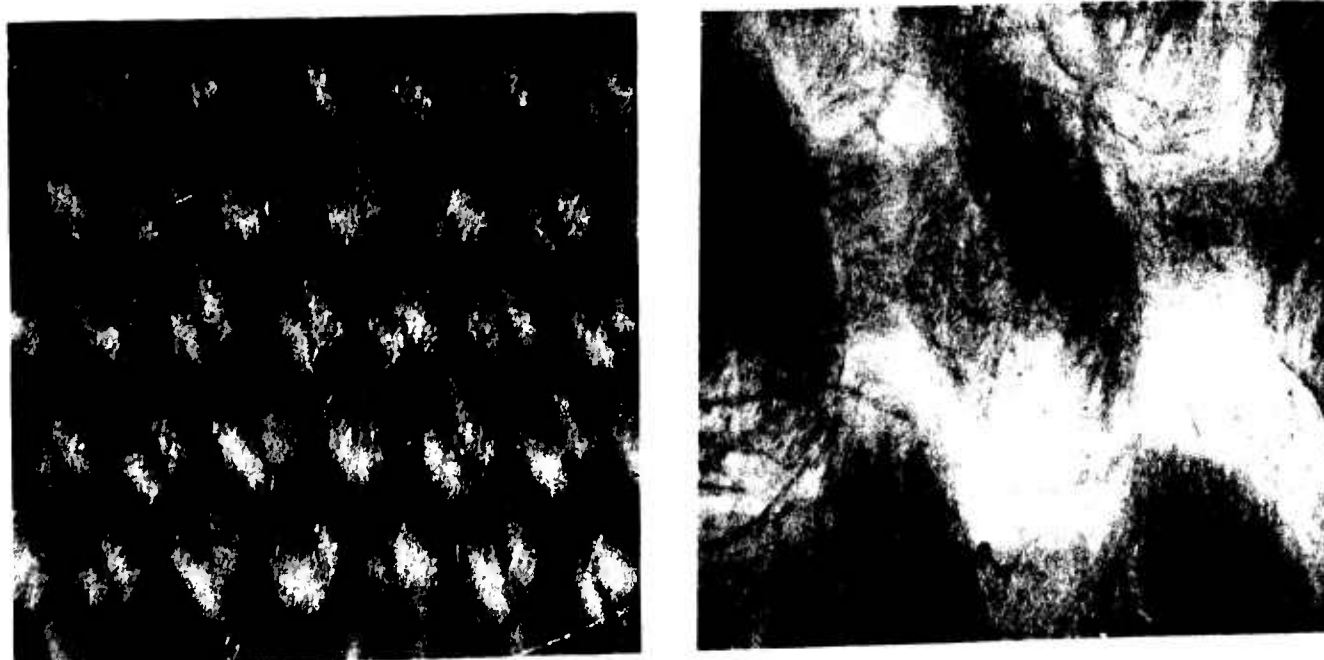
FIGURE 13.   PHOTOMICROGRAPHS OF PP BARRIER FABRIC.   REFLECTED
LIGHT , 12X (LEFT); TRANSMITTED LIGHT, 40X (RIGHT)
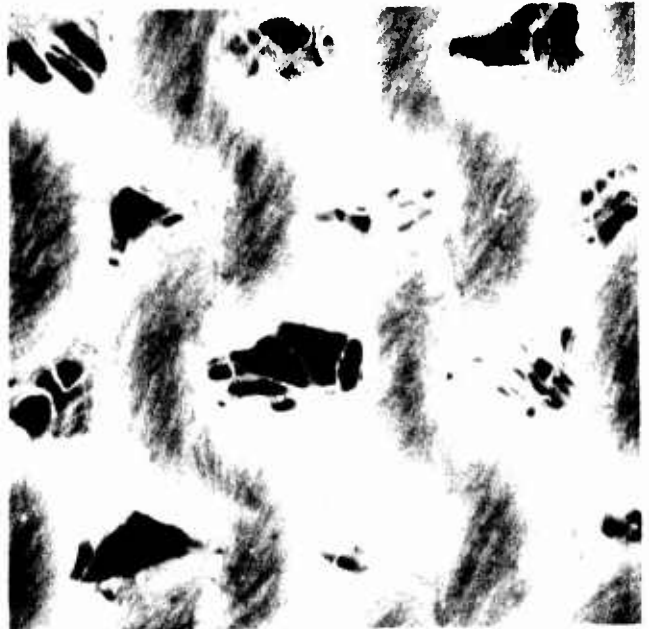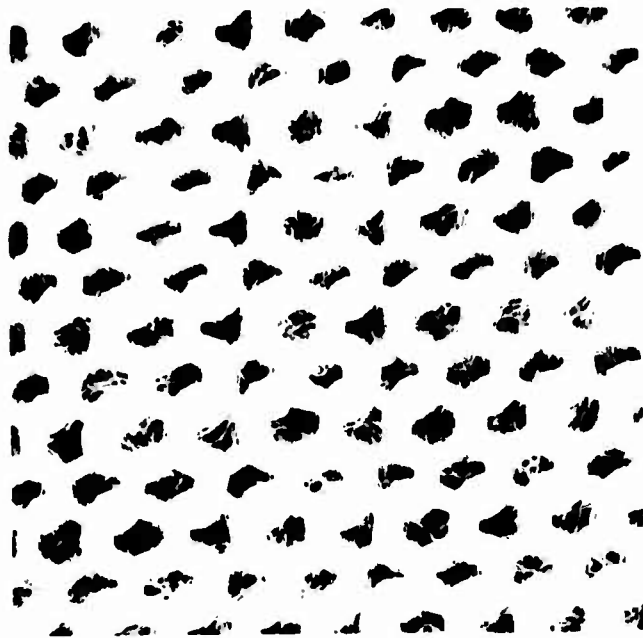
FIGURE 14. PHOTOMICROGRAPHS OF THE FRONT AND BACK SIDES OF
PET/COTTON RECEIVER FABRIC. REFLECTED LIGHT, 12X
(LEFT); TRANSMITTED LIGHT, 40X (RIGHT)

TABLE 6. FABRIC PROPERTIES

Barrier Fabric	% Light Transmittance	Thickness, mm
PBI	0.5	0.62
Rayon	0.2	0.64
PET	1.0	0.59
PP	0.0	0.97

TABLE 7. FABRIC PROPERTIES DETERMINED BY TRI

Fabric	Air Permeability $ft^3/ft^2/min$	Spontaneous Rate $mg/s/cm^2$	Uptake Total mg/cm^2	Pore Size Distribution Prevalent Pore Sizes μm
PBI	7.1	0.81	19.8	5, 55
Rayon	20.8	1.96	19.3	3, 53
PET	65.9	0.15	7.5	5, 55
PP	32.8	0.58	28.0	9, 76
PET/ Cotton	408	3.67	20.0	5, 60

fabric (Figure 12) are evidently not detected by this method. Although no continuous transplanar pores were observed by light transmission for the PP fabric, the TRI method implied interyarn spaces with an average size of 76 μm. This would also agree with the high air permeability for this fabric. The smaller of the prevalent pore sizes are generally ascribed to intrayarn spaces.

4.4 Penetration Studies

The penetration studies were performed by Celanese Fibers Operations with a constant barrier-receiver contact pressure of 50 cm water for a duration of 20 seconds. The delivery of a constant liquid drop was practiced by measuring the weight delivered to a filter paper for at least 10 drops. It was assumed that the same amounts were delivered under the actual experimental conditions to the barrier fabrics. The calculated percentages of liquid penetrated are given in Table 8. The observed average weights, standard deviations and general observations are given in Appendix A, Tables A-10 through A-13. The PET barrier fabric showed the highest degree of penetration and the polypropylene barrier fabric the lowest one. The relative ranking of the different liquids was, however, surprisingly independent of the type of barrier fabric.

29

TABLE 8. PERCENT LIQUID PENETRATED AFTER 20 SECONDS CONTACT
THROUGH THE BARRIER FABRICS INTO THE RECEIVER MATERIAL
CALCULATED FROM PENETRATION STUDIES PERFORMED AT
CELANESE FIBERS OPERATIONS.

Liquid	Rayon %	PBI %	PET %	Polypropylene %
Water	11	83	4	2
Dimethylsulfoxide	38	47	100	50
N-Methyl-2-Pyrrolidone	55	41	100	50
Dimethylacetamide	51	41	89	43
Diethylmalonate	57	30	99	43
Triethylphosphate	47	40	74	35
Formamide	30	38	94	23
Acetic Acid	59	33	75	30
Hexadecane	37	39	91	23
Ethylene Glycol	37	33	56	1
Ethanol	36	32	61	16
Propanol	35	19	37	12
Methylene Iodide	26	12	93	31
Pyridine	16	25	49	21
Methanol	19	26	21	2
Acetonitrile	6	4	49	3
1,2 Dichloroethane	3	1	50	4
t-Butylamine	11	0	8	5
Diisopropylether	7	0	3	4
Cyclohexane	4	1	7	4
4-Methyl-2-Pentanone	6	1	7	1
2-Butanone	4	2	7	3
Ethylacetate	3	1	6	3
Dichloromethane	2	1	5	3
Toluene	1	0	7	3

A restudy of the penetration behavior of pure liquids was performed using the very careful control of all experimental parameters found to be necessary. The penetration time of 20 seconds was kept although time studies showed the penetration to be very fast and to occur within the first seconds. The liquids were chosen among the original set of liquids to represent a wide range of physico-chemical properties. The most volatile liquids were omitted. Only acetonitrile and 1,2-dichloroethane showed significant evaporative losses (10-20% weight loss in 10 seconds). Liquids with boiling points above 150°C showed no weight loss during 1 minute's study. The average delivered weight of liquid, its standard deviation and the average amount of liquid penetrated into the receiver material and its standard deviations are given in Appendix A, Tables A-14 through A-17. The calculated percent liquid delivered of a 50 µL drop by light contact to the barrier fabric is given in Table 9. Liquids which had shown advancing contact angles larger than 60° were not transferred to the barrier fabric. It is evident from Table 9 that although a constant size of a liquid drop was contacted with

the fabric the amount actually transferred showed large
variations. Especially the liquids with both a low surface
tension a a low viscosity delivered much less than the desired 4
mm drop.

The calculated percentages of penetrated liquid after 20
seconds contact are given in Table 10. The PET fabric shows
again the highest level of penetration. However, the rayon
fabric showed considerable penetration for all liquids but
water. It was observed that the water drop transferred extremely
fast from the capillary onto the rayon where it wicked out to
cover a large variable area. The polypropylene fabric was not
wetted by the drops of four of the liquids. It showed in general
the lowest penetration of the four barrier fabrics. The PBI
barrier fabric showed least penetration of the two simulants
diethylmalonate and triethylphosphate. Acetonitrile was the
liquid which showed the highest penetration through all barrier
materials in average. It was, however, also a liquid with a
small volume transferred.

TABLE 9. PERCENT LIQUID DELIVERED OF A 50 μ L DROP BY LIGHT
CONTACT TO THE BARRIER FABRIC IN THE PRESENCE OF A
BARRIER-RECEIVER CONTACT PRESSURE OF 50 CM WATER.

LIQUID	γ_{LV} DYN/CM	η CPS	RAYON %	PBI %	PET %	PP %
Water	72.6	0.891	80	86	-	-
Formamide	58.0	3.30	82	84	89	-
Ethylene Glycol	47.8	13.50	85	86	88	-
Dimethylsulfoxide	43.3	2.00	69	75	70	-
Pyridine	36.7	0.88	46	48	44	77
1,2-Dichloroethane*	32.2	0.73	23	22	21	41
Diethylmalonate	31.5	1.94	50	56	48	69
Triethylphosphate*	29.7	1.70	48	47	46	63
Acetonitrile	28.6	0.33	30	35	24	56
Toluene	28.1	0.56	32	35	31	43
Hexadecane	27.2	3.34	72	70	75	74
Acetic Acid	26.6	1.04	32	27	33	44
Propanol	23.6	1.72	52	54	46	62
4-Methyl-2-Pentanone	23.6	0.54	35	24	22	30

*45 μl drops

31

TABLE 10. PERCENT LIQUID PENETRATED AFTER 20 SECONDS CONTACT
THROUGH THE BARRIER FABRICS INTO THE RECEIVER
MATERIAL CALCULATED FROM PENETRATION STUDIES
PERFORMED AT CELANESE RESEARCH COMPANY USING A
REVISED PROCEDURE.

LIQUID	RAYON %	PBI %	PET %	POLYPROPYLENE %
Water	26	57	–	–
Formamide	55	79	84	–
Ethylene Glycol	62	57	80	–
Dimethylsulfoxide	58	43	70	–
Pyridine	63	39	82	51
1,2-Dichloroethane	67	31	66	19
Diethylmalonate	55	38	74	40
Triethylphosphate	71	36	60	48
Acetonitrile	80	46	78	53
Toluene	69	30	66	23
Hexadecane	66	44	72	32
Acetic Acid	72	45	71	38
Propanol	66	35	77	23
4-Methyl-2-Pentanone	62	43	74	24

5. DISCUSSION

5.1 Capillary Flow

The driving force for liquid flow in a capillary is determined by the capillary pressure,

$$\frac{2\ \gamma_{LV}\ \cos\theta_a}{r_i} \tag{7}$$

where

γ_{LV} = surface tension of the liquid
θ_a = advancing contact angle
r_i = radius of the capillary

and the hydrostatic pressure

$$\rho g l \tag{8}$$

where

ρ = density of the liquid
g = gravitational acceleration
l = distance of liquid flow into the capillary

The general theory for the capillary flow is described by Washburn's equation:

$$\frac{dl}{dt}\ =\ \frac{r_i{}^2}{8\eta\,l}\ \left(\frac{2\ \gamma_{LV}\ \cos\theta_a}{r_i}\right)\ \pm\ \rho g l \tag{9}$$

32

where

    t = time
    η = viscosity of the liquid
    - = for capillary rise
    + = for capillary down flow

The contributions from the hydrostatic pressure are generally regarded negligibly small for the movement of a limited liquid volume as a small drop in a fabric. This reduces Washburn's equation to:

$$\frac{dl}{dt} = \frac{1}{4} \cdot \frac{\gamma_{LV} \cdot \cos\theta_a}{\eta} \cdot \frac{r_i}{l} \qquad (10)$$

An integration gives:

$$l = \left(\frac{\gamma_{LV} \cdot \cos\theta_a}{\eta} \cdot \frac{r_i}{2} \right)^{1/2} \cdot t^{1/2} \qquad (11)$$

or

$$V = \pi \left(\frac{\gamma_{LV} \cdot \cos\theta_a}{2\eta} \right)^{1/2} \cdot r_i^{5/2} \cdot t^{1/2} \qquad (12)$$

The Washburn equation thus predicts that the flow rate will be much faster into the large capillaries than into the small ones and that most of the liquid will be absorbed into the large pores originally. However, when all of a liquid drop is absorbed into capillaries, the pressure gradient due to size differences of the capillaries will lead to liquid flow from the larger capillaries (j) into the smaller ones (i).

$$\Delta P_{ij} = \frac{2\gamma_{LV} \cdot \cos\theta_{ai}}{r_i} - \frac{2\gamma_{LV} \cdot \cos\theta_{rj}}{r_i} \qquad (13)$$

where

    ΔP_{ij} = pressure gradient for capillaries i and j
    θ_{ai} = advancing contact angle of small capillary i
    θ_{rj} = receding contact angle of large capillary j

Only very large contact angle hysteresis would prevent this redistribution of liquid. The Washburn relation also predicts that a liquid with a large penetrating power or driving force, $\gamma_{LV} \cos\theta/\eta$, will show a higher flow rate than one with a small one. Capillary flow should occur for all liquids which have an advancing contact angle less than 90°. However, analysis of the wetting through of fabrics shows that the non-cylindrical capillaries of a fabric will lead to an opposing pressure for

contact angles less than 0°[23]. Break through would thus occur only if the hydrostatic pressure of the drop is larger than this pressure.

The final distribution of liquid between the barrier fabric and the receiver fabrics should be a function of the flow rate in the capillaries of both materials. The applied drop will experience the finer intrayarn capillaries, the larger interyarn capillaries at yarn cross-over points as well as the transplanar pores. Some liquid will enter all of these capillaries but the fastest transport and the largest volume will be in the transplanar pores. The transfer rate of liquid to the receiver material will depend on the properties of the capillaries between the two materials which will be a function both of the materials and of the contact pressure. Maximal penetration should result when the rate of penetration into the receiver material is larger than that of planar wicking in the barrier fabric.

5.2 Experimental Results

Most of the liquids used in the present study have densities within the range of 1.0 ± 0.2 g/cm^2. The only liquid with a significant larger density was the methylene iodide (Appendix A, Table A-1). The open transplanar pores of the PBI, rayon and PP were of the order of 50 μm or less. Calculations show that contributions from the hydrostatic pressure to be negligible compared to the capillary force for these barrier fabrics. The PET barrier fabric has much larger transplanar pores and the contribution from the hydrostatic pressure of the drop will be significant. Both the larger pore size and the hydrostatic pressure will thus contribute to the higher penetration observed for the PET fabric especially in the case of the dense methylene iodide. The somewhat lower penetrations observed for the polypropylene barrier fabric might also be related to the construction. The denier of the polypropylene staple yarn is thus much higher than the other yarns. This leads to much fewer transplanar pores per unit area (e.g., compare Figures 12 and 13) and to a thicker fabric (Table 6) i.e., longer path length of diffusion to the receiver.

The penetration data were first analyzed to see if the penetration was governed by Washburn's equation. The percent penetrated liquid was thus plotted against the driving force $\gamma_{LV} \cos \theta / \eta$ as determined from the wettability studies (Appendix A, Tables A-2, A-4, A-6 and A-8) (Figure 15). Liquids with a high driving force showed, in general, a low penetration, although Washburn's equation predicted the highest transport rates through the larger transplanar pores for these liquids. Planar wicking within the finer intrayarn pores appeared to dominate for these liquids i.e., the transfer of liquid into the finer pores caused by their higher capillary pressure was taking place.

A three dimensional representation in the form of contour maps of the penetration data was next made for the PBI and PP

34
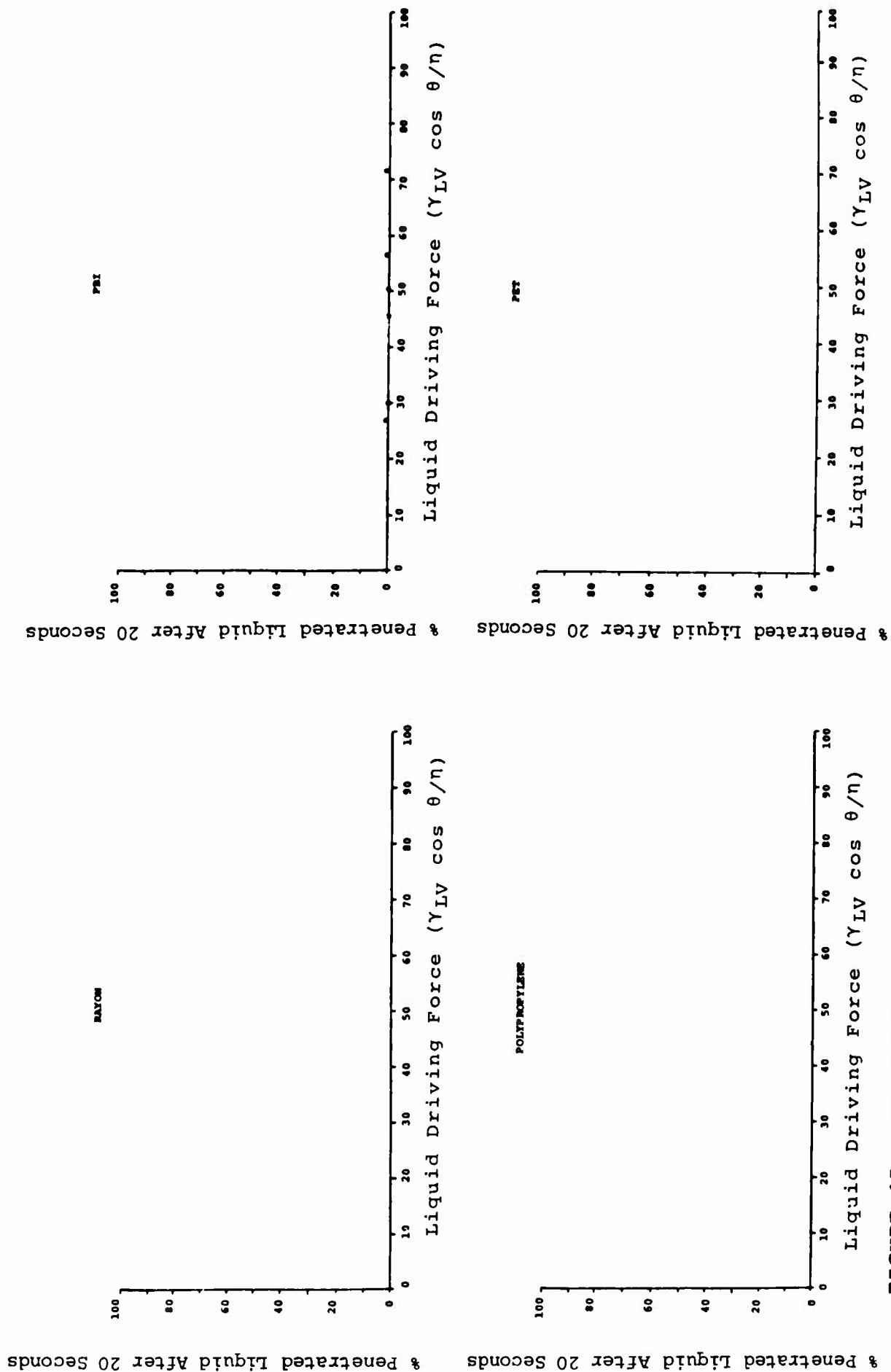
FIGURE 15. ANALYSIS OF OBSERVED PENETRATION RATES AS FUNCTION OF THE PENETRATION POWER ACCORDING TO WASHBURN'S EQUATION FOR CAPILLARY FLOW

barrier fabrics in an attempt to separate the effect of the capillary force assuming constant pore radii and the viscous drag (Figure 16). The contour maps implied that the viscosity of the liquids was the determining factor for the penetration. Low penetration was observed for liquids with an inverse viscosity larger than 1.1 or a viscosity less than approximately 1 cps. It thus appeared that extensive planar wicking took place only for liquids with a very low viscosity although general capillary theory for a limited liquid volume predicts the wicking in the fine intrayarn capillaries to become the dominating transport mechanism for all liquids which do not show high contact angle hysteresis. Mainly, water, ethylene glycol and formamide showed significant contact angle hysteresis. A plausible explanation was the fact that the intrayarn capillaries of a staple yarn will show large variability in diameter, especially at yarn cross over points when the fabric is under tension due to an applied pressure across the fabric. An analysis of a simplified model system such as a corrugated tube shows that the viscous friction losses caused by tube diameter variations can qualitatively explain the observed viscosity dependence for the planar wicking and thus the penetration.

However, the subsequent penetration studies showed these results to be an artifact. The explanation is that the organic liquids with a low viscosity exhibited low degrees of transfer to the barrier fabric under the experimental conditions (Table 9). They also had comparatively low boiling points. Thus, considerable evaporation took place during the experiments, especially when performed in a fume hood.

All liquids but for dichloroethane and triethylphosphate formed stable 50 µL drops at the end of the glass capillary used to deliver the liquids to the fabric. The shape of the drops was very similar for all liquids. Analysis showed that the primary physico-chemical properties determining how much of the drops were transferred, were the contact angle and the viscosity. Secondary factors were the surface tension and the density of the liquid. Liquids with an advancing contact angle larger than approximately 60° did not transfer at all (Table 9, Appendix A, Tables A-2, A-4, A-6, and A-8). They did not penetrate when sheared off into the fabric. Liquids which gave contact angles in the range of 40-60° with some of the barrier fabric materials and with other materials 0°, appeared to transfer more under the poorer wetting conditions. A contact angle less than 90° was thus not enough for the liquid to enter the pores of the fabric. Evidently, the irregular shape of the pores of a fabric and the resulting changes in the capillary pressure with the position of the liquid front[23] caused too high a resistance to be overcome by the hydrostatic pressure of the drop in the case of systems with a contact angle larger than 60°. This is true even in the case of the PET fabric with its comparatively large transplanar pores.

Previous investigations had shown[6], that the degree of penetration depended on the drop volume. Plots of the percent liquid penetrated vs. the percent liquid transferred showed a

36
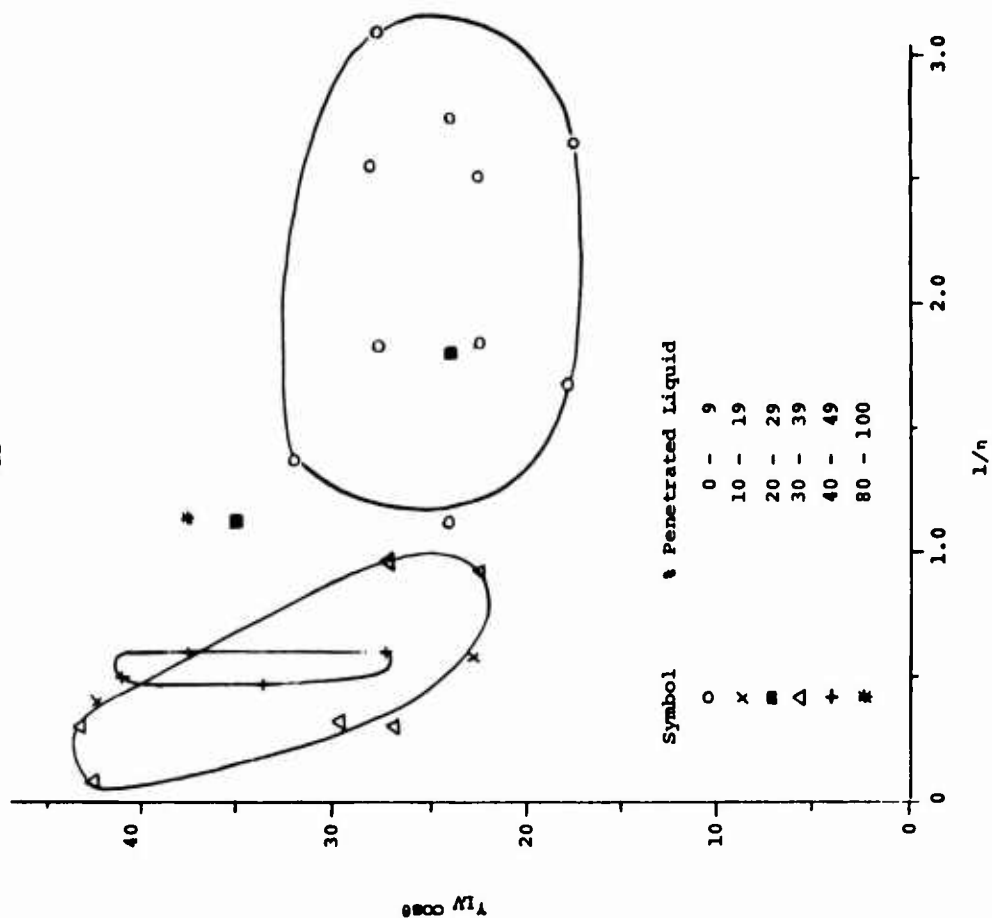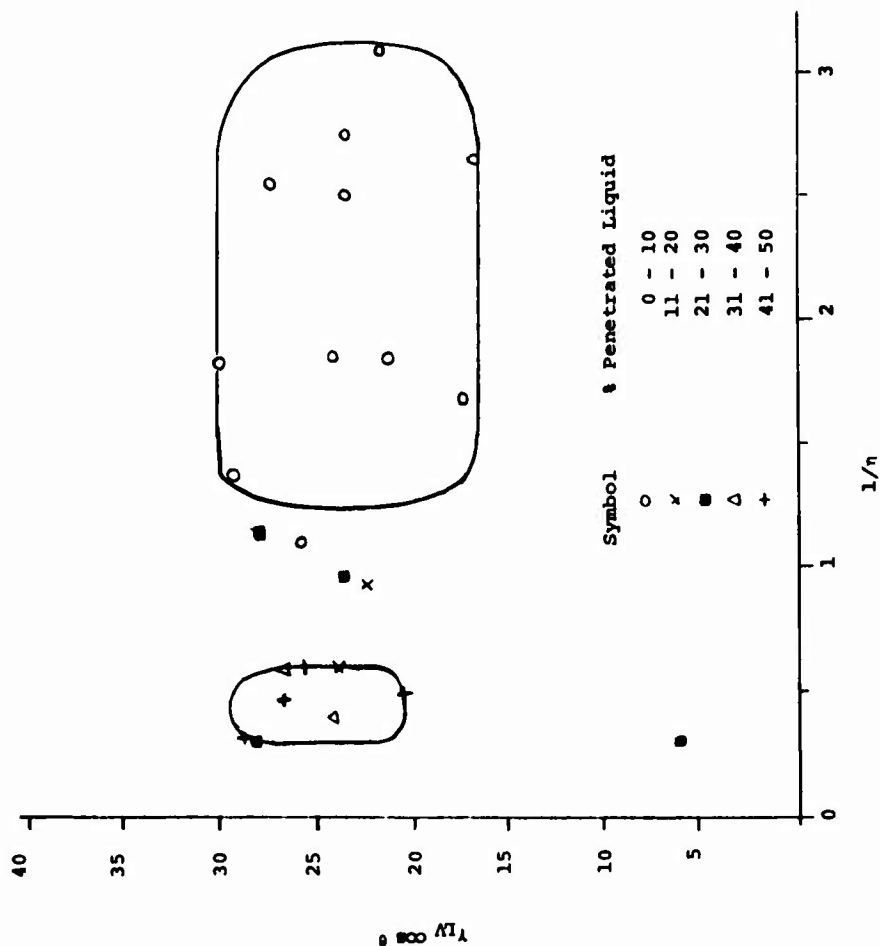
FIGURE 16. CONTOUR MAP OF PENETRATION DATA AS FUNCTION OF CAPILLARY DRIVING FORCE ($\gamma_{LV} \cdot \cos\theta / \Sigma r_i = $ const. $\gamma_{LV} \cdot \cos\theta$) AND VISCOUS DRAG ($1/\eta$) FOR THE PP AND PBI BARRIER MATERIALS

weak trend of increase for PBI, PET and polypropylene and of decrease for rayon. The drop volume did not govern the degree of penetration for any of the barrier fabrics.

The thickness of the barrier fabric as well as the pore size distribution will determine the length of the penetration path. It will also affect the maximum liquid volume that can be held by the fabric per unit area. The thickness of the rayon, PBI and PET fabric was approximately the same, while the polypropylene fabric was approximately 50% thicker (Table 6). The difference was also translated into the maximum free volume. More liquid should therefore be expected to be retained in the polypropylene fabric than the other fabrics. A comparison of the different barrier fabrics (Table 10) showed that the PBI fabric did not follow the expected behavior. The PBI fabric thus showed the highest relative retention. This had to originate from the physico-chemical properties of the PBI fibers since the construction of the rayon, PBI and PET fabric were similar. However, the PET fabric had comparatively large transplanar pores which might account for the high penetration of this fabric.

Analysis of the penetration data by Washburn's equation showed a poor correlation (Figure 17). The size of the capillary driving force thus appeared to have low impact on the relative amount of penetration. A partial explanation to this could be the fact that the capillary driving forces were determined from equilibrium wetting behavior while the penetration was shown to be very fast. The whole penetration process was completed within less than a second for most of the liquids. This would corre-spond to flow rates of the order of mm/sec. Deviations from the equilibrium advancing contact angle have been observed to start at a velocity as low as 0.8 mm/min for water and PET[24] and at cm/minutes for many systems[25]. Inverarity[25] studied the dynamic wetting of glass and polymer fibers plunging into a liquid. He found that a common master curve was obtained when the cosine of the dynamic contact angle was plotted against the logarithm of the product of the viscosity and the velocity for all liquid/solid pairs which had a zero advancing contact angle at equilibrium conditions. A low viscosity liquid thus retained its equilibrium contact angle at higher velocities than a liquid with a high viscosity. Significant changes in the contact angle was observed already at velocities of cm/min. Jing et al derived a correlation from experimental data for liquids with high viscosities which suggested that the dynamic contact angle could be calculated from the capillary number and the static contact angle. (The capillary number is the ratio of the viscosity forces to interfacial forces.) The calculated flow rates needed to cause significant changes in the advancing contact angle of liquids with low viscosities were orders of magnitude higher than those observed by Gillberg and Kemp[24] and Inverarity[25]. Further studies would be needed to determine if the spontaneous flow of a liquid due to capillary forces could lead to dynamic contact angles.

% Penetrated Liquid After 20 Seconds

Liquid Driving Force ($\gamma_{LV} \cos \theta /\eta$)

% Penetrated Liquid After 20 Seconds

Liquid Driving Force ($\gamma_{LV} \cos \theta /\eta$)

% Penetrated Liquid After 20 Seconds

Liquid Driving Force ($\gamma_{LV} \cos \theta /\eta$)

% Penetrated Liquid After 20 Seconds

Liquid Driving Force ($\gamma_{LV} \cos \theta /\eta$)
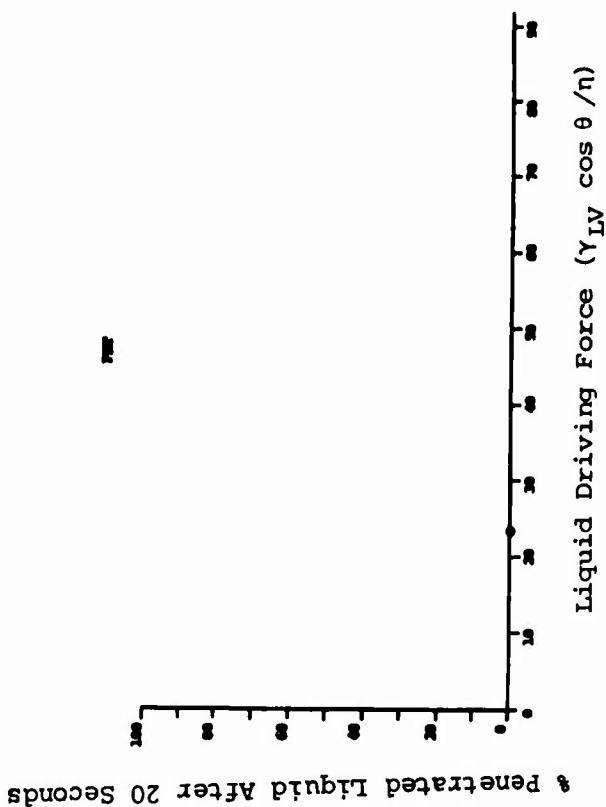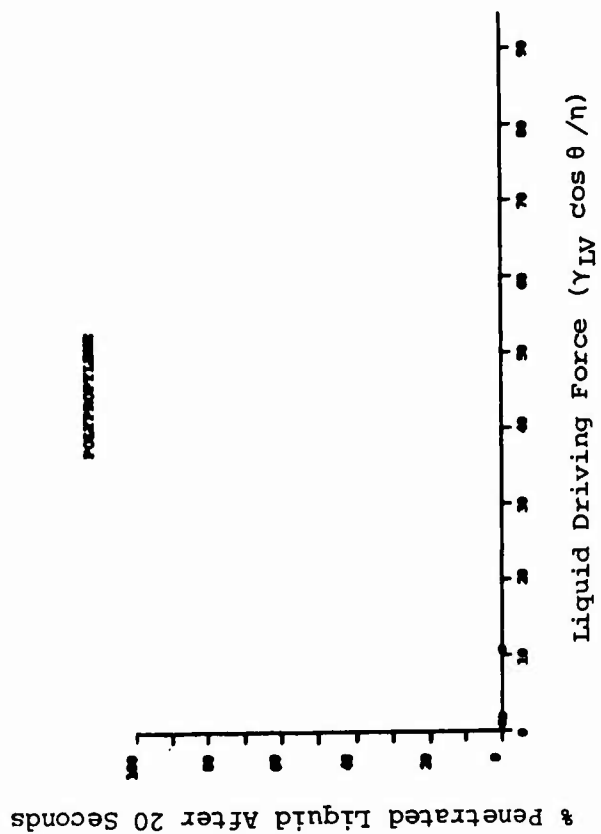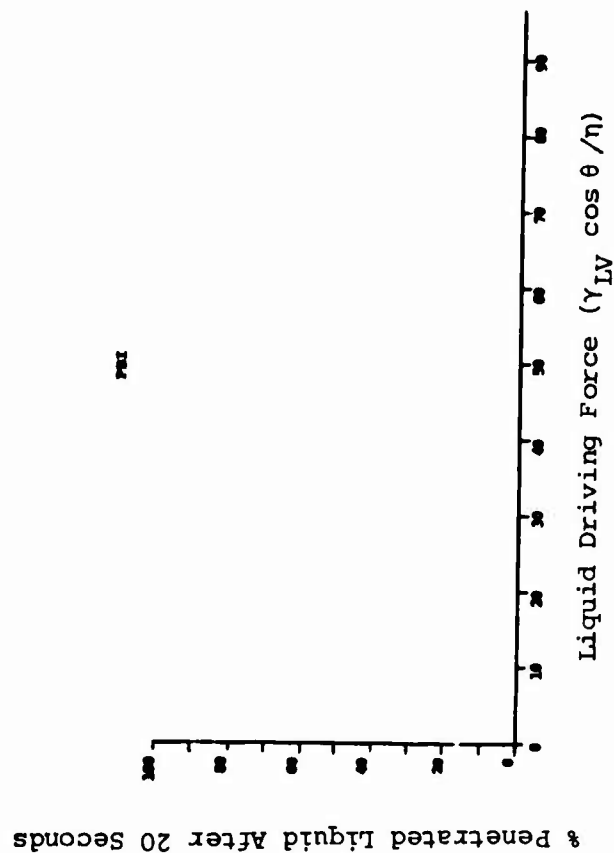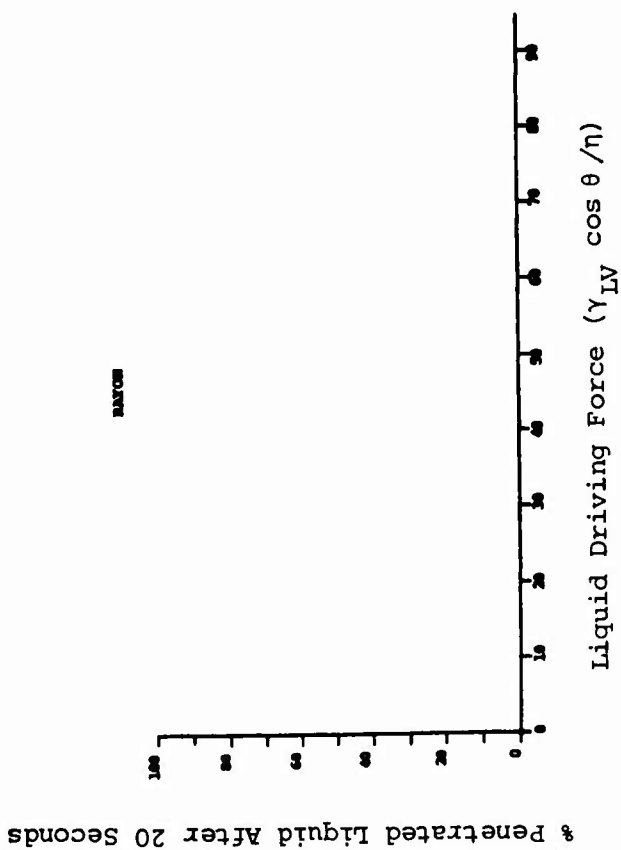
FIGURE 17.   ANALYSIS OF OBSERVED PENETRATION RATES AS FUNCTION OF THE PENETRATION POWER ACCORDING TO WASHBURN'S EQUATION FOR CAPILLARY FLOW

The very fast penetration process also meant that a redis-
tribution of liquid from the receiver to the barrier fabric
caused by differences in capillary pressure might have taken
place during the 20 seconds of experimental time. The possibil-
ity of redistribution was studied for a few liquids within the
time range of 2 seconds to 10 minutes. No redistribution of
these liquids were observed. The use of several receiver layers
might decrease the tendency of reversal although this was
observed by Miller and Perkins using the same experimental con-
ditions[6].

The relative fabric wettability, as described by the contact
angle, determined if a liquid would be transferred to the fabric
and thus the limit of zero penetration. The general analysis by
Clark and Miller of the resistance to flow in a fabric predicted
the resistance to be higher and also more sensitive to the
advancing contact angle for finer pores. A penetration of liquid
through the longer transplanar pores should thus be favored for
liquids which wetted the fabric but had high contact angles. A
plot of the relative amount penetrated liquid vs. the advancing
contact angle are given in Figure 18 for PBI, PET and polypropyl-
ene. A general trend of an increased degree of penetration with
increasing contact angle is observed as predicted.

All liquids except methylene iodide gave a zero advancing
contact angle with rayon due to its high surface energy (larger
than 70 dyn/cm). The rayon also showed high penetration for all
liquids except for water. The water was observed to wick out
very rapidly. The rayon fabric could be expected to show high
affinity to the water due to its hydroxyl rich surface and high
water regain (15%). Attempts to correlate the penetration data
of rayon with various physico-chemical parameters (the partial
solubility parameters, Kamlet and Taft's solvatochromic parame-
ters, surface tension) gave in all cases poor correlation. There
was a general trend to a higher degree of penetration with a
decreasing surface tension of the liquid i.e., an increasing
difference between the estimated surface energy of the fabric and
the surface tension of the liquid. Similar analysis for the
other three fabrics also gave poor correlations.
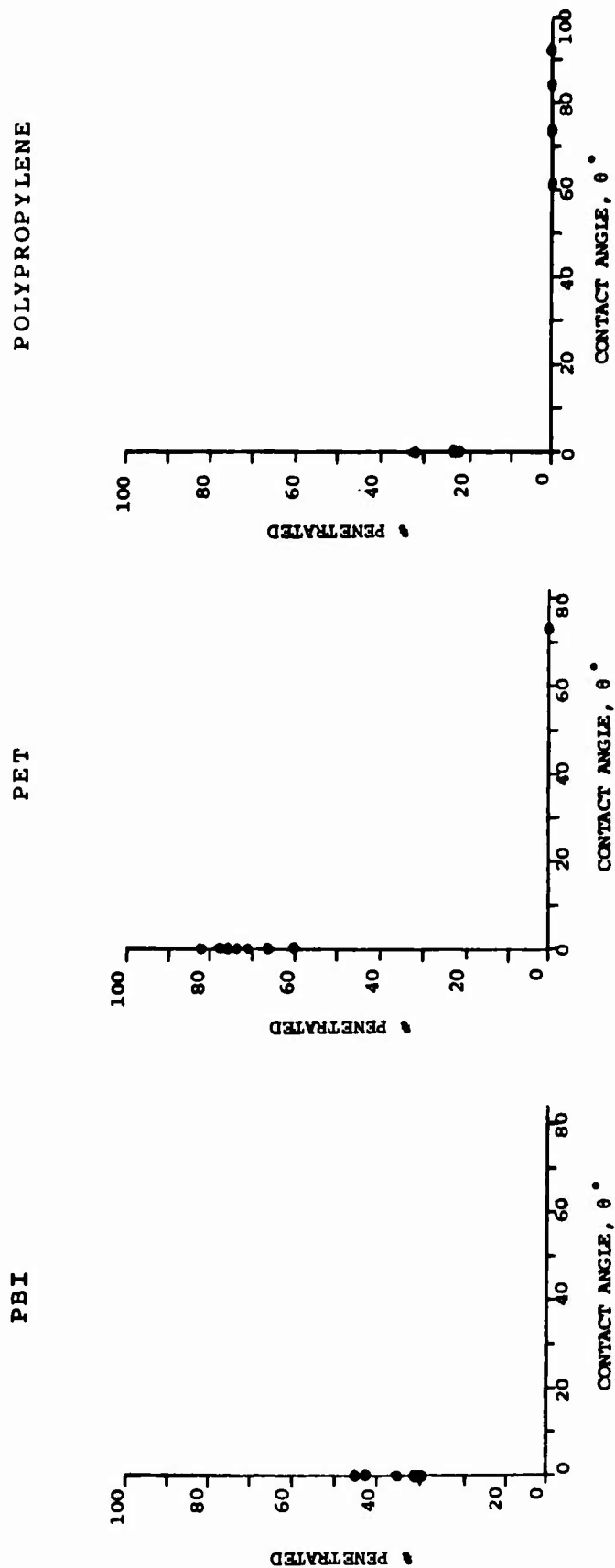
FIGURE 18. ANALYSIS OF OBSERVED PENETRATION RATES AS FUNCTION OF THE CONTACT ANGLE, θ°

41

SECTION 6. CONCLUSIONS AND RECOMMENDATIONS

a. The study of the penetration of pure liquids through a barrier fabric into a receiver fabric using the apparatus and the general procedure developed by B. Miller and H. K. Perkins under contract DAAK11-82-C-0143 shows that very careful control of all experimental parameters is essential for reliable and reproducible data to be obtained. The amount of liquid actually transferred to the barrier fabric by contacting a drop of constant size has to be determined under the experimental conditions since the volume transferred was shown to depend on the viscosity of the liquid, the wettability of the fabric by the liquid, the evaporation rate of the liquid and the contact pressure across the fabric and the receiver material.

b. The penetration process is very fast for pure liquids with viscosities less than 15 cps and takes place within a second. Differences in penetration rates cannot be determined with the procedure specified.

c. The fabric construction and its wettability control the penetration. The degree of penetration decreases with increasing fabric thickness and yarn crimp and with a decreasing size of the transplanar pores. Liquids will not wet (transfer and penetrate) the barrier fabric if their contact angle is larger than 60°. The degree of penetration will increase with an increase in the contact angle below 60°. Liquids with zero contact angle will generally show a higher degree of penetration the larger the difference in surface energy between the liquid and the solid. However, no good correlation has been found between the physico-chemical parameters of the liquid and the degree of pentration. The PBI barrier fabric shows a much higher liquid retention than expected from its construction and wettability.

d. The specific interaction between a liquid and a polymer as described by the work of adhesion can be modeled by a linear relationship using the solvatochromic parameters of Kamlet and Taft for liquid/polymer pairs which yield a finite contact angle.

e. Mixtures of liquids containing a very volatile component could drastically affect the penetration rate if large changes in wettability behavior results from the evaporation of the volatile component.

REFERENCES

1. Minor, F. W., Schwartz, A. M. Buckles, L. C. and Wulkow, E. A., *Am. Dyestuff Reptr.*, 49, 419 (1960).

2. Minor, F. W., Schwartz, A. M., Wulkow, E. A. and Buckles, L. C., *Textile Research J.*, 29, 931 (1959).

3. Minor, F. W., Schwartz, A. M., Wulkow, E. A. and Buckles, L. C., *Textile Research J.*, 29, 940 (1959).

4. Minor, F. W., Schwartz, A. M. Buckles, L. C. Wulkow, E. A., Marks, M. P. and Fielding, G. H., *Textile Research J.*, 31, 525 (1961).

5. Rader, C. A. and Schwartz, A. M., *Textile Research J.*, 3?, 140 (1962).

6. Miller, B. and Perkins, H. K., *Final Report Contract No. DAAK 11-82-C-0143*, Chemical Systems Laboratory, U.S. Army AMCCOM.

7. Kamlet, M. J., Abboud, J. L. M., Abraham, M. H. and Taft, R. W., *J. Org. Chem.*, 48, 2877 (1983).

8. Barton, A. F. M., *Handbook of Solubility Parameters and Other Cohesion Parameters*, CRC Press, Bora Raton, (1983).

9. Riddick, J. A. and Bunger, W. B., *Organic Solvents*, Wiley Interscience, New York, (1970).

10. Adamson, A. W., *Physical Chemistry of Surfaces*, Interscience Publishers, New York, (1967), Second Ed. p. 21.

11. Neumann, A. W. and Tanner, W. P., *Proc. 5th Int. Cong. Surf. Activity*, 2, 727 (1968).

12. Zisman, W. A., in *Contact Angles, Wettability and Adhesion*, Gould, R. F. Ed., Amer. Chem. Soc., Washington, (1964), p. 1.

13. Kaelble, D. H. and Uy, K. C., *J. Adhes*, 2, 50 (1970).

14. Owens, D. K. and Wendt, R. C., *J. Appl. Polym. Sci.*, 13, 1741 (1969).

15. Fowkes, F. M. in *Adhesion and Adsorption of Polymers*, Lee, L. H. Ed., Plenum, New York, (1980), Part A, p. 43.

16. Taft, R. W., Abboud, J. L. M., Kamlet, M. J. and Abraham, M. H., *J. Solution Chem.*, 14, 153 (1985).

17. Braun, J. M. and Gillet, J. E., in *Mechanisms of Polyreactions - Polymer Characterization, Adv. Polymer Sci.*, 21, 108 (1976).

18. Schreiber, H. P., Wertheimer, M. R. and Lambla, M., J. Appl. Polymer Sci., 27, 2269 (1982).

19. Gozdz, A. S. and Weigmann, H. D., J. Appl. Polymer Sci., 29, 3965 (1984).

20. Miller, B. and Tyomikin, I., Textile Research J., 54, 706 (1984).

21. Miller, B. and Tyomkin, I., Proceedings of the 11th Technical Symposium of the Association of Nonwoven Fabrics Industry (INDA), Baltimore, MD, September 13-15, (1983), p. 73.

22. Washburn, E. W., Phys. Rev., 17, 273 (1921).

23. Clark, D. B. and Miller, B., Textile Res. J 48, 256 (1978).

24. Gillberg, G. and Kemp, D., J. Appl. Polym. Sci. 26, 2023 (1981).

25. Inverarity, G., Br. Polym. J. 1, 245 (1969).

26. Jing, T. S., Oh, S. G. and Slattery, J. C., J. Coll. Interface Sci. 69, 74 (1979).

GLOSSARY

C_A	=	Drago's parameter for acid strength
C_B	=	Drago's parameter for basic strength
E_A	=	Drago's parameter for acid strength
E_B	=	Drago's parameter for basic strength
F	=	Observed force
F_W	=	Wetting force
F_B	=	Buoyance force
g	=	Gravitational acceleration
IGC	=	Inverse gas chromotography
l	=	Distance of liquid flow into capillary
P	=	Perimeter
p	=	Vapor pressure of liquid
P_O	=	Pressure of saturated vapor
ΔP_{ij}	=	Pressure gradient for capillaries i and j
PBI	=	Polybenzimidazole
PET	=	Polyethylene terephthalate
PP	=	Polypropylene
R	=	Ideal gas constant
r	=	Outer radius of vertical tube
r_i	=	Radius of capillary
SP	=	Solubility properties
T	=	Absolute temperature
TRI	=	Textile Research Institute
V	=	Volume of liquid drop
$\overline{V}_2$	=	Solute molar volume
W_{ADH}	=	Work of adhesion
W_A^P	=	Dipole-dipole interaction forces
α	=	Measure of hydrogen bond donar (acidity) of solvent
β	=	Measure of hydrogen bond acceptor (basicity) of solvent

Γ = Gibbs' absorption excess per unit area

γ^D = Dispersive part of surface tension/energy

γ^P = Polar part of surface tension/energy

γ_{LV} = Surface tension of liquid

γ_S = Surface energy of solid

γ_{SL} = Interfacial tension between liquid and solid

γ_{SV} = Surface energy of solid in equilibrium contact with liquid

δ = Hildebrand solubility parameter

δ_d = Hansen dispersion parameter

δ_h = Hansen hydrogen bonding parameter

δ_p = Hansen polar parameter

η = Viscosity of liquid

θ = Contact angle

θa = Advancing contact angle

θ_r = Receding contact angle

π^* = Solvent dipolarity/polarizability

πe = Surface pressure of vapor

ρ = Density of liquid

APPENDIX A

EXPERIMENTAL DATA

TABLE A-1   PHYSICOCHEMICAL PARAMETERS FOR THE PURE LIQUIDS USED IN THE STUDIES

Solvent	γ_{LV}, dyn/cm	η, cps	ρ, g/cm³	Kamlet and Taft's Solvatochromic Parameters			Solubility Parameters			
				π^*	β	α	δ	δd	δp	δh
Water	72.6	0.890	1.000	1.09	0.18	1.17	23.5	7.6	7.8	20.7
Acetic Acid	26.6	1.040	1.043	0.64	(0.40)	1.12	10.6	7.1	3.9	6.6
Methanol	22.5	0.544	0.787	0.60	0.62	0.93	14.3	7.4	6.0	10.9
Ethanol	22.2	1.078	0.785	0.54	0.77	0.83	12.9	7.7	4.3	9.5
Propanol	23.6	1.722	0.800	0.52	0.37	0.78	12.0	7.8	3.3	8.5
Ethylene Glycol	47.8	13.500	1.110	0.92	0.52	0.90	16.1	8.3	5.4	12.7
Formamide	58.0	3.302	1.129	0.97	0.55	0.71	17.9	8.4	12.8	9.3
Acetonitrile	28.8	0.325	0.777	0.75	0.31	0.19	11.9	7.5	8.8	3.0
Dimethylsulfoxide	43.3	1.996	1.095	1.00	0.76	0.00	12.9	9.0	8.0	6.0
N-Methyl-2-Pyrrolidone	41.4	1.666	1.028	0.92	0.77	0.00	11.2	8.8	6.0	3.5
Dimethylacetamide	35.7	2.140	0.937	0.88	0.76	0.00	11.1	8.2	5.6	5.0
Triethylphosphate	29.7	1.700	1.073	0.72	0.77	0.00	10.9	8.2	5.6	4.5
Diethylmalonate	31.3	1.940	1.052	0.64	(0.40)	0.00	10.3	7.6	2.3	5.3
Ethylacetate	23.0	0.400	0.895	0.55	0.45	0.00	9.1	7.7	2.6	3.5
Pyridine	36.7	0.884	0.978	0.87	0.64	0.00	10.6	9.3	4.3	2.9
T-Butylamine	17.4	0.600	0.691	0.25	0.69	0.00	7.8	6.0	3.4	3.4
4-Methyl-2-Pentanone	23.6	0.542	0.796	0.67	0.48	0.00	8.5	7.5	3.0	2.0
2-Butanone	24.3	0.365	0.800	0.67	0.48	0.06	9.4	7.8	4.4	2.5
Diisopropylether	17.4	0.379	0.718	0.27	0.49	0.00	7.0	6.6	2.3	0.7
Dichloromethane	26.7	0.393	1.316	0.82	0.00	0.30	9.9	7.5	3.0	1.9
1,2,-Dichloroethane	32.2	0.730	1.245	0.81	0.00	0.10	10.2	9.2	3.6	2.0
Methylene Iodide	50.8	2.500	3.300	1.12	0.00	0.00	9.3	8.7	1.9	2.7
Toluene	28.1	0.551	0.858	0.54	0.11	0.00	8.9	8.8	0.7	1.0
Cyclohexane	25.2	0.898	0.774	0.00	0.00	0.00	8.2	8.2	0.0	0.0
Hexadecane	27.2	3.340	0.773	-0.08	0.00	0.00	8.0	8.0	0.0	0.0

TABLE A-2 THE AVERAGE ADVANCING WETTING FORCE AND THE CALCULATED ADVANCING CONTACT ANGLE, θ, ADHESION TENSION, $\gamma_{LV} \cos \theta$, AND LIQUID PENETRATING POWER, $\gamma_{LV} \cos \theta / \eta$, FOR RAYON FIBERS.

LIQUID	AVG. ADVANCING FORCE (mg)	ST. DEV	COSINE OF AVG. ADVANCING CONTACT ANGLE	AVG. ADVANCING CONTACT ANGLE	ADHESION TENSION	PENETRATING POWER
METHANOL	0.213	0.007	1.03	0	23.21	42.7
ETHANOL	0.198	0.014	0.97	0	21.58	20.0
DIMETHYLSULFOXIDE	0.399	0.019	1.00	0	43.49	21.8
N-METHYL-2-PYRROLIDONE	0.368	0.021	0.97	0	40.11	24.1
DIMETHYLACETAMIDE	0.326	0.015	0.99	0	35.53	16.6
DICHLOROMETHANE	0.261	0.008	1.07	0	28.45	72.4
TOLUENE	0.261	0.012	1.01	0	28.45	51.6
CYCLOHEXANE	0.234	0.008	1.01	0	25.51	28.4
HEXADECANE	0.249	0.003	1.00	0	27.14	8.1
FORMAMIDE	0.700	0.044	1.32	0	58.00	17.6
ETHYLENE GLYCOL	0.431	0.006	0.98	0	46.98	3.5
PYRIDINE	0.349	0.011	1.04	0	38.04	43.0
4-METHYL-2-PENTANONE	0.216	0.011	1.00	0	23.54	43.4
T-BUTYLAMINE	0.168	0.008	1.05	0	18.31	30.5
1-PROPANOL	0.211	0.005	0.97	0	22.99	13.4
2-BUTANONE	0.229	0.002	1.03	0	24.96	68.4
ETHYL ACETATE	0.208	0.010	0.98	0	22.67	56.7
DIISOPROPYL ETHER	0.165	0.006	1.03	0	17.98	47.4
WATER	0.836	0.021	1.26	0	72.60	81.6
ACETONITRILE	0.257	0.008	0.97	0	27.90	85.8
1,2-DICHLOROETHANE	0.295	0.016	1.00	0	32.16	44.1
ACETIC ACID	0.247	0.008	1.01	0	26.92	25.9
METHYLENE IODIDE	0.429	0.023	0.92	23	46.76	18.7
DIETHYL MALONATE	0.297	0.015	1.03	0	32.37	16.7
TRIETHYL PHOSPHATE	0.272	0.006	1.00	0	29.65	17.4

The fibers were cleaned ultrasonically with methanol and then stored at 65% RH and 25°C to a constant water regain of 13%. The average fiber perimeter was determined from wettability studies to be 90 μm.

TABLE A-3   THE AVERAGE RECEDING WETTING FORCE, F mg, AND THE CALCULATED RECEDING CONTACT ANGLE, θ , FOR RAYON FIBERS.

WETTABILITY STUDIES RAYON RETARDING AFTER CLEANING IN METHANOL

LIQUID	AVG. RECEDING FORCE (mg)	ST. DEV.	COSINE OF AVG. RECEDING CONTACT ANGLE	AVG. RECEDING CONTACT ANGLE
METHANOL	0.221	0.007	1.07	0
ETHANOL	0.198	0.014	0.97	0
DIMETHYLSULFOXIDE	0.399	0.019	1.00	0
N-METHYL-2-PYRROLIDONE	0.367	0.022	0.96	0
DIMETHYLACETAMIDE	0.325	0.014	0.99	0
DICHLOROMETHANE	0.261	0.008	1.07	0
TOLUENE	0.259	0.003	1.00	0
CYLCOHEXANE	0.235	0.008	1.01	0
HEXADECANE	0.249	0.003	1.00	0
FORMAMIDE	0.704	0.044	1.32	0
ETHYLENE GLYCOL	0.430	0.015	0.98	0
PYRIDINE	0.348	0.011	1.04	0
4-METHYL-2-PENTANONE	0.216	0.011	1.00	0
T-BUTYLAMINE	0.164	0.007	1.03	0
1-PROPANOL	0.211	0.005	0.97	0
2-BUTANONE	0.229	0.002	1.03	0
ETHYL ACETATE	0.209	0.010	1.00	0
DIISOPROPYL ETHER	0.164	0.006	1.03	0
WATER	0.874	0.014	1.31	0
ACETONITRILE	0.255	0.008	0.97	0
1,2-DICHLOROETHANE	0.294	0.016	1.00	0
ACETIC ACID	0.246	0.008	1.01	0
METHYLENE IODIDE	0.449	0.019	0.96	0
DIETHYL MALONATE	0.297	0.015	1.03	0
TRIETHYL PHOSPHATE	0.271	0.006	1.00	0

The fibers were cleaned ultrasonically with methanol and then stored at 65% RH and 25°C to a constant water regain of 13%. The average fiber perimeter was determined from wettability studies to be 90 μm.

50

TABLE A-4   THE AVERAGE ADVANCING WETTING FORCE, F mg, AND THE CALCULATED ADVANCING CONTACT ANGLE, θ , ADHESION TENSION, γ_{LV} COSθ , WORK OF ADHESION, W_{ADH}, AND LIQUID PENETRATING POWER, γ_{LV} COS θ/η, FOR PBI FIBERS.

LIQUID	AVG. ADVANCING FORCE (mg)	ST. DEV.	COSINE OF AVG. ADVANCING CONTACT ANGLE	AVG. ADVANCING CONTACT ANGLE	ADHESION TENSION	WORK OF ADHESION	PENETRATING POWER
METHANOL	0.112	0.003	1.06	0	23.9	46.4	43.9
ETHANOL	0.104	0.001	0.99	0	22.2	44.4	20.6
DIMETHYLSULFOXIDE	0.192	0.004	0.95	19	40.9	84.2	20.5
N-METHYL-2-PYRROLIDONE	0.176	0.005	0.91	25	37.5	78.9	22.5
DIMETHYLACETAMIDE	0.156	0.003	0.93	21	33.3	69.0	15.6
DICHLOROMETHANE	0.132	0.004	1.05	0	28.1	54.8	71.5
TOLUENE	0.130	0.004	0.99	0	27.7	55.8	50.3
CYCLOHEXANE	0.113	0.007	0.96	0	24.1	49.3	26.8
HEXADECANE	0.124	0.001	0.97	0	26.4	53.6	7.9
FORMAMIDE	0.203	0.005	0.75	42	43.3	101.3	13.1
ETHYLENE GLYCOL	0.200	0.013	0.89	27	42.6	90.4	3.2
PYRIDINE	0.164	0.007	0.95	18	34.9	71.7	39.5
4-METHYL-2-PENTANONE	0.106	0.001	0.96	0	22.6	46.2	41.7
T-BUTYLAMINE	0.084	0.004	1.03	0	17.9	35.3	30.0
1-PROPANOL	0.106	0.001	0.96	0	22.6	46.2	13.1
2-BUTANONE	0.113	0.004	0.99	0	24.1	48.4	66.0
ETHYL ACETATE	0.106	0.002	0.95	17	22.6	46.3	56.5
DIISOPROPYL ETHER	0.081	0.002	0.99	0	17.3	34.7	45.6
WATER	0.176	0.016	0.52	59	37.5	110.1	42.1
ACETONITRILE	0.131	0.005	0.97	14	27.9	56.7	85.8
1,2-DICHLOROETHANE	0.150	0.003	0.99	0	32.0	64.2	43.8
ACETIC ACID	0.127	0.002	1.02	0	27.1	54.5	26.0
METHYLENE IODIDE	0.198	0.012	0.83	34	42.2	93.0	16.9
DIETHYL MALONATE	0.138	0.004	0.94	20	29.4	60.7	15.2
TRIETHYL PHOSPHATE	0.127	0.001	0.91	24	27.1	56.8	16.0

The fibers were cleaned ultrasonically with methanol and then stored at 65% RH and 25°C to a constant water regain of 15%. The average fiber perimeter was determined from wettability studies to be 46 μm.

TABLE A-5 THE AVERAGE RECEDING WETTING FORCE, F mg, AND THE CALCULATED RECEDING
CONTACT ANGLE, θ , FOR PBI FIBER.

LIQUID	AVG. RECEDING FORCE (mg)	ST. DEV	COSINE OF AVG. RECEDING CONTACT ANGLE	AVG. RECEDING CONTACT ANGLE
METHANOL	0.112	0.003	1.06	0
ETHANOL	0.107	0.001	1.03	0
DIMETHYLSULFOXIDE	0.196	0.006	0.96	0
N-METHYL-2-PYRROLIDONE	0.176	0.005	0.91	25
DIMETHYLACETAMIDE	0.155	0.003	0.93	22
DICHLOROMETHANE	0.132	0.004	1.05	0
TOLUENE	0.130	0.004	0.99	0
CYCLOHEXANE	0.113	0.007	0.96	0
HEXADECANE	0.124	0.001	0.97	0
FORMAMIDE	0.241	0.005	0.88	27
ETHYLENE GLYCOL	0.210	0.002	0.94	20
PYRIDINE	0.165	0.007	0.96	0
4-METHYL-2-PENTANONE	0.106	0.001	0.96	0
T-BUTYLAMINE	0.084	0.004	1.03	0
1-PROPANOL	0.106	0.001	0.96	0
2-BUTANONE	0.113	0.004	0.99	0
ETHYL ACETATE	0.106	0.002	0.95	17
DIISOPROPYL ETHER	0.081	0.002	0.99	0
WATER	0.227	0.015	0.67	48
ACETONITRILE	0.133	0.001	0.98	0
1,2-DICHLOROETHANE	0.149	0.002	0.99	0
ACETIC ACID	0.127	0.002	1.01	0
METHYLENE IODIDE	0.216	0.008	0.91	25
DIETHYL MALONATE	0.139	0.003	0.95	19
TRIETHYL PHOSPHATE	0.127	0.001	0.91	24

The fibers were cleaned ultrasonically with methanol and then stored at 65% RH
and 25°C to a constant water regain of 15%. The average fiber perimeter was
determined from wettability studies to be 46 μm.

TABLE A-6 THE AVERAGE ADVANCING WETTING FORCE, F mg, AND THE CALCULATED ADVANCING CONTACT ANGLE, θ, ADHESION TENSION γ_{LV} COS θ, WORK OF ADHESION, W$_{ADH}$, AND LIQUID PENETRATING POWER, γ_{LV} COS θ/η, FOR PET FIBERS.

LIQUID	AVG. ADVANCING FORCE (mg)	ST. DEV.	COSINE OF AVG. ADVANCING CONTACT ANGLE	AVG. ADVANCING CONTACT ANGLE	ADHESION TENSION	WORK OF ADHESION	PENETRATING POWER
METHANOL	0.165	0.007	1.00	0	22.40	44.9	41.2
ETHANOL (ABSOLUTE)	0.164	0.003	1.00	0	22.26	44.4	20.7
DIMETHYLSULFOXIDE	0.303	0.016	0.95	18	41.13	84.4	20.6
N-METHYL-2-PYRROLIDONE	0.302	0.011	0.99	0	41.00	82.4	24.6
DIMETHYLACETAMIDE	0.263	0.002	1.00	0	35.70	71.4	16.7
DICHLOROMETHANE	0.250	0.009	1.27	0	33.43	60.1	85.1
TOLUENE	0.206	0.007	1.00	0	27.96	56.0	50.7
CYCLOHEXANE	0.191	0.014	1.03	0	25.93	51.1	28.9
HEXADECANE	0.201	0.005	1.00	0	27.28	54.5	8.2
FORMAMIDE	0.261	0.007	0.61	52	35.43	93.4	10.7
ETHYLENE GLYCOL	0.272	0.021	0.77	39	36.92	84.7	2.7
PYRIDINE	0.284	0.013	1.05	0	38.55	75.3	43.6
4-METHYL-2-PENTANONE	0.174	0.006	1.00	0	23.62	47.2	43.6
T-BUTYLAMINE	0.134	0.010	1.05	0	18.19	35.6	30.3
1-PROPANOL	0.177	0.010	1.02	0	24.03	47.6	14.0
2-BUTANONE	0.186	0.004	1.04	0	25.25	49.5	69.2
ETHYL ACETATE	0.171	0.005	0.98	0	23.21	46.9	58.0
DIISOPROPYL ETHER	0.126	0.003	0.98	0	17.10	34.5	45.1
WATER	0.155	0.026	0.29	73	21.04	93.6	23.6
ACETONITRILE	0.210	0.005	0.99	0	28.51	57.3	87.7
1,2-DICHLOROETHANE	0.244	0.014	1.03	0	33.12	65.3	45.4
ACETIC ACID	0.202	0.006	1.00	0	27.42	54.8	26.4
METHYLENE IODIDE	0.303	0.024	0.81	36	41.43	92.2	16.5
DIETHYL MALONATE	0.230	0.006	1.00	0	31.22	62.5	16.1
TRIETHYL PHOSPHATE	0.213	0.023	0.97	0	28.91	58.6	17.0

The fibers were cleaned ultrasonically with methanol and then stored at 65% RH and 25°C. The average fiber diameter was determined from wettability studies to be 23 μm.

TABLE A-7   THE AVERAGE RECEDING WETTING FORCE, F mg, AND THE CALCULATED RECEDING CONTACT ANGLE, θ , FOR PET FIBERS.

LIQUID	AVG. RECEDING FORCE (mg)	ST. DEV.	COSINE OF AVG. RECEDING CONTACT ANGLE	AVG. RECEDING CONTACT ANGLE
METHANOL	0.165	0.008	1.00	0
ETHANOL	0.164	0.004	1.00	0
DIMETHYLSULFOXIDE	0.306	0.017	0.96	16
N-METHYL-2-PYRROLIDONE	0.302	0.010	0.99	8
DIMETHYLACETAMIDE	0.263	0.002	1.00	0
DICHLOROMETHANE	0.257	0.012	1.31	0
TOLUENE	0.204	0.006	0.99	0
CYLCOHEXANE	0.190	0.015	1.02	0
HEXADECANE	0.203	0.003	1.01	0
FORMAMIDE	0.343	0.016	0.80	36
ETHYLENE GLYCOL	0.339	0.010	0.96	15
PYRIDINE	0.284	0.013	1.05	0
4-METHYL-2-PENTANONE	0.174	0.006	1.00	0
T-BUTYLAMINE	0.133	0.013	1.03	0
1-PROPANOL	0.176	0.010	1.01	0
2-BUTANONE	0.185	0.004	1.03	0
ETHYL ACETATE	0.169	0.005	0.97	0
DIISOPROPYL ETHER	0.126	0.003	0.98	0
WATER	0.306	0.029	0.57	55
ACETONITRILE	0.212	0.005	1.00	0
1,2-DICHLOROETHANE	0.251	0.017	1.06	0
ACETIC ACID	0.202	0.005	1.00	0
METHYLENE IODIDE	0.327	0.005	0.87	29
DIETHYL MALONATE	0.229	0.005	0.99	29
TRIETHYL PHOSPHATE	0.213	0.023	0.97	0

The fibers were cleaned ultrasonically with methanol and then stored at 65% RH and 25°C. The average fiber diameter was determined from wettability studies to be 23 μm.

54

TABLE A-8 THE AVERAGE ADVANCING WETTING FORCE, F mg, AND THE CALCULATED ADVANCING CONTACT ANGLE, θ, ADHESION TENSION, $\gamma_{LV} \cos \theta$, WORK OF ADHESION, W_{ADH}, AND LIQUID PENETRATING POWER, $\gamma_{LV} \cos \theta / \eta$ FOR POLYPROPYLENE FIBERS.

LIQUID	AVG. ADVANCING FORCE (mg)	ST. DEV.	COSINE OF AVG. ADVANCING CONTACT ANGLE	AVG. ADVANCING CONTACT ANGLE	ADHESION TENSION	WORK OF ADHESION	PENETRATING POWER
METHANOL	0.086	0.003	0.95	17	21.48	43.98	39.5
ETHANOL	0.090	0.004	1.01	0	22.48	44.68	20.9
DIMETHYLSULFOXIDE	0.083	0.005	0.48	61	20.73	64.03	10.4
N-METHYL-2-PYRROLIDONE	0.103	0.007	0.62	52	25.73	67.13	15.4
DIMETHYLACETAMIDE	0.107	0.003	0.75	41	26.72	62.42	12.5
DICHLOROMETHANE	0.110	0.003	1.03	0	27.47	54.17	69.9
TOLUENE	0.121	0.004	1.00	0	30.22	58.32	54.8
CYCLOHEXANE	0.103	0.008	1.02	0	25.73	50.93	28.7
HEXADECANE	0.113	0.003	1.04	0	28.22	55.42	8.5
FORMAMIDE	0.024	0.008	0.10	84	5.99	63.99	1.8
ETHYLENE GLYCOL	0.059	0.007	0.31	73	14.73	62.53	1.1
PYRIDINE	0.112	0.003	0.76	40	27.97	64.77	31.6
4-METHYL-2-PENTANONE	0.095	0.003	1.00	0	23.73	47.33	43.8
T-BUTYLAMINE	0.073	0.004	1.00	0	17.53	34.93	29.2
1-PROPANOL	0.096	0.003	1.02	0	23.98	47.58	13.9
2-BUTANONE	0.095	0.001	0.98	0	23.73	48.08	65.0
ETHYL ACETATE	0.095	0.001	1.00	0	23.73	47.43	59.3
DIISOPROPYLETHER	0.068	0.005	0.98	0	16.98	34.39	44.8
WATER	<0	-	-	(94)	-5.24	67.36	-5.9
ACETONITRILE	0.088	0.003	0.76	40	21.98	50.78	67.6
1,2-DICHLOROETHANE	0.118	0.001	0.92	24	29.47	61.67	40.4
ACETIC ACID	0.095	0.007	0.87	30	23.73	51.13	22.8
METHYLENE IODIDE	0.097	0.001	0.48	61	24.23	75.03	9.7
DIETHYL MALONATE	0.110	0.008	0.88	28	27.47	58.77	14.2
TRIETHYL PHOSPHATE	0.107	0.003	0.90	26	26.72	56.42	15.7

The fibers were cleaned ultrasonically with methanol and then stored at 65% RH and 25°C. The average fiber diameter was determined from wettability studies to be 12.5 μm.

TABLE A-9 THE AVERAGE RECEDING FORCE, F mg, AND THE CALCULATED RECEDING CONTACT ANGLE, θ, FOR POLYPROPYLENE FIBERS.

LIQUID	AVG. RECEDING FORCE (mg)	ST. DEV.	COSINE OF AVG. RECEDING CONTACT ANGLE	AVG. RECEDING CONTACT ANGLE
METHANOL	0.088	0.004	0.98	0
ETHANOL	0.089	0.003	1.00	0
DIMETHYLSULFOXIDE	0.087	0.005	0.50	60
N-METHYL-2-PYRROLIDONE	0.108	0.005	0.65	49
DIMETHYLACETAMIDE	0.108	0.003	0.75	41
DICHLOROMETHANE	0.110	0.003	1.03	0
TOLUENE	0.120	0.004	1.07	0
CYCLOHEXANE	0.106	0.011	1.05	0
HEXADECANE	0.113	0.003	1.04	0
FORMAMIDE	0.048	0.001	0.21	78
ETHYLENE GLYCOL	0.078	0.018	0.41	66
PYRIDINE	0.114	0.003	0.77	39
4-METHYL-2-PENTANONE	0.095	0.003	1.00	0
T-BUTYLAMINE	0.073	0.004	1.05	0
1-PROPANOL	0.096	0.003	1.02	0
2-BUTANONE	0.095	0.001	0.98	0
ETHYL ACETATE	0.095	0.001	1.00	0
DIISOPROPYL ETHER	0.070	0.005	1.01	0
WATER	-		-	-
ACETONITRILE	0.093	0.002	0.81	36
1,2-DICHLOROETHANE	0.116	0.003	0.90	26
ACETIC ACID	0.095	0.007	0.87	30
METHYLENE IODIDE	0.098	0.001	0.48	62
DIETHYL MALONATE	0.111	0.008	0.89	27
TRIETHYL PHOSPHATE	0.111	0.003	0.93	21

The fibers were cleaned ultrasonically with methanol and then stored at 65% RH and 25°C. The average fiber diameter was determined from wettability studies to be 12.5 μm.

TABLE A-10   DROP PENETRATION TEST DATA FOR RAYON

Solvent	Ave. Weight Gain (Grams)	St. Dev.	Weight of 4 mm Droplet
Water	0.0038	0.0012	0.0334
Methanol	0.0049	0.0013	0.0263
Hexadecane	0.0095	0.0023	0.0258
Dimethylsulfoxide	0.013^	0.0032	0.0365
Formamide	0.011.	0.0071	0.0377
Ethyl Acetate	0.0010	0.0004	0.0299
N-methyl-2-pyrrolidinone	0.0189	0.0016	0.0344
Dichloromethane	0.0009	0.0002	0.0441
DMAC-	0.0160	0.0010	0.0313
1-Propanol	0.0095	0.0022	0.0268
Cyclohexane	0.0011	0.0001	0.0258
Ethylene Glycol	0.0138	0.0019	0.0372
Toluene	0.0003	0.0001	0.0287
Pyridine	0.0052	0.0026	0.0327
4-methyl-2-pentanone	0.0016	0.0003	0.0265
Tert-butylamine	0.0025	0.0006	0.0230
Diisopropyl Ether	0.0016	0.0003	0.0239
1,2-dichloroethane	0.0010	0.0002	0.0322
Glacial Acetic Acid	0.0206	0.0023	0.0349
Trifluoro Acetic Acid	0.0226	0.0020	0.0494
Acetonitrile	0.0016	0.0002	0.0261
Ethanol	0.0094	0.0022	0.0262
2-Butanone	0.0010	0.0008	0.0270
Methylene Iodide	0.0294	0.0086	0.1114
Triethyl Phosphate	0.0169	0.0022	0.0358
Diethyl Malonate	0.0202	0.0025	0.0353

NOTE: All solvents penetrated a small surface area.   Penetration
was   complete   and   instantaneous.   None   of   the   solvents
formed a droplet which remained on the top of the fabric.

DMAC = Dimethylacetamide

TABLE A-11 DROP PENETRATION TEST DATA FOR PBI

Solvent	Ave. Weight Gain (Grams)	St. Dev.	Weight of 4 mm Droplet
Water	0.0277	0.0026	0.0334
Methanol	0.0068	0.0019	0.0263
Hexadecane	0.0100	0.0052	0.0258
Dimethylsulfoxide	0.0170	0.0021	0.0365
Formamide	0.0143	0.0090	0.0377
Ethyl Acetate	0.0004	0.0003	0.0299
N-methyl-2-pyrrolidinone	0.0141	0.0005	0.0344
Dichloromethane	0.0002	0.0004	0.0441
DMAC	0.0129	0.0035	0.0313
1-Propanol	0.0052	0.0020	0.0268
Cyclohexane	0.0003	0.0003	0.0258
Ethylene Glycol	0.0122	0.0021	0.0372
Toluene	0.0001	0.0001	0.0287
Pyridine	0.0080	0.0022	0.0327
4-methyl-2-pentanone	0.0007	0.0006	0.0265
Tert-butylamine	0.0003	0.0002	0.0230
Diisopropyl Ether	0.0001	0.0001	0.0239
1,2-dichloroethane	0.0001	0.0001	0.0322
Acetonitrile	0.0010	0.0002	0.0261
Glacial Acetic Acid	0.0114	0.0022	0.0348
Ethanol	0.0064	0.0006	0.0262
2-Butanone	0.0006	0.0007	0.0270
Methylene Iodide	0.0131	0.0038	0.1114
Diethyl Malonate	0.0104	0.0026	0.0353
Triethyl Phosphate	0.0144	0.0014	0.0358
Trifluoro Acetic	0.0177	0.0017	0.0494

NOTE: The DMAC and formamide formed droplets which remained on the barrier fabric throughout the test. The methylene iodine penetrated a larger surface area than the other solvents. The other solvents penetrated a small surface area.

DMAC = Dimethylacetamide

TABLE A-12   DROP PENETRATION TEST DATA FOR POLYESTER

Solvent	Ave. Weight Gain (Grams)	St. Dev.	Weight of 4 mm Droplet
Water	0.0014	0.0003	0.0334
Methanol	0.0054	0.0016	0.0263
Hexadecane	0.0234	0.0016	0.0258
Dimethylsulfoxide	0.0425	0.0019	0.0365
Formamide	0.0353	0.0036	0.0377
Ethyl Acetate	0.0017	0.0004	0.0299
N-methyl-2-pyrrolidinone	0.0376	0.0012	0.0344
Dichloromethane	0.0021	0.0004	0.0441
DMAC	0.0277	0.0036	0.0313
1-Propanol	0.0098	0.0018	0.0268
Cyclohexane	0.0017	0.0004	0.0258
Ethylene Glycol	0.0207	0.0023	0.0372
Toluene	0.0020	0.0013	0.0287
Pyridine	0.0162	0.0036	0.0327
Tert-butylamine	0.0018	0.0006	0.0230
4-methyl-2-pentanone	0.0018	0.0006	0.0265
Diisopropyl Ether	0.0008	0.0004	0.0239
1,2-dichloroethane	0.0162	0.0013	0.0322
Trifluoro Acetic Acid	0.0306	0.0015	0.0494
Glacial Acetic Acid	0.0262	0.0014	0.0349
Acetonitrile	0.0129	0.0013	0.0261
Ethanol	0.0159	0.0017	0.0262
2-Butanone	0.0020	0.0007	0.0270
Methylene Iodide	0.1039	0.0147	0.1114
Triethyl Phosphate	0.0264	0.0040	0.0358
Diethyl Malonate	0.0350	0.0017	0.0353

NOTE: No solvents remained on the surface of the fabric in drop-
let form.   All solvents penetrated completely and instan-
taneously within a small area.

DMAC = Dimethylacetamide

TABLE A-13 DROP PENETRATION TEST DATA FOR POLYPROPYLENE

Solvent	Ave. Weight Gain (Grams)	St. Dev.	Weight of 4 mm Droplet
Water	0.0005	0.0003	0.0334
Methanol	0.0004	0.0001	0.0263
Hexadecane	0.0059	0.0017	0.0258
Dimethylsulfoxide	0.0182	0.0042	0.0365
Formamide	0.0087	0.0131	0.0377
Ethyl Acetate	0.0010	0.0002	0.0299
N-methyl-2-pyrrolidinone	0.0172	0.0039	0.0344
Dichloromethane	0.0012	0.0003	0.0441
DMAC	0.0136	0.0011	0.0313
1-Propanol	0.0031	0.0011	0.0268
Cyclohexane	0.0009	0.0004	0.0258
Ethylene Glycol	0.0005	0.0001	0.0372
Toluene	0.0008	0.0002	0.0287
Pyridine	0.0068	0.0006	0.0327
4-methyl-2-pentanone	0.0003	0.0002	0.0265
Tert-butylamine	0.0012	0.0006	0.0230
Glacial Acetic Acid	0.0106	0.0021	0.0349
Diisopropyl Ether	0.0010	0.0004	0.0239
1,2-dichloroethane	0.0012	0.0003	0.0322
Acetonitrile	0.0009	0.0007	0.0261
Ethanol	0.0041	0.0007	0.0262
2-Butanone	0.0008	0.0010	0.0270
Methylene Iodide	0.0349	0.0040	0.1114
Diethyl Malonate	0.0152	0.0015	0.0353
Trifluoro Acetic Acid	0.0146	0.0046	0.0494
Triethyl Phosphate	0.0124	0.0045	0.0358

NOTE: No surface area of the droplet penetration was of a medium size, slightly larger than for rayon or PET. The methylene iodine penetrated a smaller area than the other chemicals mentioned. The DMAC, formamide, ethylene glycol and water formed droplets on the fabric surface which remained throughout the test.

DMAC = Dimethylacetamide

TABLE A-14. DROP PENETRATION DATA FOR RAYON

All Weights In Grams

	Receiver/Barrier		Receiver	
	Grams	S.D.	Weight	S.D.
Water	.0398[A]	.0016	.0105	.0042
Acetic Acid	.0167	.0039	.0120	.0017
Propanol	.0208	.0013	.0137	.0006
Ethylene Glycol	.0469	.0013	.0292	.0013
Formamide	.0462	.0015	.0254	.0012
Acetonitrile	.0118	.0011	.0094	.0006
Dimethylsulfoxide	.0378	.0014	.0218	.0015
1,2-Dichloroethane	.0130[B]	.0012	.0087	.0010
Hexadecane	.0280	.0007	.0184	.0007
Toluene	.0137	.0007	.0094	.0006
4-Methyl-2-Pentanone	.0090	.0017	.0056	.0012
Pyridine	.0227	.0020	.0144	.0012
Triethylphosphate	.0233[B]	.0023	.0165	.0018
Diethylmalonate	.0265	.0012	.0146	.0019

A - Drop transferred very rapidly to fabric.
B - 45 μl drop used, since 50 μl drop would not form.

TABLE A-15.   DROP PENETRATION DATA FOR PBI

All Weights In Grams

	Receiver/Barrier		Receiver	
	Grams	S.D.	Weight	S.D.
Water	.0430[A]	.0018	.0244	.0056
Acetic Acid	.0139	.0014	.0063	.0011
Propanol	.0215	.0009	.0075	.0004
Ethylene Glycol	.0476[A]	.0005	.0271	.0060
Formamide	.0477	.0013	.0376	.0045
Acetonitrile	.0136	.0006	.0063	.0006
Dimethylsulfoxide	.0411	.0020	.0176	.0008
1,2-Dichloroethane	.0121[B]	.0017	.0037	.0003
Hexadecane	.0270	.0010	.0118	.0007
Toluene	.0149	.0015	.0044	.0006
4-Methyl-2-Pentanone	.0097	.0017	.0042	.0006
Pyridine	.0234	.0014	.0092	.0012
Triethylphosphate	.0227[B]	.0012	.0081	.0017
Diethylmalonate	.0298	.0011	.0114	.0012

A - Drop transferred slowly to fabric.
B - 45 μl drop used, since 50 μl drop would not form.

TABLE A-16. DROP PENETRATION DATA FOR PET

All Weights In Grams

| | Receiver/Barrier | | Receiver | |
	Grams	S.D.	Weight	S.D.
Water	_ [A]	–	–	–
Acetic Acid	.0170	.0021	.0121	.0010
Propanol	.0185	.0019	.0142	.0011
Ethylene Glycol	.0490[C]	.0007	.0391	.0016
Formamide	.0503	.0012	.0424	.0015
Acetonitrile	.0095	.0012	.0074	.0008
Dimethylsulfoxide	.0383	.0016	.0269	.0010
1,2-Dichloroethane	.0116[B]	.0021	.0076	.0013
Hexadecane	.0289	.0004	.0209	.0007
Toluene	.0135	.0011	.0089	.0012
4-Methyl-2-Pentanone	.0089	.0011	.0066	.0010
Pyridine	.0213	.0022	.0174	.0008
Triethylphosphate	.0220[B]	.0013	.0132	.0016
Diethylmalonate	.0255	.0020	.0188	.0014

A - Drop would not transfer to fabric.
B - 45 μl drop used, since 50 μl drop would not form.
C - Drop transferred slowly to fabric.

TABLE A-17. DROP PENETRATION DATA FOR POLYPROPYLENE

All Weights In Grams

	Receiver/Barrier		Receiver	
	Grams	S.D.	Weight	S.D.
Water	- [A]	-	-	-
Acetic Acid	.0232	.0027	.0089	.0012
Propanol	.0248	.0016	.0057	.0005
Ethylene Glycol	- [A]	-	-	-
Formamide	- [A]	-	-	-
Acetonitrile	.0216	.0022	.0115	.0017
Dimethylsulfoxide	- [A]	-	-	-
1,2-Dichloroethane	.0227[B]	.0013	.0044	.0006
Hexadecane	.0288	.0007	.0092	.0010
Toluene	.0183	.0020	.0042	.0004
4-Methyl-2-Pentanone	.0119	.0015	.0028	.0007
Pyridine	.0378	.0029	.0193	.0014
Triethylphosphate	.0306[B]	.0020	.0148	.0020
Diethylmalonate	.0367	.0016	.0147	.0003

A - Drop would not transfer to fabric.
B - 45 μl drop used, since 50 μl drop would not form.

APPENDIX B

ESTIMATE OF THE SURFACE ENERGY OF POLYMERS

The work of adhesion between a solid and a liquid is defined as:

$$W_{ADH} = \gamma_S + \gamma_{LV} - \gamma_{SL} \qquad (B-1)$$

where

W_{ADH} = work of adhesion
γ_S = surface energy of the solid
γ_{LV} = surface tension of the liquid
γ_{SL} = interfacial tension between liquid and solid

Combining equation B-1 with the Young-Dupre equation

$$\gamma_{SV} - \gamma_{SL} = \gamma_{LV} \cos\theta \qquad (B-2)$$

where

γ_{SV} = the surface energy of the solid in equilibrium contact with the liquid
θ = the contact angle

gives

$$W_{ADH} = \gamma_S - \gamma_{SV} + \gamma_{LV} (1 + \cos\theta) =$$
$$\pi_e + \gamma_{LV} (1 + \cos\theta) \qquad (B-3)$$

π_e is called the surface pressure of the vapor and describes any reduction of the surface energy of the solid due to the absorption of the vapor of the test liquid. For vapors obeying the ideal gas law π_e can be determined according to:

$$\pi_e = RT \int_0^{p_o} \Gamma d(\ln p) \qquad (B-4)$$

where

R = ideal gas constant
T = absolute temperature
p = vapor pressure of liquid
p_o = pressure of the saturated vapor
Γ = Gibbs absorption excess per unit area

The surface pressure has been shown to be negligibly small for liquids which give a finite contact angle.

The work of adhesion can also be written as the sum of the contributions from the different types of interactions such as Londen dispersion forces (D) and various types of polar interactions (P).

$$W_{ADH} = W^D + W^P \tag{B-5}$$

It has been shown that the dispersion force interactions can correctly be described by the use of a geometric mean expression:

$$W^D = 2\sqrt{\gamma_1^D \cdot \gamma_2^D} \tag{B-6}$$

where

γ_i^D = dispersion component of the surface tension of component

It is reasonable to treat dipole-dipole interactions in the same way. Owens and Wendt group all types of polar interactions into one component denoted by P and assumes a geometric mean for the interaction

$$W^P = 2\sqrt{\gamma_1^P \cdot \gamma_2^P} \tag{B-7}$$

and the work of adhesion between a liquid (L) and a solid (S) thus becomes

$$W_{ADH} = 2\sqrt{\gamma_{LV}^D \cdot \gamma_S^P} + 2\sqrt{\gamma_{LV}^P \cdot \gamma_S^P} \tag{B-8}$$

A combination of equations B-3 and B-8 and rearrangements give

$$\frac{W_{ADH}}{2\sqrt{\gamma_{LV}^D}} = \frac{\gamma_{LV}(1 + \cos\theta)}{2\sqrt{\gamma_{LV}^D}} + \pi e =$$

$$= \sqrt{\gamma_S^D} + \frac{\sqrt{\gamma_{LV}^P}}{\sqrt{\gamma_{LV}^D}} \cdot \sqrt{\gamma_S^P} \tag{B-9}$$

The determination of the contact angle for liquids with published partial surface tensions and the assumption that the πe term is negligibly small will thus allow a determination of the partial surface energies of the solid either graphically (Kaelble plots) or by the solution of simultaneous equations. Kaelble plots with calculated partial surface energies are given for PBI, PET and PP in Figures B-1 - B-3.
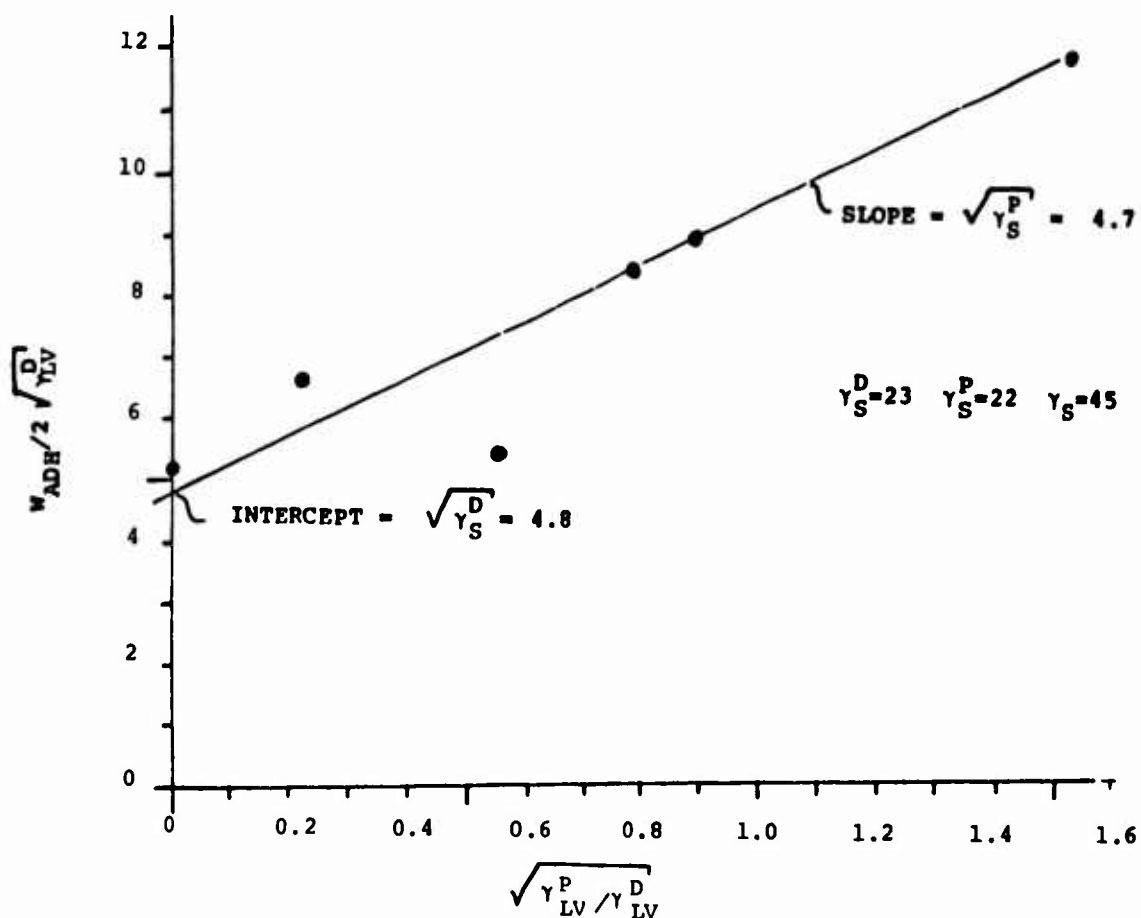
Appendix B

FIGURE B-1. PBI - ESTIMATE OF THE SURFACE ENERGY OF PBI
FIBERS (PERIMETER 46 μm) BY KAELBLE'S METHOD
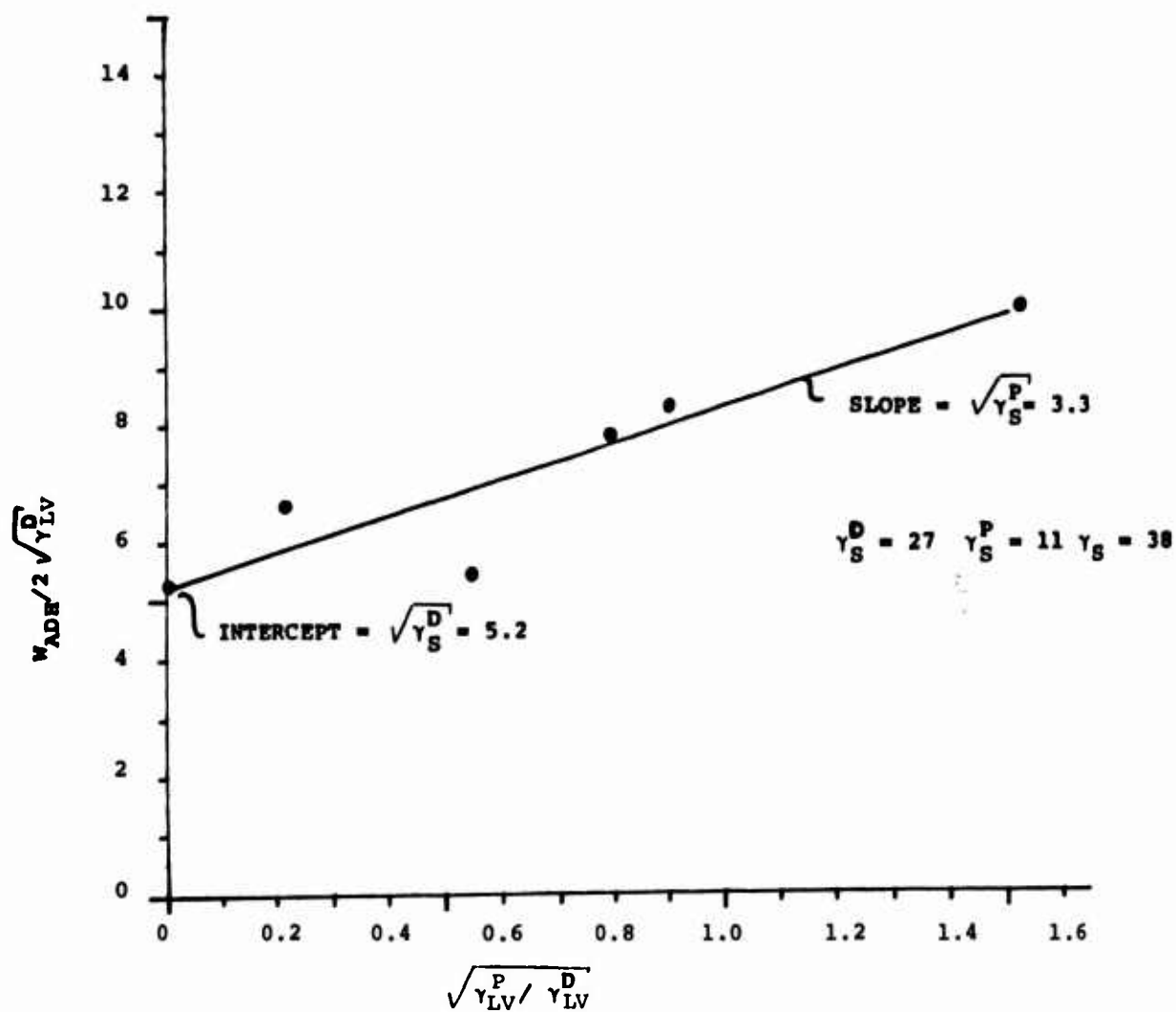
Appendix B

FIGURE B-2. PET – ESTIMATE OF THE SURFACE ENERGY OF PET
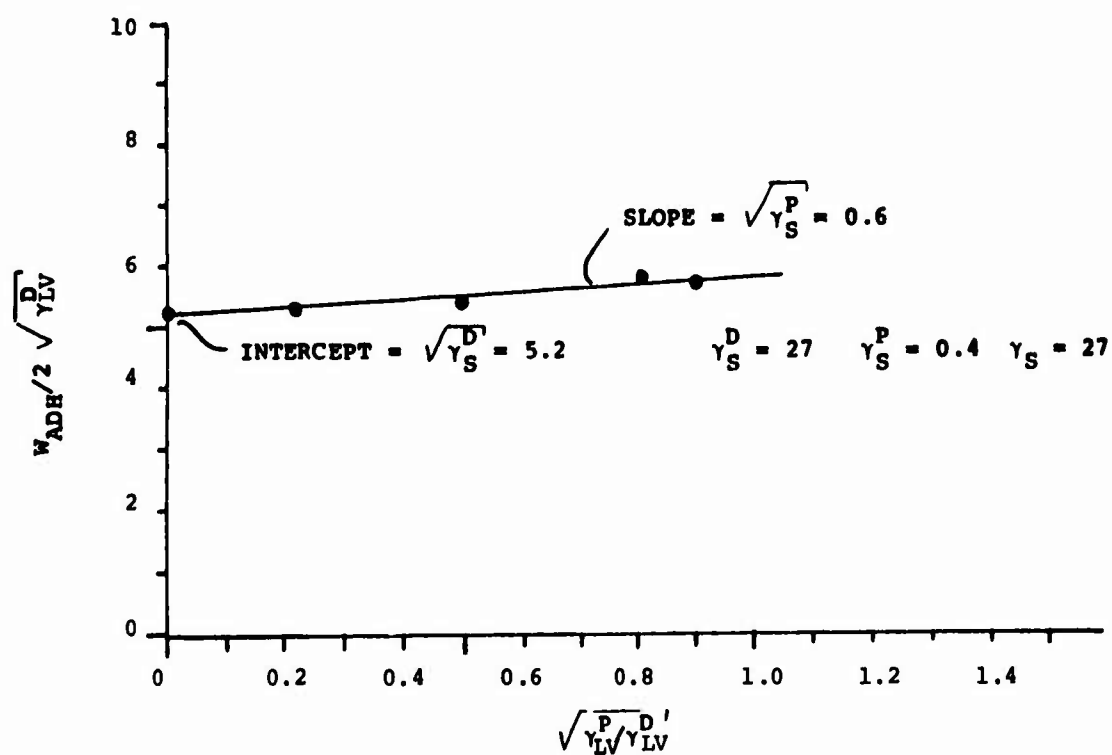FIBERS (DIAMETER 23 μm) BY KAELBLE'S METHOD

FIGURE B-3.   POLYPROPYLENE – ESTIMATE OF THE SURFACE ENERGY
OF POLYPROPYLENE FIBERS (DIAMETER 13 μm) BY
KAELBLE'S METHOD

Appendix B

Blank

APPENDIX C

INVERSE GAS CHROMATOGRAPHY (IGC) OF INTACT FIBERS

P. N. CHEN

Purpose

The purpose of this study was to investigate the interactions between probe molecules and commercial fibers using IGC.

Summary

IGC was applied to study the inherent surface characteristics/ interactions of four commercially available fibers, polyethylene terephthalate (PET), polybenzimidazole (PBI), Rayon (regenerated cellulose) and polypropylene (PP). The effects of experimental parameters (flow rate, sample injection size and column temperature) on the interactions between the fibrous packings and organic probes were investigated and the results suggested fundamental GC theories could be used to rationalize the IGC behavior of intact fibers. Generally speaking, an increase in sample injection size or column temperature decreased the retention volume of organic probes, whereas, the effect of flow rate on column efficiency followed the Van Deemter plot (i.e. the correlation between flow rate and column efficiency was parabolic). Using a set of selected empirical conditions, correlations between the parameters of column temperature and retention volume could be established for all probes on all four columns. PP with its high hydrophobicity and low glass transition temperature (Tg) exhibited the greatest degree of fiber-probe interaction among all tested fibers. The inherent acidlike or baselike properties of each fiber was elucidated by using acidic (t-butanol), neutral (n-heptane) and basic (n-butylamine) probes. The preliminary results suggested PBI, Rayon and PP fibers had acidlike properties; whereas, PET showed baselike properties. Probe-fiber interaction enthalpies were also estimated.

Introduction

The morphology, surface characteristics and chemical functionality of a polymer strongly affect many of its physical and chemical properties. The sorption of various gases, vapors and solutes on porous resins, coatings and films have been widely studied and many processes involving the use of porous materials have long been developed for analytical and industrial separations. Investigations of sorption behavior of non-porous fibrous materials were limited because these textile grade fibers generally had low surface area and low surface energy which resulted in small sorption and slow diffusion of solvents into the noncrystalline regions of the fiber.

During the past decade, a new technique, inverse gas chromatography (IGC), has been sufficiently developed to study various polymer-solvent interactions and fundamental polymer properties despite the fact that IGC remains complicated by experimental and theoretical factors which are not completely understood[1].

A. S. Gozdz et. al. [2] applied IGC to characterize the surface behavior of many commercially available fibers. Gozdz used normal-alkanes as the IGC probes for the study of fiber - probe interactions. In this study the interactions between probes having different functionality and fibers having various degrees of hydrophobicity were investigated. Based on relative sorption of organic vapors, the inherent chemical/surface properties of these fibers were studied as part of the program of future penetration mechanism. Specifically this work explored the correlations between the volatility, acidity and IGC retention volume of various probes, the effect of experimental conditions (i.e. temperature, flow rate and sample injection size) on the IGC separations, the interaction mechanism between probes and fibrous packings, and the sorptivity differences between probes and fibrous packings, and the sorptivity differences between conventional fibers (PET, PP and Rayon) and the new generation/high-performance PBI fiber.

Experimental

Apparatus and Procedure

All IGC experiments were carried out by using a semi-automatically controlled Varian 3700 gas chromatograph equipped with a highly sensitive thermal conductivity detector. High purity (>99.99%) helium gas was used as the column carrier and the flow rate (FR) was controlled by a precision needle valve and a soap bubble flowmeter. Seven organic probes were used to analyze four commercially available fibers, polyethylene terephthalate (PET), sulfonated-polybenzimidazole (PBI), Rayon (regenerated cellulose) and polypropylene (PP). The seven probes were acidic t-butanol, basic n-butylamine and neutral alkanes from C-6 to C-10. A 0.5 µl Hamilton syringe was used to inject a 0.05 µl sample into the column, and the GC injector and detector were kept at 150° and 200°C respectively. Three selected column temperatures (30°, 60° and 90°C) having a fixed flow rate (4.44 ml/min) were used to perform most of the IGC studies. Initial IGC results indicated the PP column exhibited a high degree of affinity towards all probes, so additional experiments were carried out by using faster flow rates (66.6 and 10.0 ml/min), a larger sample size (0.5 µl) or different temperatures (75°, 90° and 105°C).

Material

Four continuous multi-filament fibers (PET, PBI, Rayon and PP) were washed with methanol to remove possible additives and the dried fibers were subsequently used to pack four stainless steel columns (3 ft. length x 1/8 inch O.D.) by pulling the filaments from one end of the column to another end. The physical properties of these four fibers are shown in Table C-1.

Calculation/Data Treatment

The retention time of each probe was determined as the time of peak maximum by the Hewlett Packard 3354 laboratory computer. The corresponding retention volume were obtained by multiplying the retention time by the column flow rate.

According to Koing's equation [3], the qualitative interaction enthalpy (ΔH_p) of each probe depends upon the retention volume and the column temperature.

Koing's Equation: $\Delta H_p = -R \dfrac{d(\ln V_R)}{d(1/T)}$ (eq. 1)

ΔH_p = interaction enthalpy between the probe and the column
$[erg(ml)(g\ mole)^{-1}]$

R = gas constant; T = column temp. (°C); V_R = retention volume $(ml)^{-1}$

In other words, a linear correlation should exist between the "$\ln V_R$" and the "1/T" (see eq. 2).

$$\ln V_R = -(\Delta H_p/R)(1/T) + K \quad\quad (eq.\ 2)$$

K is the intercept when (1/T) approaches zero.

Based on the vapor phase separation theory, at very high temperature (when 1/T approaches zero), the interaction between the probe and the column is negligible; therefore, the retention volume of all probes approach the column void volume. K may be rationalized as the "ln" of the void volume, hence, it is an intrinsic factor for each column.

Results and Discussion

The Effect of Flow Rate (FR) on Retention Volume (V_R)

In order to define the fundamental separation characteristics of our experiments, we studied the effect of temperature, flow rate and sample injection size on the retention volume. The Rayon column was chosen for the initial study because its specific surface area

was between PBI (or PP) and PET (see Table C-1). At 60°C, the retention volume of t-butanol, n-butylamine and n-octane under six different flow rates (i.e. 1.06; 1.92; 3.04; 4.44; 6.02 and 7.94 ml/min) were determined by measuring the peak maximum. The results (see Table C-2) indicated the retention volume of all three probes increased with increasing flow rate up to around 6 ml/min and then dropped off at 7.9 ml/min. (see Fig. C-1). The existence of a retention volume max. at ca 6 ml/min. might be qualitatively rationalized via the famous Van Deemter equation (see Fig. C-2). In this equation, Van Deemter indicated the column efficiency expressed by HETP (height equivalents to theoretical plate) and the flow rate had a parabolical relationship. In other words, there was an optimum flow rate for obtaining max. column efficiency and selectivity. Since both efficiency and selectivity would directly affect the shape and retention volume of a given GC peak (see Fig. C-3), the max. performance of the Rayon column was apparently reached at a flow rate of ca. 6 ml/min. (see Figure C-1 - C-4) . In other words, at 6 ml/min., the diffusivity of organic probes reached an optimized stage between the gas carrier and the column packing. In this stage, there was a max. interaction between probes and fiber packings and this max. interaction resulted in max. retention volume for all probes.

The Separation of Neutral Alkanes

Five normal alkanes (C-6 to C-10) having boiling points (b.p.) ranging from 69 to 174°C were selected for initial IGC studies. The purpose of selecting n-alkanes was to explore the effect of probe volatility (b.p.) on the retention volume since no specific chemical interaction was anticipated between the inert alkane and fibrous packings. The peak max. retention volume of these hydrocarbon probes on PET, PBI and Rayon columns were determined at 30°, 60 and 90°C with a common flow rate of 4.44 ml/min. The initial results (see Table C-3) indicated that near linear correlations could be established between the n-alkane's b.p. and their corresponding retention volumes on all three columns. (See, e.g., Fig. C-5 while the data is plotted for PBI). These results suggested no abnormal chemical interactions existed between n-alkanes and the fibers so the separation of inert n-alkanes was mainly based on their relative volatilities and their physical interactions, such as van der Waals forces, with column packings. The existence of a linear correlation on PET column (see Table C-3) also suggested the glass transition temp.(Tg) of PET had little impact on the retention volume of n-alkanes because the IGC experiments were carried at temperatures both below and above the Tg (69°C) of PET.

Plotting the data as $\ln V_R$ vs $1/_T$ yielded essentially straight lines in the temperature range studied. Hence, for simple comparison purposes, the qualitative interaction enthalpy (ΔH_D) of n-alkanes on each column were estimated according to eq. 2 and these estimated results (see Table C-6) did not suggest the existence of any simple or

Appendix C

77

direct relationship between ΔH_p and the effective column surface area (see Table C-1). Generally speaking, the interactions between probes and fibers were exothermic with negative reaction enthalpy. The overall results suggested the presence of inherent differences among each column. Using n-heptane as an example, the near linear correlations between the ln of retention volume and the reciprocal of the column temperature are shown for PET, PBI and Rayon columns in Fig. C-6. According to eq. 2, the slope of these linear curves were proportional to the interaction enthalpy and revealed the degree of n-heptane and fiber interaction. Based on these slopes, the sorptivity of PBI and Rayon appeared to be greater than PET despite the fact that PET was more hydrophobic. The effective surface area, polymer crystallinity, amorphous density and chain orientation might all affect the probe-column interactions. At this time, additional efforts aimed to study the impact of these factors on probe-column interactions have not been pursued.

The interaction between n-alkanes and PP was much stronger than the corresponding interactions between n-alkanes and the other fibers (PET, PBI and Rayon) because no alkane peaks could be observed on PP column at a temperature below 60°C. Factors which might contribute to these strong interactions were the PP's high hydrophobicity and low glass transition temp. (Tg). The low Tg(-20°C) of PP might allow the n-alkane to fully diffuse into its hydrophobic/amorphous structure; consequently, n-alkanes might spread themselves in the entire PP matrix and form a non-detectable broad peak which could merge into the chromatographic baseline. In order to confirm this speculation, an experiment aimed at depressing the PP and n-alkane interactions might enhance the possibility of eluting the probe out from the PP column at an early stage as well as increase the opportunity of obtaining the probe's retention volume. The first experiment designed to depress these interactions was pursued by using higher column temperatures (75°, 90° and 105°C). As expected, clearly defined IGC peaks were observed and the retention volume of all tested n-alkanes (except n-decane) could be obtained (see Table C-7). Similar to the other columns, the obtained results suggested near linear correlations existed between the n-alkane's b.p. and their V_R and the separation of alkanes on the PP column depended upon their relative volatility. Qualitative interaction enthalpies (ΔH_p) of n-alkanes at the flow rate of 4.44 ml/min were estimated according to eq. 2 and these results revealed the relative sorptivity differences between PP and other fibers (see Table C-6).

Additional efforts aimed to elucidate the impact of flow rate and sample injection size on the degree of n-alkane and PP interaction

Appendix C

78

were pursued by using n-heptane as the reference probe. Based on the basic GC theory, an increase in flow rate and injection size would depress the probe-column interaction; therefore, the retention volume of n-heptane might be obtainable at a temperature below 75°C. As expected, the result (see Table C-6) indicated the retention volume of n-heptane was observable at 60° by increasing the flow rate from 4.44 to 6.66 ml/min or by increasing the sample injection size from 0.05 to 0.5 ul. An alternate method which may be pursued in the future for studying low temperature (<60°C) interactions between n-alkanes and PP fiber is described below.

- Increase column efficiency by using highly crimped and/or more porous fibers. Schreiber[4] coated polyethylene on Chromosorb W and obtained n-octane peak at 30° and 60°C. The reason for Schreiber's capability to obtain n-octane's retention volume at low temp. might be attributed to the high efficiency of his polyethylene coated column. A coated Chromosorb W column would have much higher efficiency than a non-porous fiber column because Chromosorb is a typical GC packing with high surface area and uniform particle size distribution (see Fig. C-3 for the effect of efficiency on GC peaks).

The Interaction of Acidic and Basic Probes with Fibrous Columns

Using IGC, H. P. Schreiber[4] characterized the inherent acidlike and baselike properties of polyvinyl chloride and polyethylene polymers. Neutral (n-octane), acidic (t-butanol) and basic (n-butylamine) probes were used by Schreiber as the probing compounds. In our efforts to characterize the chemical properties of PET, PBI, Rayon and PP fibers, it was decided to use n-heptane, t-butanol and n-butylamine because their b.p. were closer to each other. Using the typical flow rate (4.44 ml/min), the retention volume of the probes on PET, PBI and Rayon columns were measured and the results are listed in Table C-9. Based on the results, near linear correlations between the reciprocal of the column temperature and the ln of the retention volume could be established for all three probes and the retention volume for each probe decreased with the increase of column temperature (see Fig. C-7).

Efforts aimed at estimating the interaction enthalpies (ΔH_p) of these probes were pursued by generating the correlation between "$\ln V_p$" and "$1/T$" (see Tables C-9 & C-13). Based on the ΔH_p ratio of n-butylamine and t-butanol, the inherent acidlike and baselike properties of each fiber could be estimated. For PBI and Rayon, the absolute ΔH_p of the amine was greater than the corresponding ΔH_p of the alcohol, so PBI and Rayon fibers exhibited acidlike properties (Table C-13). The ΔH_p ratio also indicated PBI having sulfonic acid groups had a much stronger acid strength than the Rayon fiber having free hydroxy groups. Unlike PBI and Rayon, the ΔH_p ratio of PET was 0.5, thus, PET

Appendix C

had baselike properties and showed a strong affinity toward t-butanol (Table C-13). The basicity of PET might be caused by its carbonyl ester groups.

Similar to the previously discussed n-alkane and PP interactions, PP having a low Tg and strong hydrophobicity exhibited great affinities towards t-butanol and n-butylamine. Some efforts (increasing flow rate or sample injection size) were pursued in order to obtain the retention volume of acidic and basic probes on the PP column. The overall IGC results including retention volume and interaction enthalpy (ΔH_R) are listed in Table C-13 & C-14. In general, the PP column showed the following inherent properties:

- PP exhibited strong affinities (low ΔH_R) toward all probes regardless of their acidity or basicity. The low Tg of PP might be one of the contributing factors.

- PP is extremely hydrophobic so it showed the strongest interaction with neutral alkanes.

- PP had acidlike properties despite its neutral chemical structure. The interaction between PP and n-butylamine was greater than the corresponding interaction between PP and t-butanol.

Conclusions

The preceeding results demonstrated the utility of performing IGC on intact fibers. The basic GC theory could be used to rationalize the effect of empirical parameters (temperature, flow rate and sample injection size) on IGC separations. On the Rayon column, we observed the existence of an optimized flow rate which gave the maximum retention volume and possibly the highest column efficiency for all probes despite the differences of their chemical properties. This observation could be rationalized by using the Van Deemter equation. The effect of sample injection size on IGC was investigated by using the PP column and organic probes having different acidity or b.p. The overall results indicated an increase on sample size would decrease the degree of peak spreading as well as to suppress the interaction between probes and column packings. The temperature effect in IGC was basically the same as its effect on regular GC. In other words, the IGC results indicated the retention volume and the probe-column interactions decreased with the increase of column temp.

The n-alkanes were successfully used to elucidate the relationship between the probe volatility (b.p.) and their corresponding retention volume. No specific chemical interaction existed between n-alkanes and all tested fibers (PET, PBI, PP and Rayon) and the separation of hydrocarbons on IGC columns depended on their relative

Appendix C

volatility and their van der Waals interactions with the column packings. Compared to other fibers PP with its low Tg and high hydrophobicity displayed the greatest affinity toward organic probes.

The inherent acidlike or baselike properties of all four fibers were studied with the use of neutral (n-heptane), acidic (t-butanol) and basic (n-butylamine) probes. Based on the relative retention volume and interaction enthalpies of t-butanol and n-butylamine, it was found that all fibers (except PET) had acidlike properties. Qualitative interaction enthalpies (ΔH_p) of all probes were estimated and the results suggested the interactions between probes and columns were exothermic.

References

1. T. W. Card, Z. Y. Al-Saigh and P. Munk, Macromolecules 18, 1030 (1985).

2. A. S. Gozdz and H. D. Weigmann; J. Appl. Poly. Sci. 29, 3965 (1984).

3. P. K. Koning and T. C. Ward, Abstract, The Adhesion Society 8th Annual Meeting, p21a. (1985).

4. H. P. Schreiber, M. R. Wertheimer and M. Lambla, J. Appl. Poly. Sci., Vol. 27, 2269 (1982).

82

TABLE C-1. PHYSICAL PROPERTIES OF IGC COLUMNS

Fiber	Specific Surface Area[a]	T_g[a]	Neat Wt.	Effective Surface Area[b]	Pretreatments
PET (polyethylene terephthalate)	0.13 m^2/g	69°C	1.77 gm	0.23 m^2/column	Preconditioned at 105°C for 24 hrs. at 10.0 ml flow rate
PBI (sulfonated polybenzimidazole)	0.33	N.E.[c]	1.79	0.59	Preconditioned at 200°C for 24 hrs at 30.0 ml/min flow rate
Rayon (Regenerated Cellulose)	0.25	N.E.[c]	1.10	0.28	Preconditioned at 150°C for 24 hrs at 10.0ml/min flow rate
PP (Polypropylene)	0.38	-20°	1.00	0.38	Preconditioned at 130°C for 24 hrs at 10.0 ml/min flow rate

Note: (a) T_g (literature published glass transition temp.); specific surface areas were measured by Dr. Gunilla E. Gillberg.

(b) Effective surface area = specific surface area x neat fiber weight for each column.

(c) N.E. means does not exist.

TABLE C-2. THE EFFECT OF FLOW RATE (FR) ON RETENTION VOLUME (V_R)

(Results obtained on Rayon column at 60°C)

FR (ml/min)	t-Butanol	n-Butylamine	n-Octane
1.06	3.26 ml	3.78 ml	3.15 ml
1.92	3.95	4.62	3.76
3.04	4.44	5.80	4.37
4.44	5.26	6.44	4.99
6.02	5.68	6.46	5.74
7.94	5.00	5.67	5.10

TABLE C-3. LINEAR CORRELATIONS BETWEEN HYDROCARBON B. P. AND RETENTION VOLUME ON PBI COLUMN

H. C. (b.p. °C)	COLUMN TEMP. (°C) AND RETENTION VOLUME (ML)		
	30°C	60°C	90°C
n-Hexane (69°C)	5.33 ml	4.22 ml	3.07 ml
n-Heptane (97°C)	8.84	5.47	3.51
n-Octane (125°C)°	10.98	7.06	4.79
n-Nonane (151°C)	14.27	10.53	5.42
n-Decane (174°C)	N.D.	10.67	8.84

Least Square analysis

(b.p. vs V_R)

Coeff.	0.996	0.972	0.918
Slope	9.384	13.877	16.802
Intercept	18.019	17.877	37.073

*Note: (1) The column flow rate was 4.44 ml/min.

(2) N.D. = not determined.

Appendix C

TABLE C-4.   LINEAR CORRELATIONS BETWEEN HYDROCARBON B. P. AND RETENTION VOLUME ON RAYON COLUMN

H. C. (b.p. °C)	COLUMN TEMP. (°C) AND RETENTION VOLUME (ML)		
	30°C	60° C	90°C
n-Hexane (69°C)	4.81 ml	3.96 ml	3.67 ml
n-Heptane (97°C)	6.08	4.36	3.73
n-Octane (125°C)	8.39	4.98	3.87
n-Nonane (151°C)	13.50	6.62	4.18
n-Decane (174°C)	16.67	9.50	4.80

Least Square Analysis

(b.p. vs V_R)

Coeff.	0.971	0.918	0.934
Slope	8.046	16.948	80.990
Intercept	43.627	23.478	-203.675

Note: (1) The column flow rate was 4.44 ml/min.

Appendix C

85

TABLE C-5. LINEAR CORRELATIONS BETWEEN HYDROCARBON B. P. AND RETENTION VOLUME ON PET COLUMN

H. C. (b. p. °C)	COLUMN TEMP. (°C) AND RETENTIN VOLUME (ML)		
	30°C	60°C	90°C
n-Hexane (69°C)	3.20 ml	2.98 ml	2.85 ml
n-Heptane (97°C)	3.65	3.18	2.89
n-Octane (125°C)	4.34	3.24	2.95
n-Nonane (151°C)	7.04	3.95	3.11
n-Decane (174°C)	13.82	5.01	3.37

Leasts Square analysis

(b.p. vs V_R)

	30°C	60°C	90°C
Coeff.	0.865	0.900	0.924
Slope	8.212	45.150	181.766
Intercept	70.56	-42.621	-428.277

Note: (1) The column flow rate was 4.44 ml/min.

TABLE C-6. ESTIMATED INTERACTION ENTHALPIES OF N-ALKANES ON
IGC COLUMNS (DATA CALCULATED BY USING EQ. 2)

N-Alkanes	ΔH_p x R (R is the gas constant)			
	PBI	Rayon	PET	PP
n-Hexane	-22.3R	-12.7R	-4.8R	-168.9R
n-Heptane	-38.6R	-21.7R	-10.3R	-226.9R
n-Octane	-34.9R	-34.3R	-17.6R	-278.0R
n-Nonane	-38.0R	-50.4R	-36.1R	-254.2R
n-Decane	-33.9R	-50.8R	-63.0R	-

Note: (1) For baselike PET column, the absolute ΔH_p increases
proportionally with the increase of molecular weight (or
b.p.); whereas, for acidlike PBI and Rayon columns, this
simple correlation does not exist. Hence, the van der Waals
interaction between n-alkanes and PET appeared to be a
dominant factor in affecting the retention volume.

(2) The unit of ΔH_p is erg (ml) (g mole) $^{-1}$.

Appendix C

87

TABLE C-7. IGC RETENTION VOLUME OF n-ALKANES ON PP COLUMN

	COLUMN TEMP. (°C) AND RETENTION VOLUME (ML)		
H. C. (B.P.°C)	75°C	90°C	105°C
n-Hexane (69°C)	14.87 ml	10.52 ml	7.77 ml
n-Heptane (97°C)	27.88	16.64	11.86
n-Octane (125°C)	55.41	28.53	19.40
n-Nonane (151°C)	94.31	56.76	35.34
n-Decane (174°C)	N.E.	N.E.	60.18

Least Square Analysis
(b.p. vs V_R)

Coeff.	0.973	0.942	0.936
Slope	0.981	1.625	1.829
Intercept	63.323	64.805	73.971

Note: (1) N.E. (not eluted out from the column).

(2) The flow rate was set at 4.44 ml/min. and the injection size of each probe was 0.05 µl.

TABLE C-8. THE EFFECTS OF FLOW RATE (FR) AND SAMPLE INJECTION SIZE (SIS) ON THE INTERACTION OF N-HEPTANE AND PP COLUMN

SIS	FR	Column Temp.(°C) and Retention Volume (ml)				
		30°C	60°C	75°C	90°C	105°C
0.05 μl	4.44 ml/min.	N.E.	N.E.	27.88	16.64	11.86
	6.66	N.E.	50.02	N.S.	18.05	N.S.
	10.0	N.E.	46.10	N.S.	19.70	N.S.
0.5 μl	4.44	N.E.	42.00	N.S.	17.32	N.S.

Note: (1) N.E. (not eluted out from the column).

(2) N.S. (not studied).

(3) It is hard to rationalize the 90°C abnormal result, the retention volume increases with the increase of column flow rate (see data listed under 0.05 μl SIS).

TABLE C-9. CORRELATIONS BETWEEN COLUMN TEMP. AND RETENTION VOLUME (V_R) OF PROBES ON PET COLUMN

Probes (b.p. °C)	COLUMN TEMP. (°C) AND V_R (ML)			$\ln V_R$			Slope $(-\Delta H_p/R)$	K (Column Constant)
	30°C	60°C	90°C	30°C	60°C	90°C		
n-Butylamine (77°)	3.54 ml	3.44 ml	3.14 ml	1.264	1.236	1.144	4.556	1.122
n-Butanol (82°)	3.51	3.07	2.85	1.256	1.122	1.047	9.108	0.956
n-Heptane (97°C)	3.65	3.18	2.89	1.295	1.157	1.061	10.302	0.967

Note:

1. Based on Eq. 2, the interaction enthalpy (ΔH_p) between probes and column packings were related to the $\ln V_R$ and the reciprocal of the column temp.

$$\ln V_R = (-\Delta H_p/R)(1/T) + K \qquad \text{(Eq. 2)}$$

2. The absolute value of the slope ($-\Delta H_p/R$) revealed the degree of probe-column interaction.

3. The flow rate and sample size were set at 4.44 ml/min. and 0.05 µl respectively.

TABLE C-10. CORRELATIONS BETWEEN COLUMN TEMP. AND RETENTION
VOLUME (V_R) OF PROBES ON PBI COLUMN

Probes (B.P.°C)	COLUMN TEMP(°C) AND V_R			lnV_R			SLOPE	K
	30°C	60°C	90°C	30°C	60°C°	90°C	(- $\Delta H_p/R$)	(COLUMN CONSTANT)
n-Butylamine(77°)	N.E.	6.44 ml	3.60 ml	N.E.	1.863	1.281	103.928	Not established
t-Butanol (82°)	7.85	4.98	3.78	2.061	1.605	1.330	31.682	1.020
n-Heptane (97°)	8.84	5.47	3.51	2.179	1.699	1.256	38.586	0.923

Note 1. Based on Eq. 2, the interaction enthalpy (ΔH_p) between probes and column packings were related to the lnV_R and the reciprocal of the column temp.

$lnV_R = (-\Delta H_p/R) (1/T) + K$ (eq. 2)

2. The absolute value of the slope (- $\Delta H_p/R$) revealed the degree of probe-column interaction.

3. The flow rate of sample size were set at 4.44 ml/min. and 0.05 μl respectively.

TABLE C-11. CORRELATIONS BETWEEN COLUMN TEMP. AND RETENTION
VOLUME (V_R) OF PROBES ON RAYON COLUMN

Probes (b.p. °C)	COLUMN TEMP. (°C) AND V_R			$\ln V_R$			SLOPE $(-\Delta H_p/R)$	K (COLUMN CONSTANT)
	30°C	60°C	90°C	30°C	60°C	90°C		
n-Butylamine (77°)	10.20 ml	6.04 ml	4.17 ml	2.322	1.798	1.428	38.281	1.070
t-Butanol (82°)	7.83	5.11	4.13	2.058	1.631	1.418	28.120	1.130
n-Heptane (97°)	6.08	4.36	3.73	1.805	1.472	1.316	21.680	1.092

Note 1. Based on eq. 2, the interaction enthalpy (ΔH_p) between probes and column packings were related to the $\ln V_R$ and the reciprocal of the column temp.

$$\ln V_R = (-\Delta H_p/R)\,(1/T) + K \qquad \text{(eq. 2)}$$

2. The absolute value of the slope ($-\Delta H_p/R$) revealed the degree of probe-column interaction.

3. The flow rate and sample size were set at 4.44 ml/min and 0.05 μl respectively.

TABLE C-12. CORRELATIONS BETWEEN COLUMN TEMP. AND RETENTION
VOLUME (V_R) OF PROBES ON PP COLUMN

| Probes (b.p.°C) | COLUMN TEMP. (°C) AND V_R | | | $\ln V_R$ | | | $\dfrac{\text{SLOPE}}{(-\Delta H_p/R)}$ | $\dfrac{K}{(\text{Column Constant})}$ |
	75°C	90°C	105°C	75°C	90°C	105°C		
n-Butylamine (77°)	16.69 ml	11.47 ml	8.88 ml	2.815	2.440	2.184	165.827	0.603
t-Butanol (82°)	8.21	6.00	5.28	2.105	1.792	1.664	117.371	0.525
n-Heptane (97°)	27.88	16.64	11.86	3.328	2.812	2.473	226.870	0.326

Note 1.   Based on eq. 2, the interaction enthalpy (ΔH_p) between probes and column packings were related to the $\ln V_R$ and the reciprocal of the column temp.

$$\ln V_R = (-\Delta H_p/R)\,(1/T) + K \qquad \text{(eq. 2)}$$

2.   The absolute value of the slope ($-\Delta H_p/R$) revealed the degree of probe-column interaction.

3.   The flow rate and sample size were set at 4.44 ml/min. and 0.05 μl respectively.

TABLE C-13. **ESTIMATED INTERACTION ENTHALPES (ΔH_p) of n-HEPTANE, n-BUTYLAMINE AND t-BUTANOL ON IGC COLUMNS**

ΔH_p X R (R IS THE GAS CONSTANT)

Probe (b.p°C)	PET	PBI	RAYON	PP
I) n-Butylamine (77°)	-4.56	-103.93	-38.28	-165.83
t-Butanol (82°)	-9.11	-31.68	-28.12	-117.37
n-Heptane (97°)	-10.30	-38.59	-21.68	-226.87
II) ΔH_p(Amine)/ΔH_p(alcohol)	0.50	3.28	1.36	1.38
Acidity/Basicity	Basic	Very Acidic	Acidic	Acidic

Note 1.   The flow rate and sample size were set at 4.44 ml/min. and 0.05 μl respectively.

2.   All data were calculated according to eq. 2 and Table 7 .

3.   Based on the ratios of the ΔH_p, the relative acidity or basicity of the fibers could be estimated.

TABLE C-14. THE EFFECT OF FLOW RATE (FR) AND SAMPLE INJECTION SIZE (SIS) ON THE PERFORMANCE OF PP COLUMN

I) <u>SIS WAS TYPICAL (0.05 µl FOR EACH PROBE) BUT FR WAS INCREASED</u>

	FR (6.66 ML/MIN.)			FR (10.0 ML/MIN.)		
SAMPLE	30°C	60°C	90°C	30°C	60°C	90°C
n-Heptane	N.E.	50.02 ml	18.05 ml	N.E.	46.10 ml	19.70 ml
t-Butanol	N.E.	8.92	7.13	N.E.	7.80	7.30
n-Butylamine	N.E.	26.91	12.90	N.E.	25.40	12.52

II) <u>FR WAS TYPICAL (4.44 ML/MIN) BUT SIS WAS INCREASED TO 0.5 µl</u>

	COLUMN TEMP. (°C) AND RETENTION VOL. (ML)		
SAMPLE	30°C	60°C	90°C
n-Heptane	N.E.	42.09 ml	17.32 ml
t-Butanol	9.68	8.57	5.37
n-Butylamine	36.32	22.96	10.88

NOTE: (1) N.E. (not eluted out from the column).
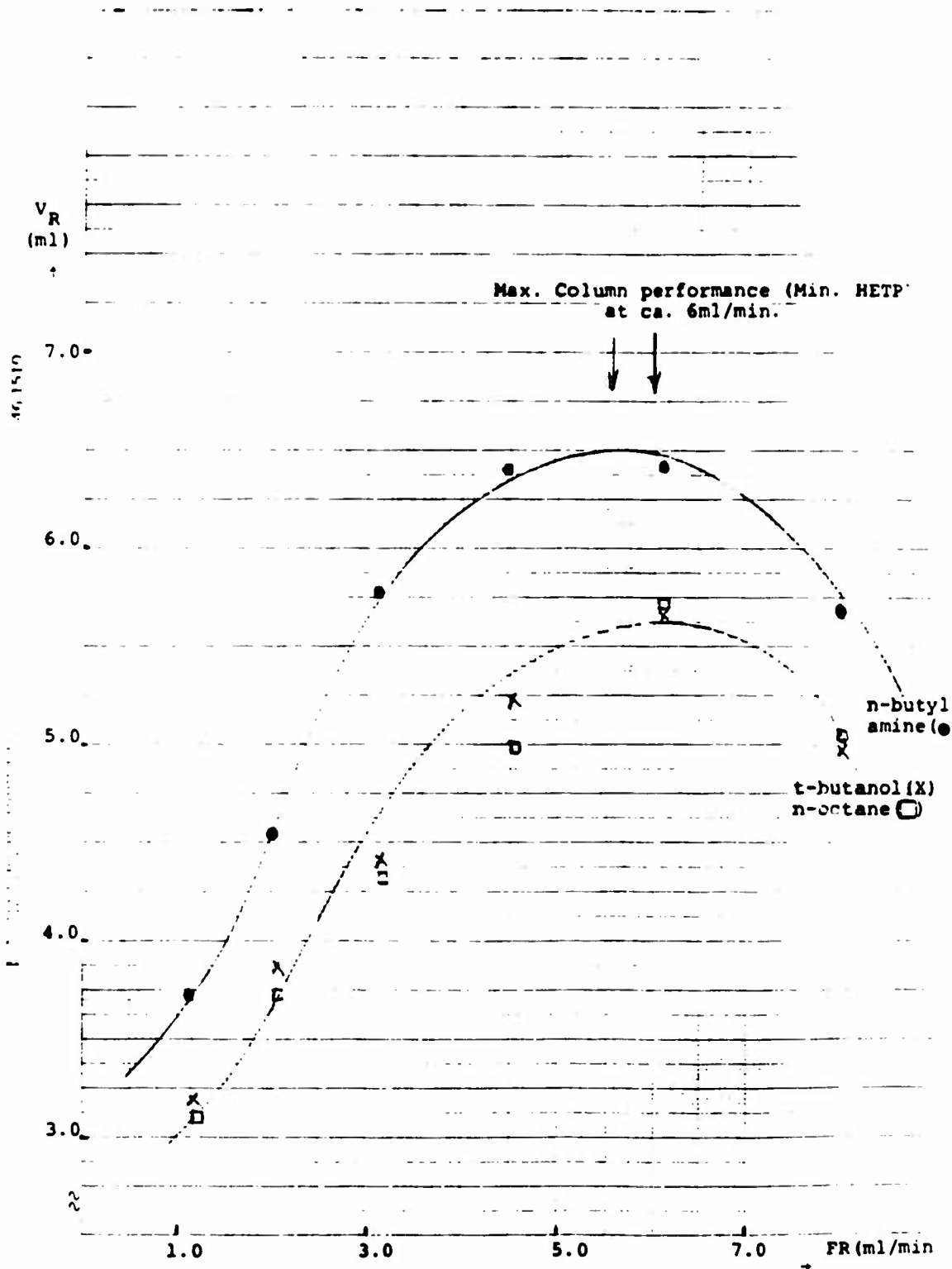
FIGURE C-1.   THE PLOT OF FLOW RATE (FR) VS. RETENTION VOLUME
              (V_R) (ON RAYON COLUMN AT 60°C: SEE TABLE C-2)
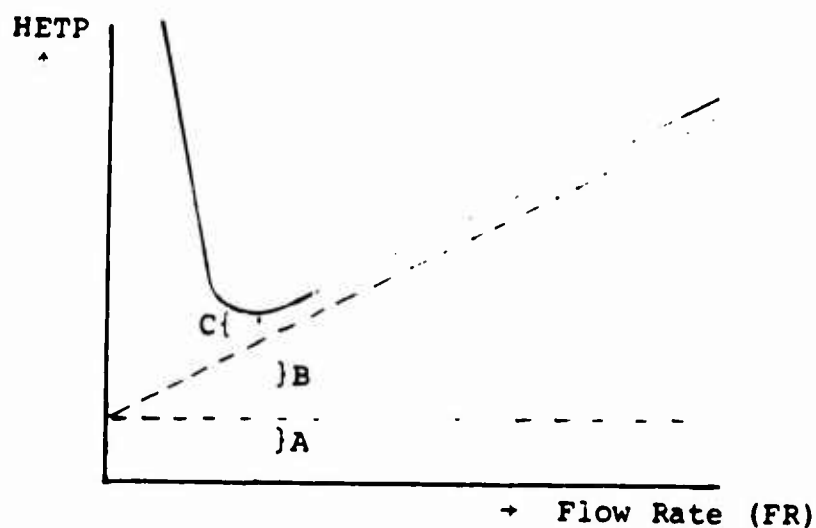
Van Deemter   Eq.

$$HETP = A + B \left(\frac{1}{FR}\right) + C \times (FR)$$

A = Eddy diffusion which corresponds to column packings.

B = Molecular diffusion which corresponds to the diffusivity of the probe in the gas carrier.

C = Resistance to mass transfer which corresponds to the diffusivity of the probe in the column packings.

Note: Higher column efficiency yields a lower HETP value.

FIGURE C-2.   THE PLOT OF COLUMN EFFICIENCY (HETP) VS. FLOW RATE (FR)

(1) Normal Condition

Injection
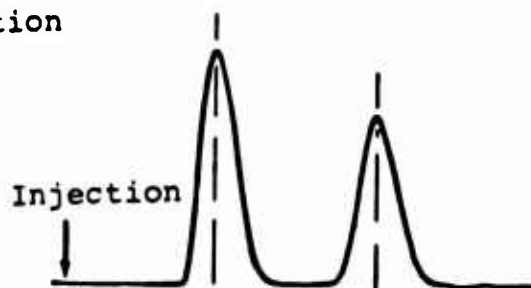
(2) Increase Efficiency

(3) Increase Selectivity
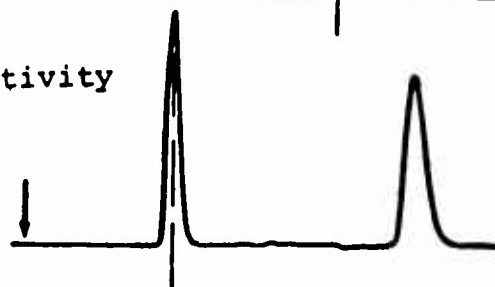
FIGURE C-3.   THE EFFECT OF EFFICIENCY AND SELECTIVITY ON GC
SEPARATION

(Retention Volume) V_R: 3.15 ml   3.76   4.37   4.99   5.74

(Flow Rate) FR: 1.06 ml/min   1.92   3.04   4.44   6.02
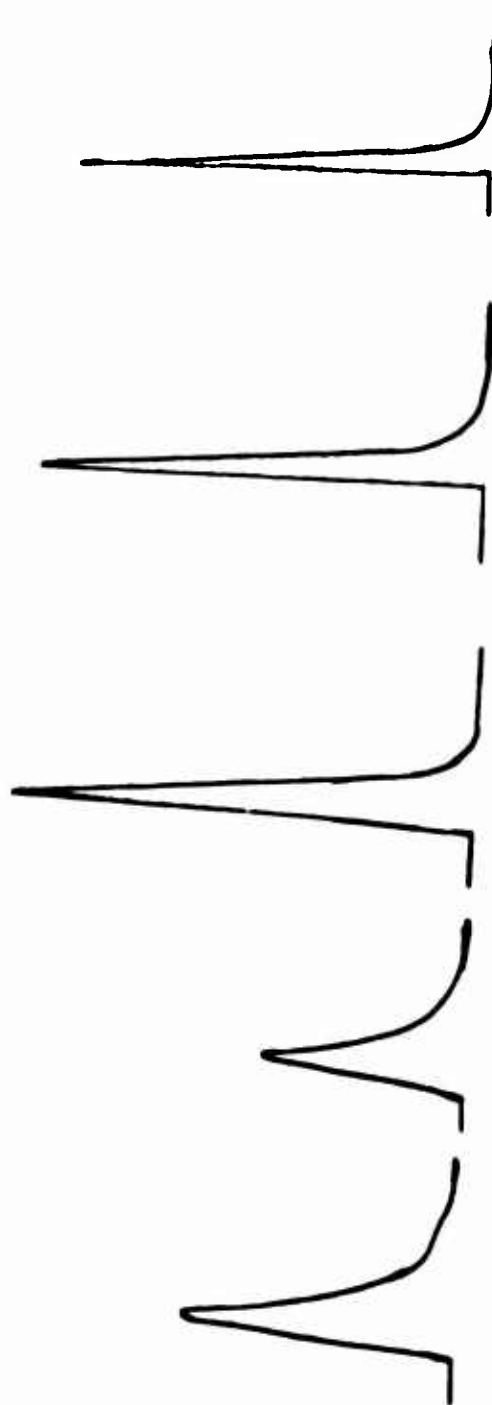
Note: The column efficiency and selectivity increased from 1.06 to 6.02 ml/min. (For detail data see Table 2).

FIGURE C-4.   THE EFFECT OF FLOW RATE ON N-OCTANE SEPARATION (ON RAYON COLUMN AT 60°C)

Appendix C

99
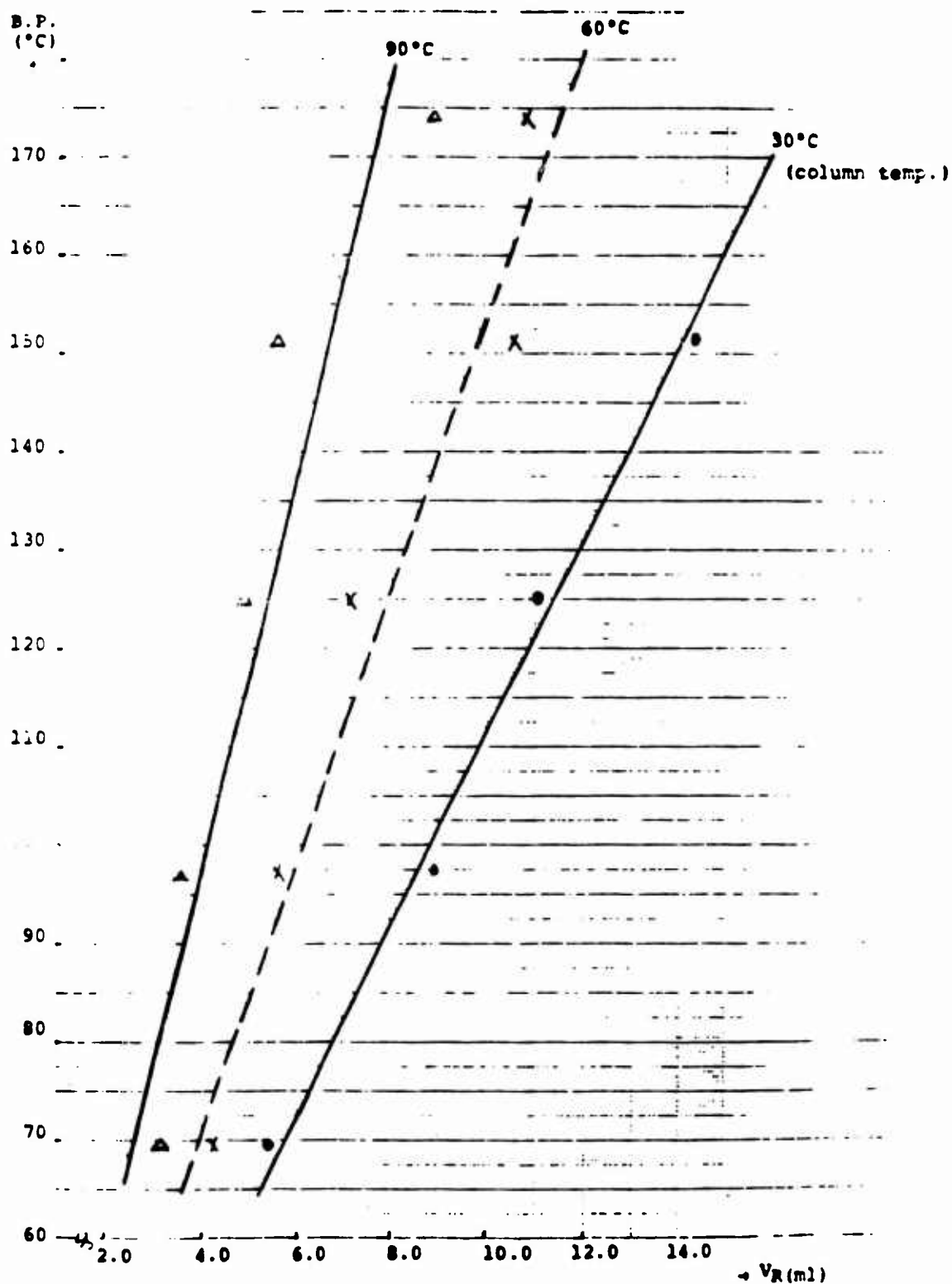
FIGURE C-5. PLOT BETWEEN n-ALKANE B.P. AND PBI COLUMN RETENTION VOLUME (SEE TABLE C-3)
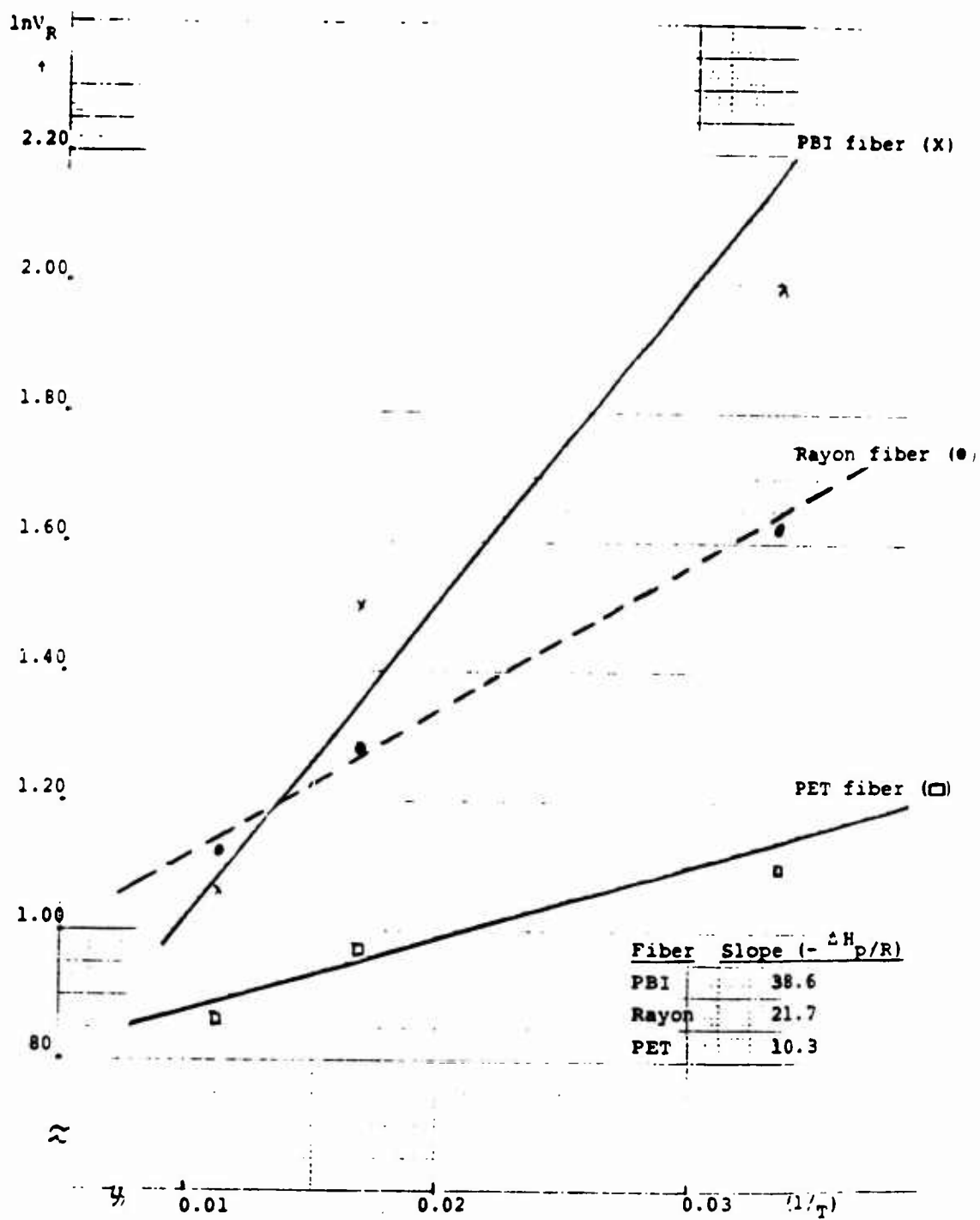
FIGURE C-6.   PLOT OF RELATIVE n-HEPTANE SORPTION ON IGC COLUMNS
(SEE TABLE C-3 AND C-6 FOR DATA, EQ. 2 FOR
CALCULATION)
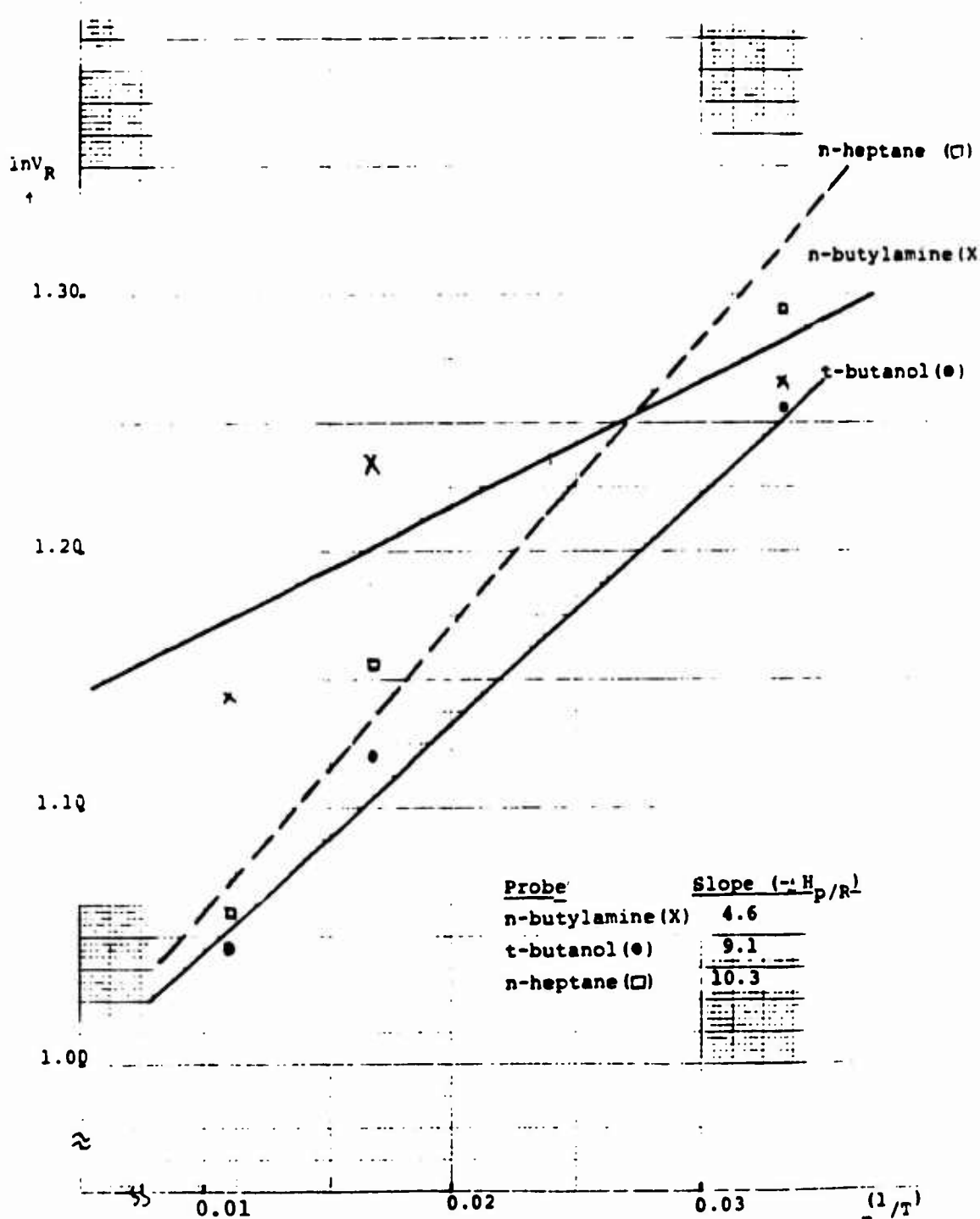
FIGURE C-7. CORRELATION BETWEEN $\ln V_R$ AND $1/T$ ON PET COLUMN
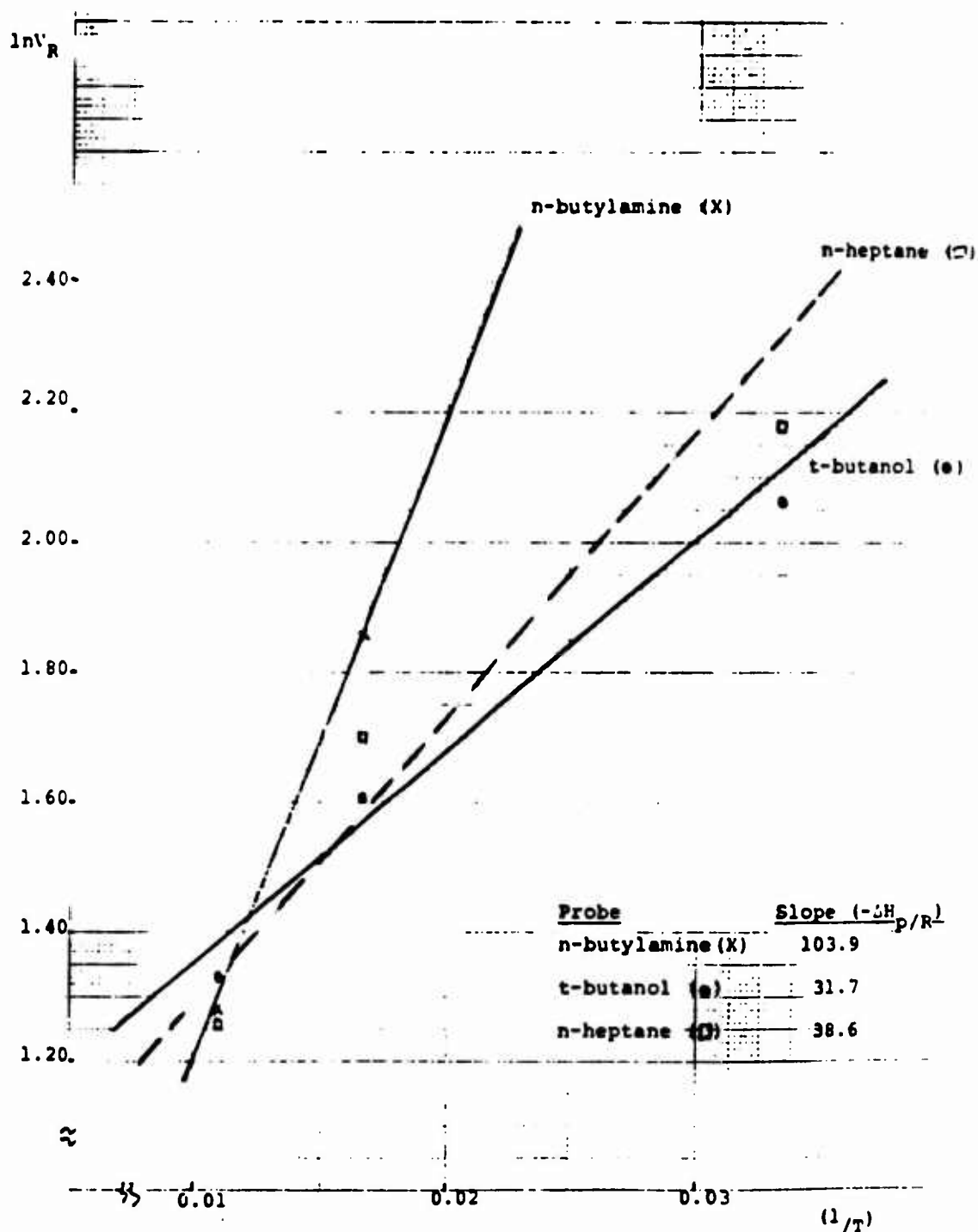(SEE TABLE C-9 FOR IGC DATA)

FIGURE C-8. CORRELATION BETWEEN $\ln V_R$ AND $1/T$ ON PBI COLUMN
(SEE TABLE C-10 FOR IGC DATA)

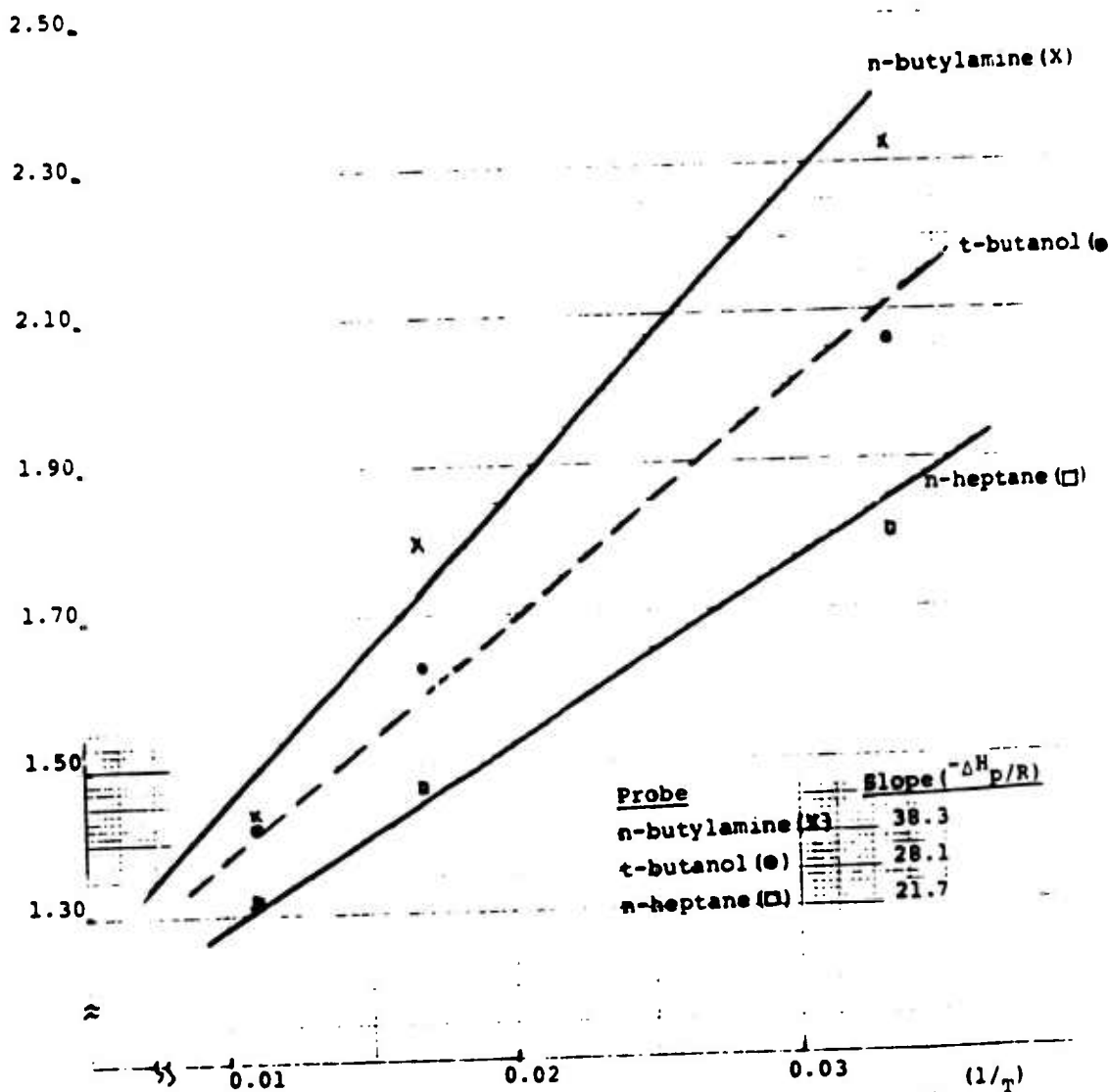FIGURE C-9. CORRELATION BETWEEN 1nV and 1/T ON RAYON COLUMN
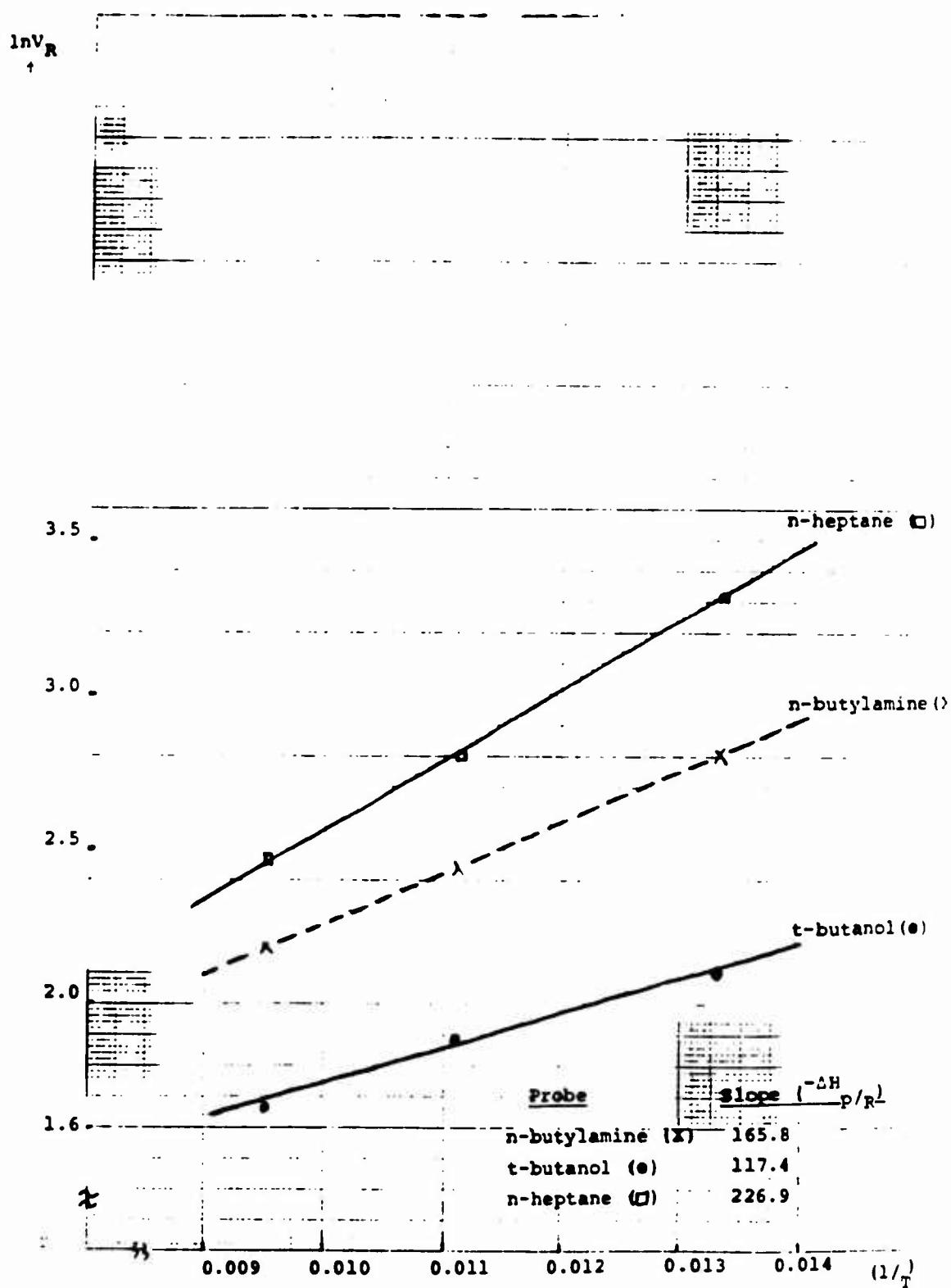(SEE TABLE C-11 FOR IGC DATA)

FIGURE C-10. CORRELATION BETWEEN lnV_R AND $1/T$ ON PP COLUMN
(SEE TABLE C-12 FOR IGC DATA)